

REVIEW OF NATURAL TERRAIN LANDSLIDE DEBRIS-RESISTING BARRIER DESIGN

GEO REPORT No. 104

D.O.K. Lo

**GEOTECHNICAL ENGINEERING OFFICE
CIVIL ENGINEERING DEPARTMENT
THE GOVERNMENT OF THE HONG KONG
SPECIAL ADMINISTRATIVE REGION**

REVIEW OF NATURAL TERRAIN LANDSLIDE DEBRIS-RESISTING BARRIER DESIGN

GEO REPORT No. 104

D.O.K. Lo

**This report was originally produced in January 2000
as GEO Special Project Report No. SPR 1/2000**

© The Government of the Hong Kong Special Administrative Region

First published, November 2000

Prepared by:

Geotechnical Engineering Office,
Civil Engineering Department,
Civil Engineering Building,
101 Princess Margaret Road,
Homantin, Kowloon,
Hong Kong.

This publication is available from:

Government Publications Centre,
Ground Floor, Low Block,
Queensway Government Offices,
66 Queensway,
Hong Kong.

Overseas orders should be placed with:

Publications Sales Section,
Information Services Department,
Room 402, 4th Floor, Murray Building,
Garden Road, Central,
Hong Kong.

Price in Hong Kong: HK\$58

Price overseas: US\$11 (including surface postage)

An additional bank charge of **HK\$50** or **US\$6.50** is required per cheque made in currencies other than Hong Kong dollars.

Cheques, bank drafts or money orders must be made payable to
The Government of the Hong Kong Special Administrative Region.

PREFACE

In keeping with our policy of releasing information which may be of general interest to the geotechnical profession and the public, we make available selected internal reports in a series of publications termed the GEO Report series. A charge is made to cover the cost of printing.

The Geotechnical Engineering Office also publishes guidance documents as GEO Publications. These publications and the GEO Reports may be obtained from the Government's Information Services Department. Information on how to purchase these documents is given on the last page of this report.



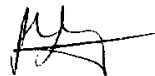
R.K.S. Chan
Head, Geotechnical Engineering Office
November 2000

FOREWORD

As part of the development of natural terrain landslide risk management strategy for Hong Kong, the Geotechnical Engineering Office is conducting a series of studies to develop techniques for quantifying natural terrain hazard and risk and to assess the range of practicable risk mitigation measures, so that a balanced and cost-effective strategy can be formulated.

This study examines the design of landslide debris-resisting barriers. The main aim is to identify methods that can produce reasonable estimates of the debris mobility and debris impact loads for use in engineering design. Various approaches suggested in the literature for assessing the mobility of debris and debris impact loads have been reviewed and evaluated in the light of laboratory and field measurements. Some suggestions are put forward to facilitate design. Given the developments in the subject, the suggestions are intended to be interim. They will be reviewed and updated when new data and results of further research become available.

This study was carried out by Dr D.O.K. Lo, under the supervision of initially Mr K.K.S. Ho and later Mr W.K. Pun and Mr Y.K. Shiu. Useful information has been provided by Prof. Z. Kang and Mr S. Zhang of the Institute of Mountainous Environment and Hazards, Chinese Academy of Sciences and Ministry of Water Conservation, Mr R. Du and Mr S. Wang of the Dongchuan Institute of Debris Flow Control, Chinese Academy of Sciences, Mr B. Hösle of Fatzer AG, Switzerland, and Mr D.F. VanDine of VanDine Geological Engineering Ltd, Canada. Their assistance is gratefully acknowledged.



P.L.R. Pang
Chief Geotechnical Engineer/Special Projects

ABSTRACT

The demand for land in the hilly terrain of Hong Kong means there is increasing pressure for developments to encroach onto the steeper parts of its natural terrain. Typically more than 300 natural terrain landslides occur in Hong Kong every year. The vast majority of these are shallow failures involving the top few metres of the ground surface and some may develop into channelised debris flows with long runout. Given the close proximity of some of the developments to natural hillsides, even a relatively small failure can potentially result in serious consequences.

Preventive works on the hillside can be extensive and prohibitively costly and landslide barriers may prove to be a cost-effective solution in certain situations. This study examines some salient aspects of the design of barriers for natural terrain landslides. Key data on some of the barriers constructed in Hong Kong are presented. Various approaches put forward in the literature for evaluating the impact loads on barriers have been reviewed and this illustrates, *inter alia*, the considerable scatter in the predictions as well as in some of the reported field measurements.

Based on the present state of knowledge, some suggestions are put forward to facilitate the assessment of debris mobility and debris impact loads in the design of landslide debris-resisting barriers. Given the developments in the subject, the suggestions are intended to be interim. They will be reviewed and updated when new data and results of further research become available.

Further research is needed to gain a better fundamental understanding of the nature and mechanisms of natural hillside failures in Hong Kong and to improve the methods for assessment of debris mobility and debris impact loads under local conditions.

CONTENTS

	Page No.
Title Page	1
PREFACE	3
FOREWORD	4
ABSTRACT	5
CONTENTS	6
1. INTRODUCTION	8
1.1 General	8
1.2 Landslide Hazards and Zones	8
1.3 Mitigation Measures	8
2. TYPES OF BARRIERS	9
2.1 Overseas Practice	9
2.2 Local Practice	11
3. REVIEW OF LOCAL DESIGN CASES	11
3.1 Design Volume	11
3.2 Impact Loading	12
3.3 Debris Mobility	14
4. DESIGN METHODOLOGIES	14
4.1 General	14
4.2 Characterisation of Landslide Hazards	15
4.3 Characterisation of Design Events	16
4.3.1 General	16
4.3.2 Methods for Estimating Debris Flow Volumes	16
4.3.3 Peak Discharge of Debris Flows	19
4.3.4 Discussion	19
4.4 Characterisation of Debris Movement	20
4.4.1 General	20
4.4.2 Methods for Estimating Debris Velocity and Runout	21

	Page No.
4.4.3 Runout Distance	27
4.4.4 Vertical Runup Distance	28
4.5 Dynamic Interaction upon Debris Impact at Barrier	30
4.5.1 Debris Impact	30
4.5.2 Boulder Impact	32
5. SUMMARY AND DISCUSSION	33
5.1 Debris Mobility	33
5.2 Runout and Runup Distance	36
5.3 Debris Impact	36
5.4 Boulder Impact	37
6. SUGGESTIONS FOR DESIGN OF BARRIERS	38
6.1 General	38
6.2 Debris Mobility	38
6.2.1 Analytical Approach	38
6.2.2 Empirical Approach	39
6.3 Debris Impact	39
6.4 Boulder Impact	40
6.5 Stability Check and Structural Design	40
7. OTHER DESIGN CONSIDERATIONS	40
8. RECOMMENDED R&D STUDIES	41
9. CONCLUSIONS	42
10. REFERENCES	43
LIST OF TABLES	50
LIST OF FIGURES	64
LIST OF PLATES	88

1. INTRODUCTION

1.1 General

The demand for land in the hilly terrain of Hong Kong means there is increasing pressure for developments to encroach onto the steeper parts of its natural terrain. Based on the Geotechnical Engineering Office's Natural Terrain Landslide Inventory, on average about 300 natural terrain landslides occur per annum (Evans & King, 1998). The vast majority of these are shallow failures within the top few metres of the ground surface and some failures have developed into channelised debris flows with a long runout. An example showing possible hazardous scenarios posed by the natural hillside is depicted in Figure 1.

1.2 Landslide Hazards and Zones

In this study, the natural terrain landslide hazards have been broadly categorised into four groups, viz. open hillside failures (debris slides and debris flows), channelised debris flows, deep-seated failures and rock/boulder falls.

In general, there are four major mechanisms involved in the landsliding and debris movement processes. These are initiation (or initial failure of the slope in the source area), transport of the mobilised debris, erosion of the natural terrain and entrainment of additional debris, and deposition of the debris. Some of these mechanisms may be absent or of minor significance depending on the landslide type. Each of these mechanisms may predominate in different zones of the path traversed by the debris, which can be broadly divided into three zones: initiation, transportation and erosion, and deposition (Figure 2). The actual gradient within each zone is a function of the composition and gradation of the debris, slope morphology and gradient, and effect of surface water. VanDine (1985) reported that for channelised debris flows, the gradients tend to decrease with increasing catchment area.

Different mechanisms of transport, erosion and deposition may occur within these zones and give rise to different hazards. For example, open hillside failures and rock/boulder falls derive the debris volume principally from the source area. For channelised debris flows, the erosion and entrainment of material within the channel in the hazard trail can add considerably to the total debris volume in addition to material derived from the source area.

1.3 Mitigation Measures

Landslide consequence can be reduced through landslide hazard mitigation measures, which can be divided into two categories: active and passive methods (Figure 3). Passive methods generally involve no direct engineering and can include land-use regulations (e.g. no-build zones and land-use planning), education and issue of landslide warnings. Active methods, on the other hand, involve engineering works and normally comprise upgrading works on the slope to reduce the likelihood of failure, or defensive works to mitigate failure consequences. Some of the active mitigation measures are summarised in Table 1. The active mitigation measures can be classified into two groups according to the locations where they are applied, viz. at the source area where the failure occurs, or on the hazard trail along which the landslide debris is transported and deposited.

Mitigation measures at the source area include strengthening of the slope by means of soil treatment, provision of reinforcement and drainage, and removal of failure initiating factors (e.g. steep gradients and unstable material) through afforestation, regrading of the slope, and construction of check dams. Protective measures such as rock/boulder fences, deflection berms and debris barriers can be constructed at the end of the hazard trail to protect the population and facilities at risk.

Protective measures have been implemented along the hazard trail for mitigating debris flows. These include, inter alia, check dams, debris racks, slit dams and steel cell dams. They help primarily to dissipate part of the energy of the debris and to screen out big boulders from the landslide debris. Unconfined deposition areas, debris containment basins and debris flow breaker screens have been provided to promote deposition by reducing the slope gradient and the confinement to flow, or enhancing the separation of water from the debris. A number of techniques have also been deployed to encourage debris to continue to flow in a controlled manner through and beyond a developed area. These include lateral walls and debris viaducts to confine and divert the flow. Lined channels and guideways are sometimes constructed to minimise segregation of debris, increase flow velocity to prevent premature deposition so as to maintain an acceptable clearance between the debris and the underside of bridges, and to minimise degradation of the channel bed. Some of these mitigation measures are shown in Plates 1 to 6.

Figure 4 is a schematic diagram showing the use of various mitigation measures. Detailed reviews of the types of active mitigation measures have been given by Hung et al (1984), Thurber Consultants Ltd (1984), VanDine (1996) and Franks & Woods (1997).

The applicability of particular mitigation measures or combination of measures depends on the types and scale of landslide hazards, the perceived elements at risk, and the consideration of costs, land-take and the associated reduction in risk that can be achieved. Preventive works on the natural hillside can be extensive and costly and barriers can be a cost-effective solution in certain situations.

This Report presents information on the various types of barriers (for both rock/boulder falls and landslide debris) used in Hong Kong and a review of their design methodologies. It then examines some salient aspects of the design of barriers for open hillside failures and channelised debris flows. Various approaches suggested in the literature for assessing the mobility of debris and debris impact loads are reviewed and evaluated in the light of laboratory and field measurements. Suggestions for the assessment of debris mobility and debris impact loads are put forward. Areas requiring further work are also suggested.

2. TYPES OF BARRIERS

2.1 Overseas Practice

A variety of rock/boulder fall barriers in the form of gabions, reinforced concrete L- or T-shaped retaining walls, reinforced fill barriers and rock/boulder fences have been constructed to retain detached debris, rocks and boulders. The required type of barrier and its dimensions depend on, inter alia, the energy of falling debris, the slope geometry, and the availability of the construction material.

The essential elements of a rock/boulder fence comprise posts anchored at a regular spacing with a net attached to it. The net will deform when impacted upon by a rock/boulder. Such deformation will prolong the impact duration and thereby reduce the impact loading and allow the use of lighter elements in construction. Description of the various types of rock fences can be found in Wyllie & Norrish (1996).

The energy-absorbing capacity of fences typically ranges from about 200 kJ to 2 300 kJ. Duffy (1998) and Thommen (1998) reported that in California, some fences have been observed to be able to retain landslide debris of a volume up to 500 m³. In one incident, a 3 000 m³ rockslide overtopped and destroyed a rock fence, before reaching the roadway. However, the fence had successfully contained a significant portion of the rockslide volume. As a result the time for clearing the debris for the reopening of the affected road section was estimated to have been reduced to one-quarter of that if the fence were not there. Haller (1999) reported that a fence installed across a streamcourse in Japan had retained up to about 800 m³ of landslide debris. The enhanced performance of these fences has been attributed partly to the conservatism built into their design. In the event of a landslide, the debris may not move as a single rigid mass, but rather as a deformable body with a leading front and a trailing tail. It is likely that the energy imparted onto the fence derives primarily from the frontal end of the debris with the trailing material which accumulates behind it acting as a static load after coming to rest (Duffy, 1998). However, the failure mechanism of these incidents is not well established.

DeNatale et al (1996) compared the energy-absorbing capacity and retention capacity of six rock fences. The fences were placed near the toe of a reinforced concrete channel which was 95 m long, 2 m wide, 1.2 m deep and inclined at 31°. The landslide debris, which was a poorly graded gravelly sand of about 10 m³ in volume, was released at the top of the channel. It reached a velocity between 5 to 9 m/s before impacting the fence. DeNatale et al (op cit) noted that by placing a chicken-wire (19 mm opening) and a chain link fence (50 mm opening), or a silt screen and a chain link fence over the netting, the fence could retain about 99% of the debris.

Gabions permit ease of construction on rugged terrain and are able to sustain considerable impact from falling rocks. However, they are susceptible to damage by impacting rocks. Also, maintenance and repair costs can be significant. Concrete barriers can be placed quickly but are less resilient than gabions.

In Europe, most debris barriers are between 5 m and 15 m in height, but some may exceed 35 m while in Japan over 80% are less than 10 m high (Czerny, 1998; Thurber Consultants Ltd, 1984; VanDine, 1985). In Canada, most of the barriers are earthfill structures whereas in Europe concrete and masonry gravity structures appear to be prevalent (Hungar et al, 1987). Prestressed concrete has also been used in the construction of barriers to achieve a lighter section (Czerny, 1998). In China, cascaded dams, each about 2 to 5 m in height, are commonly constructed in series in steep ravines to contain debris. This generally involves the construction of a base dam on solid foundation during the dry season. Dams are then constructed upstream of the previous ones resting on the debris that had piled up behind the previous dams. The debris retained behind these dams act as buttresses to the slopes adjacent to the channel bank thereby minimising the chances of further failure. The highest cascaded dam is about 50 m in height and is located in Yunnan, China (Kang, 1996 & 1999).

In European countries and in Japan, debris barriers are often constructed as the initial line of defence. They are the primary mitigation measure constructed near the mouth of a streamcourse to offer protection against debris hazards. Subsequently, a series of check dams will be constructed upstream of the barrier on the steep section of the natural streamcourse. The check dams are constructed near the point of potential initiation to 'step' the channel to reduce the steep gradient thereby lowering the likelihood of channelised debris flow occurrence. However, it is not easy to identify the location where channelised debris flow may occur in advance, and check dams are commonly constructed over much of the initiation and transportation zones of the channel. The presence of check dams also help to prevent the downcutting of the channel bed and thereby reducing the volume of debris that can be mobilised in a debris flow event.

2.2 Local Practice

Table 2 shows the types of debris- and boulder-resisting barriers that have been, or are being, constructed in Hong Kong. These include rock/boulder fences, gabions, reinforced concrete L- or T-shaped retaining walls, reinforced concrete cantilever walls, earthfill berms and check dams. These structures are generally less than 10 m high, with the majority being less than 5 m. Some of these structures are shown in Plates 7 to 14.

Boulder fences, gabions and concrete walls have been used to arrest loose boulders from encroaching development. Gabions and reinforced concrete walls are generally used to resist larger size boulders or boulders travelling at higher velocities. Boulder fences are generally designed to arrest boulders up to a certain size, above which insitu stabilisation of the boulders would be carried out to avoid the need for excessively bulky and expensive structural members.

Debris-resisting barriers commonly employed in Hong Kong comprise predominantly reinforced concrete retaining walls. To enhance the impact capacity, some of these structures are founded on minipiles and some are integral with the building structure. In one case, an earthfill berm has been constructed as a terminal barrier to protect a golf driving range from debris encroachment.

The design aspects of the various types of barriers shown in Table 2, in respect of estimation of the magnitude of the design event, debris mobility and debris impact loading, have been reviewed. These are summarised in Section 3 for the purpose of examining the current state of practice and its adequacy.

3. REVIEW OF LOCAL DESIGN CASES

3.1 Design Volume

The debris volume in most of the local design cases was estimated from slope stability analysis and was taken to be that corresponding to the slip surface with the lowest factor of safety. The design volume obtained using this approach makes little reference to the design life of the protected structure and the landslide activities at the site. This estimated volume could be unreliable because generally limited ground investigation works have been carried out over the area of the concerned natural terrain to allow the formulation of a representative

geological model for analysis.

Alternatively, at some sites information on the past landsliding activities at the site, which has been obtained from an interpretation of aerial photographs (API), an examination of site-specific landslide records and a site reconnaissance, is used to estimate the design event. The design volume of a particular landslide hazard has sometimes been taken to be equal to the largest volume of the same hazard as suggested by the historical data. In other cases, the previous landslide data have been synthesised to compile an annual landsliding frequency-debris volume relationship for the site. The design volume was then selected with reference to the design life of the structure or an arbitrary return period of the hazard.

The latter approach is sound in principle but is often limited by the scarcity of historical data, in particular, the low frequency large-scale failures. To circumvent this problem, Tse et al (1999) proposed to make use of the landslide data from areas of similar geological setting for the construction of a site-specific frequency-volume relationship for a particular site. Figure 5 shows the landsliding frequency-debris volume curves, derived from data extracted from studies carried out by Wong et al (1998) and Franks (1998), on natural terrain landslides on Lantau Island in two rainstorms in 1992 and 1993. They are broadly bilinear on a log-log plot. Tse et al's procedure involves the construction of the initial part of a site-specific annual frequency-debris volume curve using the landslide data obtained from API and site reconnaissance. The end point of this curve corresponds to the largest landslide volume with a return period equal to the inverse of the number of years of observation. To extrapolate the site-specific curve to larger landslide volumes, Tse et al assumed the trend to be similar to that for the Lantau studies and a line was drawn from the end point of the site-specific curve parallel to that for the Lantau studies. The magnitude of the design event corresponding to a particular design life was then obtained from this site-specific curve.

This approach of constructing site-specific annual frequency-debris volume curve implicitly involves a number of simplifying assumptions. It assumes that the largest recorded landslide volume corresponds to the point where the two bilinear segments meet. This assumption could in general lead to an underestimation of the magnitude of the design event, especially for areas where data on past landslides are limited. The landslides that had occurred over the observation period represent the overall responses of the terrain to a wide spectrum of rainstorms with varying characteristics whilst the landslides in 1992 and 1993 might only reflect the response of the natural terrain to the rainfall characteristics of these two rainstorms. For example, according to Wong et al (1998) the November 1993 rainstorm was extremely heavy, particularly over the medium duration range of 6-hour to 12-hour. Therefore, the frequency-debris volume curve derived from the individual storms may be different from that derived for a range of rainstorms, and the difference would depend on the characteristics of the individual storms.

3.2 Impact Loading

The approaches adopted for the design of barriers against debris impacting loading can be broadly classified into the following two groups:

- (a) energy approach, and

(b) force approach.

The energy approach is usually adopted for rock/boulder fences which are customarily designed as sacrificial structures undergoing deformation upon impact. The kinetic energy of the rock/boulder is equated to the work done to deform some of the structural components of the fence. Generally, the maximum energy-absorbing capacity of the system is designed to be mobilised assuming that the fence undergoes permanent deformation rather than elastic deformation; otherwise, very massive structural members will be needed (Chan et al, 1986). Given the energy of the rock/boulder just prior to impact, sizing of the various components of the fence can be done in accordance with structural engineering principles. Proprietary fences are also available to meet different energy-absorbing requirements.

The force approach tends to be adopted in the design of barriers which act as permanent structures, particularly where a structural wall or a mass barrier has been used. Two methods have been used to estimate the impact force: one assumes that the entire debris mass will move with the barrier as a unit upon impact and the unit will then decelerate at a rate controlled by the sliding resistance at the base of the barrier. The other involves the determination of the rate of change of momentum of the debris upon impacting the barrier. The former method, which assumes that the entire debris mass contributes towards the impact momentum, may not adequately model the impact process of a deformable body. It also requires an assumption on the proportion of the wall section that would move with the debris. In the latter approach, the impact duration has sometimes been arbitrarily defined. Alternatively, the impact force has been estimated based on the rate of debris losing momentum upon impact on the barrier. This method, which seems to be the practice favoured in a number of countries, will be further examined in this study.

Wong (1995) used the analogy of a prismatic bar undergoing lateral vibration and made some simplifying assumptions to model the dynamic effect of a reinforced concrete L- or T-shaped retaining wall impacted by debris. In this approach, the debris mass and the barrier are assumed to move together as an integral unit upon impact at a velocity determined using the principle of conservation of momentum. Upon impact by the debris, Wong (op cit) assumed that the barrier would undergo flexural vibration with a peak particle velocity equal to the translational velocity of the barrier and debris mass. Using vibration theory, the bending stresses corresponding to the state of peak particle velocity within the barrier were estimated. The energy-absorbing capacity of the barrier was derived assuming that the entire barrier was strained to the same level simultaneously.

It is worth noting that the translational velocity refers to the global velocity of the whole wall while the peak particle velocity is the transient velocity at a particular point of the wall stem when the wall stem is set to flexural vibration upon debris impact. At any given time, different parts of the wall stem will vibrate at different particle velocities which may also be in different directions at a particular time. Therefore, the translational velocity of the entire barrier and the peak particle velocity would bear no relationship with each other. The flexural strain in the barrier would vary along the barrier and is likely to be at its maximum at the base of the stem. Therefore, the assumption that the entire barrier (both the stem and the base) is strained simultaneously to the maximum would likely lead to an overestimate of the energy-absorbing capacity of the barrier.

3.3 Debris Mobility

Both the energy and the force approaches require information on debris impact velocity. In the cases examined, the velocity of rocks/boulders were assessed by various means, e.g. computer simulation (Threadgold & McNicholls, 1984; Chan et al, 1986; Tse et al, 1999), laboratory model tests wherein blocks were rolled down an inclined surface (Chan et al, 1986; Chau et al, 1998), and field trials wherein boulders were rolled down actual rock slopes (Chan et al, 1986; Mak & Bloomfield, 1986).

In the determination of the velocity of landslide debris, it was commonly assumed that the landslide mass was a rigid body undergoing translational movement. The velocity was generally estimated from the change in the position of the centre of gravity of the landslide mass before failure and when the debris had piled up against the barrier with due consideration of the sliding resistance at the base of the mass. The sliding resistance at the base of the debris mass was assumed to be frictional with the angle of friction commonly taken to be equal to the effective angle of shearing resistance of the landslide material prior to failure. No account was taken of the pore water pressure within the landslide debris. Therefore, the retardation effect of the base friction might have been overestimated leading to an underestimation of the debris impact velocity.

Recently, more rigorous methods involving the use of continuum models have been used to estimate the velocity profile and the likely thickness of debris along its path. Further details on the continuum models will be given in Section 4.4.2.

4. DESIGN METHODOLOGIES

4.1 General

The design of a barrier is intrinsically related to the assessment of the landslide hazards and is best tackled in an integrated manner. The key components of the overall design problem are described below:

- (a) Characterisation of landslide hazards - In characterising the landslide hazards, it is necessary to make reference to the types of landslide, scales and mechanisms of failure, and the mechanisms of debris movement (see below). The types of landslide and the scales and mechanisms of failure will, in general, depend on the geology, hydrogeology, geomorphology, characteristics of vegetative cover and basin terrain characteristics which control surface water flow. Different landslide hazards will have a different frequency (or likelihood) of occurrence and may be affected by different factors to a differing extent, and the corresponding debris may have different mobility. The behaviour will also be dependent on the types of triggering factors and their characteristics, e.g. long-duration rainfall versus short-duration rainfall.
- (b) Characterisation of debris movement - Unlike a man-made

slope failure, the location of a natural terrain failure may be at quite a large distance away from the affected facility. It is particularly important to consider debris mobility and the trajectory and characteristics of the debris path because these will dictate whether the debris will reach the facility, and if so, at what velocity. The depth of the debris will also be important and this is generally a function of the scale of failure, degree of entrainment along the downhill path, degree of spreading of the debris, etc. The characteristics of the debris, e.g. solids concentration and water content, will also be relevant as this can significantly influence the impact loads on a barrier.

- (c) Characterisation of the design events - Items (a) and (b) above taken together would provide the necessary information for the design events to be evaluated. The synthesis of realistic frequency-magnitude curves for the natural hillside landslide hazards threatening a given facility is an important starting point for evaluating the appropriate design events, the selection of which will also depend on the design life adopted for the barrier.
- (d) Dynamic interaction upon debris impact at barrier - Given the debris characteristics, the dynamic interaction upon impact which will be a function of the type of barrier, the foundation condition, etc, will need to be considered. For the barrier to be effective in trapping the debris, the debris movement is expected to be arrested upon impact. The capacity of the barrier and its ability to withstand the kinetic energy or impact force of the debris needs to be assessed.

4.2 Characterisation of Landslide Hazards

This involves the compilation of an inventory of different types of natural terrain landslide hazards identifiable from the aerial photograph interpretation, published information and site reconnaissance. Aerial photograph interpretation allows the identification of previous landslide activities and mapping of their locations, and assessment of the extent and nature of the landslides. Dating of landslides from aerial photograph interpretation is possible although this is constrained by the interval between sequential photographs.

The primary objective of site reconnaissance is to check the recognition and classification of landslide hazards derived using API. It allows the assessment of the geometry of the landslide scar for initial failure volume estimation, and the examination of the movement mechanism of the debris and the characteristics of the path for total debris volume estimation. It also helps to identify some of the small landslides that are not easily discernible from API.

Other useful sources of information include, inter alia, topographic maps, GASP

reports, the Natural Terrain Landslide Inventory (Evans et al, 1997) and landslide study reports (e.g. Wong et al, 1998, Franks, 1998).

4.3 Characterisation of Design Events

4.3.1 General

The determination of the design event landslide debris volume is generally based on the knowledge of the previous landslide activity in the area with reference to the life of the design structure. Information regarding previous landslide activity, viz. the types of landslide, scale and time of failure, is commonly obtained from the interpretation of aerial photographs, site reconnaissance and previous landslide investigation reports.

In principle, standard techniques of frequency analysis using extreme value theory may be applied to the landslide data to determine the recurrence intervals of landslide events of different magnitudes. In practice, the design event assessment is generally fraught with difficulties in that there is rarely sufficient information to establish the site-specific frequency-magnitude curves from past events using conventional techniques. For example, the aerial photographs, a prominent source of previous landslide data, are only available for the past fifty years. The statistics of small samples is intrinsically imprecise. The applicability of standard techniques of frequency analysis using extreme value theory, as commonly used in flood frequency analysis, can be questionable given typically incomplete data that are sometimes also of insufficient quality.

Morgan et al (1992) discussed the practical problems faced and suggested an alternative approach assuming that the individual events are statistically independent and that the number of occurrences of debris flow events exceeding a certain magnitude over the sampling period follows a binomial distribution. The proposed approach also allows room for judgement concerning non-typical conditions during the period of record or missing data and its application was illustrated using real examples in Canada.

4.3.2 Methods for Estimating Debris Flow Volumes

In Japan and China, the frequency of occurrence and the volume of a debris flow event are assumed to be related to the return period of a rainstorm and the amount of precipitation that falls within the catchment of a particular streamcourse. The total volume of a debris flow event is estimated by scaling the total runoff of rain within the catchment of the relevant streamcourse by the inverse of the porosity of the debris mass (Du et al, 1987; Public Works Research Institute (PWRI), 1988). Kang (1999) reported that this approach is primarily for high frequency events. In a recent study, Sawada et al (1999) correlated the total sediment discharge with the 10-min rainfall immediately preceding failure based on observations made in Jiangjia Ravine, in Yunnan, China.

VanDine (1985) carried out a review of different methods used in Austria, Canada and Japan for estimating the design magnitude of channelised debris flows. Most of these methods involved detailed inspection of each streamcourse upstream of the debris fan, collection of information on, inter alia, channel gradient and geometry, and nature and gradation of material on the sideslopes and within the channel, and assessment of the potential

scour depth of the streambed and of the stability of the banks. These methods can be broadly classified into two groups: area yield rate approach and channel yield rate approach.

Hungr et al (1984) and VanDine (1996) attempted to correlate the size of catchment area for streams with the magnitude of some previous debris flow events in a specific region. The ratio of the volume of debris flow to the catchment area is referred to as the area yield rate. It was assumed that the area yield rates would be similar for catchment areas of similar topography, geology, and climatic and hydrologic conditions. Figure 6 shows the area yield rates reported by Hungr et al (1984) and VanDine (1996) for a number of debris flow events in Canada. Although these values were derived from a very small region in British Columbia, they varied over a very wide range ($330 \text{ m}^3/\text{km}^2$ to $26\,200 \text{ m}^3/\text{km}^2$), with the maximum value about two orders of magnitude larger than the minimum value.

For channelised debris flows, the entrainment along their path could add considerably to the total volume of debris, e.g. the entrainment in the Tsing Shan debris flow of 1990 amounted to about 90% of the total debris volume. Hungr et al (1984) attempted to correlate the debris volume with the length of the channel (including any tributaries) upstream of the deposition area to the source area. The ratio of the debris volume to the length of channel is termed channel debris yield rate. This ranges from about $5.5 \text{ m}^3/\text{m}$ to $18.4 \text{ m}^3/\text{m}$ for five channelised debris flow events in British Columbia, with the mean channel bed gradient varying between 23° and 26° and catchment areas of less than 3 km^2 . The variation in the channel debris yield rate of these events is primarily due to differences in terms of channel erodibility. Hungr et al (1984) developed a simple classification system for stream channels, shown in Table 3, in terms of channel gradient, type of channel bed material, material type and height of side slopes, and the general stability of the channel, together with the tentative estimate of the channel debris yield rate. It is of interest to note that the channel debris yield rate observed in some natural terrain landslides on Lantau Island was estimated to be about $2.3 \text{ m}^3/\text{m}$ to $3.7 \text{ m}^3/\text{m}$ (Franks, 1998) but this could be up to about $24 \text{ m}^3/\text{m}$ as in the Tsing Shan debris flow event.

To estimate the design volume using the channel yield rate approach and Hungr et al's classification system in Table 3, one needs to sum the combined lengths of channel susceptible to erosion in each category downstream of an estimated point of landslide initiation, multiplied by the respective yield rate. Contributions from point sources of debris, e.g. individual landslides on side slopes, although difficult to identify, should be included in the total debris volume by adopting a conservatively selected yield rate. Hungr et al (1984) suggested the point of landslide initiation be taken as the highest point of any suspected branch. All major branches should be assumed to be active simultaneously. The channel yield rates given in Table 3 are applicable to catchments less than 3 km^2 in size.

A refinement to the channel yield rate approach was attempted by Hungr et al (1984) to account for the width of the channel and for application to channels with catchment areas exceeding 3 km^2 . Their approach involved dividing the channel into a number of segments. The average width of a particular section of the channel is assumed to be empirically related to the square root of the catchment area draining to that channel section. The debris volume, V_D is estimated as follows:

$$V_D = \sum_1^n A_i \frac{1}{2} \Delta L_i e_i \dots\dots\dots (1)$$

where A_i = catchment area draining to a particular channel segment
 ΔL_i = length of that channel segment
 e_i = erodibility coefficient of that channel segment

Table 3 shows the erodibility coefficients suggested by Hungr et al (1984). Although this approach was claimed to be able to allow interpolation of different catchment areas with similar erodibility characteristics and was applicable to catchment areas exceeding 3 km², the erodibility coefficients in Table 3 appear to have been derived from debris flow events with catchment areas of less than 3 km².

The applicability of the area debris yield approach and the channel debris yield approach to a particular region critically depends on the availability of a considerable number of past events in the region for deriving the relevant coefficients. Otherwise, their use could be limited. Hungr et al (1984) suggested that the area yield approach may be useful for estimating the debris volume for catchment areas that have been burnt by forest fire. The yield rates and erodibility coefficients given in Table 3 were derived from a small region and it should be cautioned that these values may not be applicable to other regions as they incorporate the effects of, inter alia, climate, geology and channel characteristics.

The channel yield rate can also be estimated based on detailed inspection of the channel by assessing the volume of loose erodible material accumulated in the channel that could be mobilised in the event of a debris flow (Hungr et al, 1984; VanDine, 1985; PWRI, 1988). This method is a viable alternative especially when data on past events are scarce. It can take account of the characteristics of the specific channel and can provide fairly reliable estimate of debris volume for channels cutting into bedrock. However, the assessment of the potential erosion depth could become difficult for channels with thick accumulation. This method has been applied to estimate the design debris volume for the mitigation works for 24 streams in British Columbia (VanDine, 1985 & 1996). These design debris volumes when plotted against the corresponding catchment areas as shown in Figure 6 appear to correspond to an area yield rate of about 10 000 m³/km². This may suggest that the volume of erodible material accumulated in the channel could be related to the catchment size which may be an indirect measure of runoff.

Figure 6 shows the data corresponding to the 1990 Tsing Shan debris flow (King, 1996). The catchment area of this event is considerably less than those reported by Hungr et al (1984) and VanDine (1996). It can be seen that area debris yield rate for the Tsing Shan debris flow is approximately 166 000 m³/km², which is about an order of magnitude greater than those recorded in Canada. It seems that the debris in the debris flow events in British Columbia reported by Hungr et al (1984) and VanDine (1985) was derived primarily from material deposited within the channel and the effect of the source volume on subsequent erosion volume could be relatively insignificant. However, the initial landslide volume at the headscarp in the Tsing Shan debris flow might have had an influence on the subsequent erosion of material along its path.

4.3.3 Peak Discharge of Debris Flows

In addition to knowledge of the scale of failure, the peak debris flow discharge (or peak flux) is also an important consideration in the design of mitigation measures as it reflects the amount and speed of debris impacting onto the barrier.

Hungr et al (1984) based on field measurements and model tests formulated an empirical correlation between peak discharge and the corresponding total debris volume as shown in Figure 7. Also shown in the figure is the correlation reported by PWRI (1988). Based on field measurements and laboratory flume tests, Mizuyama et al (1992) put forward different empirical correlations for 'stony' debris flows and those with high fines contents. Figure 7 shows that these correlations agree quite closely with those proposed by Hungr et al (1984) and PWRI (1988). This may suggest that the correlations put forward by Hungr et al and PWRI may have been derived from different types of debris flow events.

Alternatively, the peak discharge of debris flow, q_d , can be estimated from the peak discharge of rainwater q_w . PWRI (1988) reported that observations at Mt Yakedake, Japan showed that the ratio of q_d to q_w was in the range of 1 to 20. Similar measurements at Jiangjia Ravine showed that the ratio varied from 8 to as much as 43 (Du et al, 1987). A number of empirical correlations were established for the estimation of q_d based on q_w . Some of these are shown in Table 4. The results generated by these correlations are quite varied, reflecting the very many variables that could affect the peak discharge and the wide range of types of debris flow. Caution should be exercised in applying these correlations which were derived from local observations.

The peak discharge has also been estimated assuming debris building up behind a temporary dam at a location in the channel, which subsequently fails and produces a wave of debris (Hungr et al, 1984; Frenette et al, 1997)

4.3.4 Discussion

The extrapolation of past failures to predict future occurrence implicitly assumes the landsliding activities and settings at the concerned site will remain unchanged. This approach may be applicable if this implicit assumption is met and there is plentiful historical data. The debris flow history of the Val Varuna Catchment in Switzerland (Davies, 1993) shown in Figure 8 may illustrate the potential limitation of predicting debris volume based on historical records. Between 1772 and 1889, a number of debris flow events with debris volume ranging from about 12 000 m³ to 51 000 m³ occurred in Val Varuna Catchment over this period of about 110 years. At the end of the 19th century, 28 check dams were constructed over some parts of the channel at locations where it was considered to be most susceptible to erosion. This was followed by a relatively inactive period until 1987 when a debris flow event about one order of magnitude larger than the biggest event observed in the past 200 years occurred and destroyed the check dams. The rainfall intensity in the 1987 event was comparable to that in 1834. This case history serves as a reminder of the potential of underestimating the design event from historical data and the disastrous consequences. It also points to the importance of the potential effects of the environmental changes brought about by the presence of the check dams on the magnitude of failure. Ho & Wong (1999) also pointed out the importance of studying the landslide history and characteristics of an area

in an integrated manner, e.g. the occurrence of high frequency low magnitude failures may be precursor of a large-scale failure.

An impediment to improved barrier design is the difficulty in assessing the magnitude, composition and probability of occurrence of the different types of natural terrain landslides (including debris flows) for a given catchment and the assessment of the design event impacting the barrier. The formulation of the various components of the design problem in a rigorous probabilistic framework is described by Roberds & Ho (1997) but the practicality of applying such tools to real natural terrain landsliding problems has yet to be demonstrated. In practice, it is likely that a pragmatic approach, based on a comprehensive landslide database, proper classification of landslides and improved understanding of landslide triggering mechanisms and debris movement mechanics, coupled with sound judgement, is needed. Extreme caution should however be exercised in relying on, or extrapolating from, empirical data on the behaviour of natural terrain landsliding in a setting different from that at the site concerned.

4.4 Characterisation of Debris Movement

4.4.1 General

The travel distance of landslide debris is an important factor to be considered as part of the assessment of consequence or damage. The importance of having to consider the travel distance of debris is becoming recognised in recent years (e.g. Wong & Ho, 1996; Corominas, 1996).

With regard to local data on natural terrain landslides, data on the debris mobility observed during a severe rainstorm in 1993 have been reported by Wong et al (1998). The key findings of this study are summarised below:

- (a) Classification of landslide and debris movement mechanisms (e.g. planar failure versus channelised flow, effect of surface water, etc) is important.
- (b) The travel distance of landslide debris appears to be principally a function of the failure mechanisms, properties of the material that control the failure and whether channelisation and significant entrainment of debris can occur.
- (c) Debris runout appears to be affected by the scale of the failure which could affect the mechanisms of debris movement.
- (d) The apparent (or kinematic) angle of friction between the debris and the underlying material can be much lower than the angle of shearing resistance of the slope-forming materials.

Different methods may be adopted for assessing the travel angle of landslide debris

(e.g. Lau & Woods, 1997). A pragmatic approach advocated by Wong & Ho (1996) is by means of empirical observations based on good quality data and a rational classification of the landslide/debris movement mechanisms with allowance made for possible increase in debris mobility with landslide volume.

The travel angle of the debris, as defined by Cruden & Varnes (1996), is measured from the crest of the scarp to the distal end of the debris (Figure 9) and this concept is simple and appropriate in risk assessments in that it reflects directly the debris influence zone. It also resembles closely the rate of energy loss during debris movement and incorporates the effect of downslope gradient.

In the case of man-made slopes where the downslope gradient is usually fairly flat and the length of the downslope path is not significant, the travel angle concept generally provides a reasonable resolution in predicting the debris travel distance and thus can be adopted in consequence assessments. Natural terrain landslides, however, are somewhat different in that they usually involve a comparatively steep downslope profile and the use of the travel angle alone in consequence assessments may not be sufficient. This is due to the comparatively poor resolution in predicting debris travel distance because of the relatively small difference between the downslope angle and the travel angle. One possible improvement is to relate the travel angle for the different mechanisms and scale of failure to an upper bound travel distance of debris.

The growing popularity in the use of multi-variant regression analyses for establishing the correlation between debris mobility and other terrain parameters deserves some cautionary remarks. In principle, there is a potential danger that such statistical methods, when used in a 'black-box' manner with inadequate consideration of the mechanics of the physical processes involved coupled with the use of limited input/calibration data that may be of questionable reliability, are liable to result in very coarse and even misleading regression correlations. Such derived correlations are prone to errors (e.g. apparent statistical correlations that are contrary to accepted physical phenomena) and could be of doubtful validity, particularly when used as a predictive tool or for extrapolation. The numerical complexity and apparent statistical fit may in fact provide a false sense of accuracy.

4.4.2 Methods for Estimating Debris Velocity and Runout

The empirical debris runout data from the field will not, by themselves, provide any information on debris velocity which is an essential parameter for barrier design. The methods for the estimation of the motion of landslide debris can be broadly classified into three categories:

- (a) sled (lumped-mass) model,
- (b) flow equations and routing programs, and
- (c) numerical methods (e.g. continuum and distinct element method).

- (1) Sled Model. The sled model is based on the consideration of the landslide

motion at a single point (i.e. the centre of gravity of the landslide mass). In the sled model, all the energy loss during debris movement is assumed to be due to friction. The line joining the centres of gravity of the sliding mass before and after failure is referred to as the energy line, which denotes the total energy (viz. potential energy + kinetic energy) per unit weight of landslide debris (Sassa, 1988). The kinetic energy of the debris during its downslope motion is given by the vertical distance between the centre of gravity and the energy line (see Figure 9) and hence debris velocity at various points can be computed. The angle between the energy line and the horizontal is denoted as the apparent angle of friction, ϕ_a , which can be related to the angle of shearing resistance of the debris in terms of effective stress, ϕ' , as follows:

$$\tan \phi_a = \left(\frac{\sigma - u}{\sigma} \right) \tan \phi' = (1 - r_u) \tan \phi' \dots\dots\dots (2)$$

where σ = total stress
 u = pore water pressure
 r_u = pore water pressure ratio

Hungr (1998) back analysed a number of significant landslides in Hong Kong using a computer model DAN (see following Section) and found that the mean r_u values along the debris trails for these landslides range from 0.3 to 0.4, assuming a friction model for debris travel.

Sassa (1988) advocates the use of high-speed ring shear test to obtain information on the pore water pressure generated during motion for the assessment of ϕ_a .

(2) Flow Equations/Routing Programs. Morgenstern (1978) opined that in the mitigation of mobile soil and rock flows, "the motion of mobile flows and the design of protective structures should proceed using the principles of fluid mechanics rather than the more common consideration of shearing resistance in soils and rocks". In most flow models which have been developed for the estimation of debris velocity, the water-solids mixture of a debris flow is often assumed to be a single component fluid with particular rheological characteristics. Some of the commonly used rheological models are listed in Table 5. In general, the flow models are in the form of:

$$v = \text{constant} * h^a * S^b \dots\dots\dots (3)$$

where v = debris flow velocity
 h = flow depth
 S = channel bed gradient
 a & b = exponents depending on the assumption on the characteristics of the flow regime

Based on the relationship between unit discharge (i.e. discharge per unit width) and debris thickness for a number of debris flow events in British Columbia, Hungr et al (1984) suggested that the flow regime near the peak of a debris flow surge would be laminar. They found that the Newtonian laminar flow model with a viscosity of 3 kPa.s can produce flow depth - unit discharge trends very similar to those observed in selected 'debris torrent' events

in both Canada and Japan (Figure 10).

Similar good agreement was achieved with the dilatant flow model with the parameter ξ having a value of $2.17 \text{ m}^{-1/2}\text{sec}^{-1}$ (Hung et al, 1984). The dilatant flow model is for non-plastic grain-fluid dispersion and the value of ξ depends on the size and volume concentration of solid particles in the debris. Takahashi (1991) opined that the dilatant flow model is appropriate for the stony debris flows in Japan in which the effect of inter-particle collisions dominate. According to Hung et al (op cit), the Newtonian laminar flow model had been used for the prediction of debris velocity in the design of stream channels and barrier spillway in Canada, but they added that the dilatant flow model could also be used in principle.

The Newtonian laminar flow model can be extended to a Bingham model by replacing the dynamic viscosity with Bingham viscosity together with two other material constants. According to Chen (1986), the modelling of hyperconcentrated flows and mudflows with a relatively large amount of very fine sediment particles has been conducted using the Bingham model.

Hung et al (op cit) considered that the velocity formulae for turbulent flow might not be appropriate for debris flow velocity calculations. They reported that these formulae tended to overestimate the unit discharge at flow depth of less than 4 m with a Manning's roughness coefficient of 0.09. However, PWRI (1988) suggested to use Manning's equation for the determination of debris flow velocity and recommended that for debris flow in a natural river channel, the Manning's roughness coefficient should be taken as 0.1 for the first pulse and 0.06 for the subsequent pulses. For debris flow in a concrete channel, a Manning's roughness coefficient of 0.03 can be used. Zhang (1993) suggested that for intermittent debris flows the Manning's roughness coefficient could be reduced by half for subsequent pulses. Du et al (1987) reported that field measurements made in debris flow events in Yunnan, China between 1966 and 1975 had been used to back calculate the Manning's roughness coefficients. The results showed that the Manning's roughness coefficient was dependent on the flow depth in that it decreases with an increase in flow depth (Table 5).

Du et al (1987) and Wu et al (1993) reported that empirical correlations had been established for debris flows observed in different regions in China with different solids concentrations. One of these empirical correlations, developed based on field measurements in Yunnan, China, is also included in Table 5. The wide range of coefficients that have been derived for these empirical correlations reflect the varied mobility characteristics of debris flows.

Figure 10 shows the flow depth-unit discharge trends predicted by various flow formulae listed in Table 5 for channel bed angles of 10° and 22° . The two formulae derived from field measurements in China give higher values of unit discharge at flow depths of less than 4 m when compared with the field data reported by Hung et al (1984). The discrepancy could be due to the variable nature as well as the types of debris flows from which these empirical correlations were derived. For example, Takahashi (1991) and Kang (1999) pointed out that the debris flows observed in Japan and those in Jiangjia Ravine in Yunnan, China differ in the fines content and the suspended solids concentrations in the slurry which may have attributed to the different flow characteristics.

The use of average flow depth to approximate the hydraulic radius in these flow equations may not have adequately reflected the effects of channel geometry and may introduce varying degrees of inaccuracy depending on the actual channel geometry. For example, the debris flows in Jiangjia Ravine in China are in broad ravines on shallow angles whereas those in New Zealand are in narrow channels over steeper slopes. The use of average flow depth may be a reasonable approximation in the former case but may not be appropriate in the latter case.

It should be cautioned that the definition of phenomena such as debris flow and debris flood may not be consistent in the literature and that different terminologies may well have been used. The direct extrapolation of the parameters derived empirically from other places should therefore be treated with extreme caution. The various classification systems that have been developed to categorise debris flow events reflect the variable nature of debris flows. These classification systems have been based on, *inter alia*, topographic characteristics of the catchment, scale of failure, triggers, origins of the debris, frequency of occurrence, depending on the application of such systems (Kang et al, 1999). Those that are commonly adopted for engineering applications are generally in terms of unit weight of debris, solids concentration, sand content, and structure of the debris (Du et al, 1987; Kang et al, 1999; Pierson & Costa, 1987; Wu et al, 1993; Zhou et al, 1991). The use of these classification schemes is hampered by the lack of consensus regarding the boundaries between various types of debris flows and the terminology used. One of these classification schemes is shown in Figure 11.

Rickenmann & Koch (1997) developed a one-dimensional continuum model to simulate the motion characteristics of debris flows. Their model, which can accommodate various rheological flow models, was applied to simulate two debris flow events. The results of the simulation together with the field measurements for a debris flow event in Kamikamihori Valley, Japan are reproduced in Figure 12. It can be seen that almost all the models have predicted velocities that are within the measurements along some parts of the debris path. However, the velocities predicted using the Newtonian turbulent model and the Voellmy model seem to be in better agreement with the field measurements than those predicted by other flow models. This points to the importance that apparent fit between the prediction by some models and the measurements observed along certain stretches of the flow path could not ensure the appropriateness of the models. Rickenmann & Koch (*op cit*) noted that for the two cases examined, the models that have smaller exponents, namely a and b in Eq. (3) yield velocities that are in closer agreement with the measured values; those models with larger exponents tend to be very sensitive to the initial conditions. Koch (1998) noted that flow models with smaller exponents, e.g. Newtonian turbulent model, Voellmy model, seem to be more appropriate for simulations of debris flow on steep slopes or slopes with gradients over a wide range. For less steep slopes or slopes with gradients within a narrow range, the differences between the values derived from various flow models are small.

The various coefficients for the individual formulations given in Table 5 are not intrinsic material properties of the debris, but rather empirical constants that have been found to give results which could match reasonably well with the field observations. These coefficients are functions of, *inter alia*, the solids concentration, particle size, and channel characteristics and model assumptions. There is a need to systematically characterise and categorise debris flows to facilitate consolidation of experience and observations made elsewhere. This will allow a more systematic evaluation of different formulations for the

prediction of debris velocity.

The use of the equations developed requires knowledge of the flow depth. This involves the estimation of the peak discharge corresponding to the design event and subsequently the determination of the flow depth required to accommodate the peak discharge given the channel geometry.

More recently, flood routing models have been developed to assess the flood and debris flow hazards. For example, FLO-2D (Julien & O'Brien, 1997) is one such hydraulic routing program which simulates the progression of a flood hydrograph, generating information on flow velocity and flow depth along the path. It is reported that the rheological model adopted for sediment flow can account for the effect of the shearing resistance of the sediment particles, the fluid-particle viscosity and the collision of sediment clasts. The program has been used to model flow behaviour ranging from mud floods to debris flows. In practice, it is essential that such programs are properly calibrated against well-documented case histories before they are considered for predictive purposes.

(3) Simplified Continuum Models. Simplified continuum models are based on the principles of conservation of mass, momentum and energy to describe the dynamic motion of landslide debris and incorporate a rheological model to represent the flow behaviour of the debris. The DAN model, developed by Hungr (1995), is an example. It simulates the motion of landslide debris with the use of a finite difference solution of the governing dynamic equations in a Lagrangian framework. The solution is obtained in time steps for a block assembly of elements, representing the landslide debris as a continuum. Various material rheological models may be used. Some of the rheological models are summarised in Table 6. The effect of lateral confinement and mass changes (i.e. erosion and deposition along the runout path) can also be approximately allowed for. This model is capable of determining the velocity at different times for a given landslide event and can also be used to predict the debris thickness, provided that the width along the flow path is given.

Hungr & Evans (1996) and Hungr et al (1997) reported the use of DAN to back-analyse some twenty rock avalanches and coal mine waste flow slides, and summarised the material properties that were found to give a good match with observation. They found that the Voellmy model together with the combination of an apparent friction angle, $\phi_a = 11^\circ$ and a turbulence coefficient, $\zeta = 500 \text{ m/s}^2$ generally give velocity and runout prediction that are in better agreement with the observed data than those predicted using the friction model or the Bingham model.

The DAN model has been used to back analyse a number of landslides in Hong Kong, including some twenty natural terrain landslides (Hungr, 1998, Ayotte & Hungr, 1998; Hungr et al, 1999) with debris volumes ranging from about 50 m^3 to about $26\,000 \text{ m}^3$. The analysis of each landslide involved digitising the pre-failure ground surface profile at the centre-line of the path traversed by landslide debris and compiling the lateral spread of debris along its path. The material rheologies and relevant material coefficients were determined by trial and error tempered with engineering judgement to match the observed distribution of debris as far as possible. Hungr (1998) and Ayotte & Hungr (1998) made the following observations from the analyses:

- (a) The friction model predicts high velocities with the

deposition area tending to be relative short. The predicted distribution of landslide debris tends to be thicker at the location where deposition begins and gradually thinning out towards the distal end. The friction model is capable of simulating the debris mobility in most cases particularly when the debris mass is not completely saturated.

- (b) The Voellmy model predicts comparatively lower debris velocities and more uniform distribution of debris over the deposition area. As the friction coefficient increases, the difference between the Voellmy model and the friction model decreases. This model predicts a more realistic distribution of the landslide debris and velocities for landslides involving a significant proportion of water.
- (c) The Bingham model predicts very high debris velocity with debris spreading thinly over the entire length of the path. This model is more appropriate for clay rich debris and was found not suitable for the cases that have been analysed.

In general, either the friction model or the Voellmy model was used to simulate the entire motion of most landslide events. However, for incidents in which an open hillside failure subsequently became channelised, e.g. debris entering a stream channel, the friction model was used to simulate the debris movement from the source area to the stream channel, beyond which, the Voellmy model was used. In some instances, the distribution of debris and its mobility could be matched with the observations only through the use of a lower ϕ_a at the source area than along the debris trail. Ayotte & Hungr (1998) attributed this partly to the presence of a 'topographic lip' at the base of the source area and partly to the probable presence of weak planes at the source area.

The velocities back-calculated from super-elevation data allow further examination of the appropriateness of DAN in simulating debris mobility. The computed debris velocity for the Tsing Shan debris flow at Chainage 350 and Chainage 475 is 21 m/s and 25 m/s respectively using the friction model. The respective values computed using the Voellmy model are 18 m/s and 17 m/s. These values compare quite favourably with the back-calculated values from super-elevation data, viz. about 16 m/s to 18 m/s at Chainage 350 and between 11 m/s and 15 m/s at Chainage 475.

Based on these analyses, Hungr (1998) and Ayotte & Hungr (1998) concluded that the friction model could in most cases adequately model open hillside failures. The apparent friction angle, ϕ_a , could be empirically correlated to the debris volume at the source area as shown in Figure 13. The Voellmy model was more appropriate for channelised debris flow type failures and the combination of an apparent friction angle, $\phi_a = 11^\circ$ and a turbulence coefficient, $\zeta = 500 \text{ m/s}^2$ could generally give reasonable estimate of the debris mobility.

Chen & Lee (1998) developed a three-dimensional dynamic model simulating the debris movement in the longitudinal direction and the lateral spread in the transverse section. Unlike the DAN model which requires data on the lateral spread of debris as input, this model computes the lateral spread of debris. The model was applied to back-analyse the Shum

Wan Road landslide and reasonably good agreement was obtained between the predicted and observed distribution of debris deposit. The computed results derived using this model are quite similar to those using DAN. The maximum debris velocity predicted by this model was about 14.4 m/s, cf. 17.2 m/s from DAN. However, it seems that the predicted distribution of debris using the 3-D model was closer to the field observation.

Other simulation programs such as FLAC (Itasca Consulting Group, 1995) can also be used to estimate the runout of debris (Sun, 1998). The tools described above have so far been used to back-analyse the motion characteristics of some landslide events. In order to turn them into a predictive tool, there is a need to classify the natural terrain landslides into groups, assess which models will best simulate their characteristics, and to establish an appropriate range of values of parameters for use with the models.

4.4.3 Runout Distance

As discussed previously, empirical data on debris travel interpreted in a judicious manner may be used to predict the likely range of debris runout. Other methods that can be applied in assessing the runout distance are discussed by Lau & Woods (1997).

Hungr et al (1987) suggested a simplified approach to obtain a rough estimate of debris runout distance. This approach involves estimating the volume of the debris and assuming an average thickness of the deposit. The deposit is then distributed over an area downstream of the point of deposition taking due account of the topography. It is suggested that in the absence of adequate topographic mapping, a spread at a ratio of 1 (plan width) to 2 (plan length) can be assumed. The distal limit of the deposition area delineates the end of runout. Based on their experience, Hungr et al (1987) suggested that the mean deposit thickness would be about 1 m to 1.5 m for debris ranging from 10 000 to 50 000 m³ in volume. Correlations between volume and plan dimensions of debris flows have also been developed (e.g. Innes, 1983).

The runout distance, x_L , beyond the initial point of deposition can be estimated based on consideration of retardation caused by the sliding resistance at the base of the debris mass as in the 'sled' model. The formulae for the determination of the runout distance as well as the debris velocity at any distance from the initial point of deposition is given in Table 7.

Hungr et al (1984) adapted the work of Takahashi & Yoshida (1979) and developed an approach for the estimation of runout distance using the leading edge model, which was based on the principles of conservation of momentum and continuity of flow for a fluid medium. The formulae for the determination of the runout distance, x_L , beyond the initial point of deposition for a steadily moving debris front travelling over a surface with a constant low inclination, after leaving a steeply sloping channel, are given in Table 7. The solution given in Hungr et al's 1984 paper is in terms of the effective normal stresses and the effective angle of dynamic friction of the debris. Hungr & McClung (1987) presented a similar solution in terms of total stress and apparent angle of friction. Hungr et al (1984) reported that the runout distance predicted by this model compared favourably with the observed values. It was noted that the equation given in Hungr et al's paper for the determination of debris velocity at different runout distances was incorrect. The correct solution is given in Table 7.

Van Gassen & Cruden (1989) and Fang & Zhang (1988) suggested that the concept of momentum transfer could help explain the mobility of some rock avalanches. They postulated that within a rock avalanche there was redistribution and transfer of kinetic energy among the rock fragments through collisions. As a result, fragments that have surrendered their energy will come to rest and deposited along the debris trail while fragments that achieve a gain in energy will be propelled further down the trail. Incorporating the concept of momentum transfer in the friction (sled) model, they found that the travel distance for a slide which reduces its mass linearly was 1.5 times that predicted assuming constant mass using the sled model. For a slide with its mass varying exponentially with the distance from the initial point of deposition, the estimated runout distance will be twice that predicted assuming constant mass. Van Gassen & Cruden (1989) found that their model could adequately explain the mobility of large volume rock avalanches without resorting to the assumption of very low apparent friction angles for the rock fragments.

Dawson et al (1992) incorporated Van Gassen & Cruden's momentum transfer mechanism in the sled model to predict runout. Their approach involves the determination of the debris velocity when the centre of gravity of the debris mass is at the initial point of deposition. This velocity is then used as the entry velocity in Van Gassen & Cruden's equation for runout prediction.

In practice, it can be very difficult to determine the point of deposition as this can be a function of the nature of debris, the mechanism of debris movement, the energy of the debris and the characteristics of the debris path. It is worth noting that the 'frictional parameter' in each model could well be very different in magnitude. There has been very little discussion on the range and choice of the frictional parameters in each model, and further validation of these models is warranted.

4.4.4 Vertical Runup Distance

The vertical runup height could be estimated using the sled model whereby the kinetic energy of the debris is assumed to be expended in work done against friction and gain in potential energy (see Table 8). This approach assumes that the runup height is independent of the transition geometry due to changes in slope gradient and flow depth of debris.

Perla et al (1980) introduced a correction to account for changes in slope gradient. They suggested that the initial velocity, v_0 be replaced by its component parallel to the runup plane, i.e. $v_0 \cos(\theta_0 + \theta)$ to account for momentum loss in the estimation of runup as shown in Table 8. θ_0 and θ are the slope angle before the slope transition and the inclination of the runup plane respectively (see Figure 14).

The above two approaches are based on the premise that the debris behaves as a point mass and the entire mass will be raised simultaneously on the runup slope. However, in the field, the front of the debris will move up the barrier with momentum constantly fed by the oncoming materials, i.e. only the front instead of the entire mass will climb up the upstream side of the barrier and a large part of the debris mass remains behind the barrier (as shown in Figure 14).

According to Hungr & McClung (1987), Takahashi & Yoshida (1979) developed the

leading-front model which considers the mechanics for driving the leading edge of the debris mass up the barrier with most of the debris mass remaining behind. This model accounts for transfer of momentum and thrust between the main body of the debris mass and the frontal part which moves up the barrier, and continuity of flow. The vertical runup distance, Δh , derived from this model is shown below:

$$\Delta h = \frac{v_o^2 \cos^2(\theta_o + \theta) \sin \theta}{g(\tan \phi_a \cos \theta + \sin \theta)} \left(1 + \frac{gh_o \cos \theta_o}{2v_o^2} \right)^2 \dots\dots\dots (4)$$

where v_o = entry velocity
 g = gravitational constant
 ϕ_a = apparent angle of friction of debris
 θ_o = entry channel slope angle
 θ = runup slope angle
 h_o = approach debris thickness

This equation shows that if the fluid thrust between the debris mass and the debris front represented by the last term in the bracket is neglected, the vertical runup distance predicted by this equation is about twice that given by the lumped-mass formulation. The difference is due to the assumption on the portion of debris that moves up the barrier; the lumped-mass formulation assumes the entire mass while the leading-front model assumes only the frontal end. The leading-front model implicitly assumes that the presence of the barrier will not affect the flow conditions upstream. Therefore, it is not applicable to barriers with a near-vertical back.

From the consideration of conservation of energy, the theoretical maximum vertical runup distance against a barrier placed in the path of the debris can be estimated as follows:

$$\Delta h = \frac{v_d^2}{2g} \dots\dots\dots (5)$$

where v_d = velocity of debris at impact
 g = gravitational acceleration

However, field observations suggest that the observed runup of the slurry could be larger than that estimated using the above equation. Based on their experience, Du et al (1987) suggested that for barriers with a vertical back as well as for barriers with an inclined back, the vertical runup distance of slurry estimated by the above equation should be increased by 60%. According to Kang (1999) this equation is only applicable for the determination of the vertical height of the slurry rather than the debris solids.

No standard design provision has been found in the literature for debris runup on barriers with a vertical back. Hungr et al (1984) suggested that for such situations, it would be prudent to assume that some debris might have piled up against the back of the barrier forming a wedge. Hungr et al (op cit) suggested that the inclination of the upper surface of this debris wedge could be assumed to be about 15° but there was no mentioning of the probable range of dimensions of the wedge.

4.5 Dynamic Interaction upon Debris Impact at Barrier

4.5.1 Debris Impact

(1) Empirical Methods. The debris impact loading on a barrier is sometimes estimated assuming a hydrostatic pressure distribution together with an 'enhancement factor'. In Switzerland, the 'enhancement factor' is typically assumed to be 3, whereas in Austria, this is usually taken to be 3 to 5 (Thurber Consultants Ltd, 1984).

The basis of such empirical approaches is not clearly documented but these may be compared to measurements reported in the literature. For example, Scotton & Deganutti (1997) used a 9.5 m-long flume together with coal slag with an average particle size of 5.7 mm and different fluids to examine the effect of viscosity on the impact pressure on barriers. The flume was inclined at 10°, 15° and 20° in the model tests. The results are expressed in terms of the ratio of the measured impact pressure to the hydrostatic pressure at the base. This ratio was found to fall within a wide range (between about 2.5 and 7.5), with a mean value of 5.3 for a more viscous flow and 3.5 for a less viscous fluid. The impact pressure in excess of the hydrostatic pressure is likely to be related to the velocity head of the debris at impact but no information on debris velocity is given in the paper to allow an independent data interpretation. Although the mean values are similar to the empirical values adopted, it is noteworthy that the scatter of the measurements is considerable.

Wu et al (1993) reported that empirical impact pressures were prescribed for the design of barriers in Russia. The impact pressure is dependent on the magnitude of debris flow events, the flow depth and the particle size of the entrained materials. An example of such a prescriptive design approach is shown in Table 9.

(2) Analytical Methods. The average debris impact pressure imposed on a mass barrier can be estimated based on consideration of the rate of loss of momentum upon impact (Hung et al, 1984; Du et al, 1987; Matsushita & Ikeya, 1992; PWRI, 1988), as follows:

$$p = \rho_d v_d^2 \sin \beta \dots\dots\dots (6)$$

where p = average impact pressure
 ρ_d = density of debris
 v_d = velocity of debris at impact
 β = angle between the impact face of barrier and the debris motion direction

The average impact pressure is assumed to be uniform over the depth of the debris.

Field measurements of debris impact load may be interpreted using the above equation. The results of a Japanese study on the field measurement of debris impact loads were reported by Wu et al (1993). In the study, the impact load on a 15 cm by 15 cm plate was recorded (see Table 10). Figure 15 shows that the measured values are up to several times greater than the computed values using Eq. (6) assuming direct impact (i.e. $\beta = 90^\circ$). Wu et al (1993) suggested that most of the measurements could have been influenced by boulders or hard inclusions hitting the sensors.

Another instrumented field study of debris impact pressure, velocity and density of

debris was reported by Du et al (1987) for a number of debris flow events in China. Again, there was considerable scatter in the measured impact pressures. This could be due to, inter alia, the sensors being hit by debris at an oblique angle, effects of splashes or the heterogeneous nature of the debris. Table 11 shows the field measurements for direct hits on the sensors. Figure 15 shows that the computed impact pressures obtained using Eq. (6) are in general only a fraction of the measured values. In China, a factor of 3 is generally applied to Eq. (6) in the design of barriers (Du et al, 1987; Wu et al, 1993; Zhang, 1993). Also shown in Table 11 are the values of impact pressure resulting from boulders hitting the sensors, which confirm that boulder impact will induce additional pressure on the barriers.

Other alternative theoretical formulations have also been reported in the literature. According to Scheidegger (1975), the model developed by Voellmy (1955) for snow avalanches assumed that the internal structure of an avalanche is similar to that of a flowing river. This model allows the determination of impact pressure, which is dependent on the hydrostatic head and the velocity head at the moment of impact (Table 12).

Any theoretical formulation needs to be scrutinised carefully and its underlying assumptions properly understood before use. For example, in the equation proposed by Lin et al (1997) for the estimation of maximum impact pressure, it is noted that the term is dimensionally incorrect. The equation is therefore dubious and will not be examined further in this study.

The influence of the shear strength of debris on impact pressure was investigated by Armanini & Scotton (1992) using a 6 m-long flume. The trend of the results shows that for similar velocities, debris with a higher shear strength will result in higher impact pressures than that with a lower shear strength. In the experiments where debris of a high shear strength impacted the barrier, Armanini & Scotton (op cit) observed reflection waves bouncing off the barrier and the measured impact pressure was approximately twice that given by Eq. (6). This suggests that the debris does not only lose its original velocity upon impact as assumed implicitly in Eq. (6) but also is likely to attain a velocity opposite in direction to its original value, hence resulting in a larger impact pressure.

A possible explanation of the measurement of some relatively high impact pressures in China may be the size effect of the sensor relative to the particle size of the debris. If the sensors are small, the measured pressure is likely to be significantly affected by impact of large particles giving rise to local peak values, whereas for a larger sensor the measured pressure is expected to be closer to the average effect of the debris. Another plausible explanation is that when the sensors are buried by the debris, drag develops on the edges of the sensors as well as on the mass of debris in front of them, resulting in an increase in the impact pressure.

It is important to recognise that the formulation of Eq. (6) corresponds to the average pressure developed on the barrier upon impact by a fluid. Based on the available information as described above, it appears that the debris impact pressure could well be several times that given by Eq. (6), depending on the solids concentration as well as the shear strength of the debris.

4.5.2 Boulder Impact

Boulders can be entrained within landslide debris and it is important that suitable allowance be made in barrier design. According to Zhang et al (1996), the boulders will generally be in clusters aligning either transversely across the front or longitudinally along the debris trail, with the largest boulder in the front, in a debris flow. They also reported that boulders could stay afloat near the surge and travel at a velocity similar to that of the debris. The boulder size is, in general, dependent on the boulders that can be mobilised and the capacity and content of the debris flow. An overview of selected methods in estimating boulder impact load (Table 13) is given below.

PWRI (1988) recommended that the estimation of boulder impact force should be determined using the Hertz equation (Table 13), which was derived for an elastic sphere impacting an elastic medium. In determining the boulder impact force, it was recommended that the velocity of the boulder should be taken as that of the debris flow and that the design boulder size should be taken as the maximum size which can be mobilised by the debris. Hungr et al (1984) suggested that the design boulder should be assumed to be a sphere with its diameter equal to the flow depth.

As the actual impact may not be perfectly elastic and that material crushing may occur at the contact, Hungr et al (1984) cautioned that the contact forces computed using the Hertz equation could be extremely conservative and suggested to reduce them nominally by a factor of 10.

Zhou et al (1991) reported field measurements in Japan which showed the measured boulder impact forces to be about 4% to 11% of those computed using the Hertz equation. Based on the above measurements, they suggested that the boulder impact force computed using the Hertz equation should be reduced by a factor of 5 to 10.

For certain structural elements (e.g. bridge piers), flexural deformations could be more important than contact deformations in governing the magnitude of the forces generated by boulder impact. The impact forces on such structures can be estimated by equating the kinetic energy of the boulder with the work (or energy) expended by the structure in undergoing flexural deflection, as follows:

$$F = v_b \sin \beta \sqrt{m_b K_B} \dots\dots\dots (7)$$

where F = impact force
 m_b = boulder mass
 β = angle between the impact face of barrier and the debris motion direction
 v_b = boulder velocity
 K_B = stiffness factor of the barrier structure

The flexural stiffness factors for the case of simply-supported and cantilever structures are derived and summarised in Table 13. It can be seen that the impact force is proportional to the bending stiffness of the structure.

According to Huang (1996), a slightly different form of the above equation was adopted by the Chengdu Railroad Research Institute in the estimation of boulder impact force

(see Table 13 - Compressible barrier method). The coefficient η denotes the proportion of kinetic energy of the boulder imparted onto the barrier. According to Huang (op cit), the value of η may be assumed to be 0.3 for a circular impact surface, and that the sum of the coefficients of elastic deformation of the boulder and barrier may be assumed to be 0.005 m/kN, which was for bamboo or wooden rafts impacting bridge piers. A similar equation with similar coefficients has been put forward by AASHTO for estimating ship collision on bridge piers (Xanthakos, 1995). It is of interest to note that the formula adopted by the Highways Department (1993) in estimating the impact force from a vehicle is derived along the same principle as above whereby the kinetic energy of the vehicle immediately before impact is equated to the work expanded in squashing the vehicle (Table 13).

Wu et al (1993) reported that the boulder impact force could also be estimated from the change in momentum of the boulder upon impact, with the duration over which the change in momentum takes place being assumed to be 1 second.

Zhang et al (1996) noted that when a boulder impacts a barrier, the impact load will propagate at the velocity of the compressive wave generated, from the contact point to other parts of the boulder. The formula for estimating the force using wave theory depends on, inter alia, the velocity of compression wave and the contact area. The former is generally determined either from the elastic modulus and the density of the boulder, or is taken to be about 4 000 m/s. The latter, however, is very difficult to estimate with confidence in practice.

Haller & Gerber (1998) conducted a series of field tests in which boulders up to 2 700 kg in weight impacted flexible rock fences at velocities of up to 27 m/s. They used a high-speed (54 frames/second) camera to capture the trajectory and the deceleration process of the boulder. They noted that after the first contact with the rock fence, the boulder underwent a displacement of up to 5 m before coming to a halt. The entire process of bringing the boulder to rest lasted about 0.3 second and the peak deceleration force was estimated to range from 200 kN to 600 kN. For stiffer systems, the impact duration will be much shorter and consequently very large impact forces will result.

The process of boulder impacting onto a barrier may also be studied using computer modelling. An example is LS-DYNA, a non-linear 3-D finite element program which has been used recently to simulate a boulder impacting a steel fence (Ove Arup & Partners Hong Kong, 1998) to determine its probable deformations and stresses.

5. SUMMARY AND DISCUSSION

5.1 Debris Mobility

The back-analysis of the mobility of the natural terrain landslides by Hungr (1998), Ayotte & Hungr (1998) and Chen & Lee (1998) has demonstrated that the continuum model could reasonably predict the downslope motion of landslide debris. The favourable comparison between the observed and back-calculated debris velocity for the Tsing Shan debris flow using DAN as outlined in Section 4.4.2 is also an indication of the reliability of these continuum models. These back-analyses suggest that the friction model can be a reasonable rheological model for simulating the average shear resistance at the base of both open hillside failures and channelised debris flows.

In the friction model the apparent angle of friction (ϕ_a) of the landslide debris is a critical parameter that controls the mobility of the debris. It is a function of the mechanism of debris movement, structure of the debris and its behaviour under shear. The dynamic pore water pressures generated during the downslope journey of the debris have been investigated by researchers by means of laboratory shear tests and flume tests (e.g. Sassa, 1988; Iverson & Lehusen, 1989; Reid et al, 1997). Sassa (1988) advocates the use of high-speed ring shear apparatus on the finer fraction of the debris to assess ϕ_a .

The behaviour of the debris as well as its composition are likely to vary within the debris mass and along its path, i.e. there is temporal and spatial variations in the rheology of the debris mass along the debris trail. In view of this, Hungr et al (1997) opined that "it is unlikely that satisfactory predictions of the dynamic behaviour (of debris) can be achieved based on laboratory-derived constitutive relationships. Empirical determination of the bulk rheology, based on back-analysis of actual events, is more realistic." Figure 16 shows that the apparent angles of friction obtained from back-analyses of some natural terrain landslides are comparable to the corresponding travel angles observed in the field. Hence, a possible means to estimate the apparent angle of friction of the debris for a landslide of a given volume is to base it on the travel angle of landslides of similar volume and mechanism.

Figure 17 shows a compilation of travel angles for some natural terrain landslides in Hong Kong. It can be seen that the debris mobility is a function of the debris volume and the mechanism of debris motion. For a given landslide volume, the travel angle of the debris from a channelised debris flow is generally smaller than that from an open hillside failure (i.e. a channelised debris flow is more mobile than an open hillside failure). The debris mobility of the latter increases with the scale of failure whereas that for the former appears to be independent of it. These data imply that a small channelised debris flow is as mobile as a large one. For open hillside failures, the travel angle of the debris is generally between 25° and 40° for debris volumes less than 400 m^3 , and ranges from 20° to 25° for volumes equal to or exceeding 400 m^3 . The travel angle for channelised debris flows typically ranges between 20° and 25° . Based on these available data and the correlation shown in Figure 16, the apparent angle of friction could conservatively be taken as 20° for channelised debris flows. For open hillside failures, the apparent angle of friction could be taken as 25° for volumes less than 400 m^3 and 20° for volumes equal to or exceeding 400 m^3 . Given a certain landslide volume, there could be a wide range of debris mobility (in terms of mobility angle). Therefore, the lower bound values of travel angle in Figure 17 are suggested to be taken as the apparent angle of friction for design purposes, to ensure that the mobility of the debris would not be underestimated.

Hungr (1998) and Ayotte & Hungr (1998) have found that, in general, the Voellmy model tends to better predict the distribution of debris than the friction model for channelised debris flows. The latter commonly predicts slightly higher debris velocity than the former. Therefore, the Voellmy model, together with an apparent friction angle, $\phi_a = 11^\circ$ and a turbulence coefficient, $\zeta = 500 \text{ m/s}^2$ (which have been found to be appropriate by Hungr (1998) and Ayotte & Hungr (1998)), is suggested to be used to assess the mobility of debris flows.

Unlike the back-analysis of a landslide where the width of debris along its path is known, the prediction of debris mobility using a two-dimensional model, such as DAN, requires the knowledge of debris width in advance. The compilation of the width profile

along the debris path should be made with due reference to that observed in past landslides at the site and the local topographical conditions.

As there are very few measured data available regarding the velocity of debris, the results of DAN analysis of some twenty natural terrain landslides in Hong Kong have been further examined in an attempt to develop appropriate empirical correlations to facilitate the assessment of debris mobility. Although these are computed values, their quality may not be considerably inferior to the field measurements because the continuum models such as DAN (Hung, 1995) and the one developed by Chen & Lee (1998) satisfy the principles of conservation of mass, energy and momentum. They have also been calibrated against field observations.

The maximum debris frontal velocity for each natural terrain failure back-analysed by Hung (1998) and Ayotte & Hung (1998) using DAN is plotted against the corresponding maximum debris thickness in Figure 18. There is considerable scatter in the DAN data. Also shown in this figure are predictions from various flow models discussed in Section 4.4.2. There appears to be no well defined correlation between the computed maximum debris frontal velocity, maximum debris thickness and the average slope gradient for open hillside failures and none of the flow models seems to be able to adequately describe these computed data. The values of the maximum debris velocity and the maximum debris thickness have been carefully selected along the debris trail to avoid possible errors resulting from numerical inaccuracies in the model near the source area. Nonetheless, the data point marked with an asterisk in Figure 18 was believed to have been influenced by the initial conditions as the frontal velocity was abruptly reduced by half after reaching the maximum.

In this study, the debris velocity has been back-calculated from the super-elevation data reported by King (1996) at two locations for the 1990 Tsing Shan debris flow. These velocity data are shown in Figure 18 for comparison. For channelised debris flows, it seems that the estimates made by the empirical model by Du et al (1987) are quite similar to computed values using DAN as well as the back-calculated velocity data from super-elevation measurement for Tsing Shan debris flow. However, owing to the limited data currently available, it may be premature to draw conclusion as to which flow model and the associated parameters will best describe the motion characteristics of debris flows.

Figure 19 shows the maximum debris frontal velocity and maximum debris thickness obtained from DAN and plotted against the corresponding landslide volume. The observed maximum debris thicknesses along the debris trails reported by Wong et al (1998) for natural terrain landslide studies on Lantau Island are also shown in Figure 19b. Despite the scatter, both the maximum debris frontal velocity and maximum debris thickness tend to increase with debris volume. A pragmatic approach is proposed by grouping the data into four volume ranges as shown in Figure 19 and selecting the upper bound values of the debris velocity and debris thickness within each volume range for design. The proposed demarcation, although arbitrary, takes due consideration of clustering of the data. The choice of upper bound values is to account for the scatter in data and to ensure that a conservative estimate of the debris impact pressure is obtained in the absence of a detailed assessment of debris mobility.

This empirical approach makes no distinction between open hillside failures and channelised debris flows, i.e. for a given landslide volume, the debris velocity and debris

thickness will be the same for channelised debris flows and open hillside failures. This is because the currently available data are very limited and as shown in Figure 19 there is no distinct trend that debris velocity and debris thickness are dependent on mechanism of movement. However, the proposed approach should be reviewed when additional information on debris mobility becomes available.

Although the upper bound values for each volume range have been proposed for design, these values may not be adequate under some circumstances because the existing data set is very limited, e.g. there are very few data for failures with volume exceeding 3 000 m³. Therefore, it is prudent to compare these values with data from other sources, as far as possible, such as velocity estimated from super-elevation data or back-analysis of site-specific data/failures.

5.2 Runout and Runup Distance

The debris velocity values determined using the above empirical approach are for debris travelling on the slopes. Suitable adjustment to this velocity is necessary when there is an abrupt change in gradient along the debris trail, e.g. where the slope flattens out. The formulations for the determination of runout and runup given in Tables 7 and 8 may be used. These can be broadly grouped into two categories: lumped-mass (sled) model and leading-edge model.

Chu et al (1995) carried out some runup measurements of dry gravel flowing down a 5 m long flume onto the back side of a barrier placed at the tail-end of the flume. The running surface of the flume and the barrier was lined with sheet metal to keep the frictional resistance small in order to achieve a wide range of approach velocity. The inclination of the flume and the back of the barrier was varied. Their measurements allow an evaluation of the three models in Table 8. Figure 20 shows the measurements and predictions by the three models. There is considerable scatter in the data. The sled model with no correction for slope gradient overestimates the runup distance by a factor of about 4. The sled model with momentum correction and the leading-edge model tend to predict runup distances closer to the field measurements with the former tending to slightly underestimate the runup distance while the latter slightly overestimates it. A closer examination of the data suggests that Takahashi's model gives fairly reasonable estimate for runup slope angle in the range of 20° and 40° which is similar to the inclination of the slope surface of an earth embankment.

Based on this comparison and the consideration that the leading edge model seems to give runouts that compare quite favourably with field observations, it is suggested that the leading-edge solution be used for the prediction of debris runup on the back of a barrier as well as the runout distance and debris velocity on the runout path.

5.3 Debris Impact

In assessing the various approaches put forward by different investigators for the determination of impact loading, more weight has been given to those which are supported by field measurements or calibrated against field observations.

Among the various formulations available for the estimate of debris impact pressure, the one derived from rate of fluid losing its momentum upon impact onto a rigid surface closely resembles the dynamics of debris impacting onto barriers. This equation is based on the assumption that the impacting fluid has no shear strength. Unlike fluid, landslide debris exhibits shear strength which varies broadly according to its water content. The exact relationship between the shear strength of the debris and debris impact pressure is not well understood. However, the work by Armanini & Scotton (1992) and Scotton & Deganutti (1997) showed that the debris impact pressure is dependent on the shear strength of the debris and their measurements indicated that it could be up to twice that given by Eq. (6). The comprehensive field measurements of debris impact pressure carried out in China showed that the measured debris impact pressure could be 2 to 4 times that given by Eq. (6). As a first approximation, the debris impact pressure could be taken to be at least three times that given by Eq. (6), i.e.

$$p = 3\rho_d v_d^2 \sin \beta \dots\dots\dots (8)$$

5.4 Boulder Impact

Wu et al (1993) and Zhang et al (1996) reported a number of landslide events in China where structures were damaged by boulders. They gave information on the flow characteristics of the debris and estimated the loads under which these structures would have failed. It seems that the failure capacities reported by the original authors might not have accounted for the dynamic effects and hence they would likely be lower than actual values observed in the field. This information has allowed a comparison of the boulder impact loads calculated using the different formulae given in Table 13. In some cases, the information needed for the computation is not readily available from the published papers and for the purposes of the present comparative study, typical values have been adopted. The results are summarised in Table 14.

It can be seen that there is a wide scatter in the predicted results. The impact forces estimated using the Hertz equation are about one to two orders of magnitude higher than the estimated ultimate capacity of the damaged structure. It seems that the impact forces computed using the Hertz equation are unduly conservative and can be reduced by a factor of at least 10. On the other hand, the formula adopted by the Chengdu Railroad Research Institute consistently predicts much lower impact forces which are only a small fraction of the ultimate capacity of the barriers. The principal reason for the underestimation of the impact force is likely to be due to the inappropriate use of the coefficient of elastic deformation derived from bamboo and wooden rafts which are much more flexible and ductile than boulders.

The momentum equation given in Table 13 also tends to underestimate the impact forces which suggests that the assumed impact duration of 1 second may not be appropriate. This also highlights the sensitivity of the estimates to the assumption of impact duration which is very difficult to determine reliably.

The flexural stiffness equation and the wave theory tend to give estimates closer to the computed ultimate capacities of the structures. It should be noted that in the reported case studies, the only established information is that the boulder impact force exceeded the failure

capacity of the structure and therefore no definite conclusion can be drawn as to the relative reliability of the two formulae. It is noteworthy, however, that the wave theory requires the knowledge of the contact area at impact, which is very difficult to determine. The stiffness factors given in Table 13 for use in the flexural stiffness equation are for columnar structures or beam structures which are different from those for mass wall structures. In summary, the order of magnitude of the boulder impact load could be estimated using the flexural stiffness method, or taken to be nominally one-tenth of that given by the Hertz equation. As discussed in Section 4.5.2 the boulder impact could also be assessed by means of computer programs that have been calibrated against measurements.

The above exercise serves to illustrate the uncertainties in the predictions. In practice, expedients such as the possible incorporation of a soft cushion of suitable material, e.g. rubber tires, in front of the barrier may assist in reducing boulder impact loads by extending the duration of impact (see Plate 15).

6. SUGGESTIONS FOR DESIGN OF BARRIERS

6.1 General

A review of the design methodology for debris-resisting barriers has been carried out and is summarised in Section 4. These approaches have been compared and evaluated in the light of field measurements as far as possible (Section 5). Suggestions for the design of debris-resisting barriers have been drawn up based on this review to facilitate design.

Design of barriers begins with the identification and characterisation of the natural terrain hazards at a site. Different approaches can be used to determine the design event, as outlined in Section 4.3. The approach should be selected with due consideration of the available data on previous landslide activity, local topographical and geological conditions, and the limitation of the approach itself. The pros and cons of different methods are discussed in Section 4.3. After estimating the scale of the design event and its probable location, the assessment of the landslide debris mobility and debris impact loads can be carried out.

Two approaches may be used for estimating debris mobility:

- (a) analytical approach, and
- (b) empirical approach.

These are presented in Section 6.2 below. The suggested procedures for assessment of debris impact loads are presented in Sections 6.3 and 6.4.

6.2 Debris Mobility

6.2.1 Analytical Approach

Continuum models can be used to estimate debris mobility. However, due to lack of relevant experience, only those models, such as DAN, a two-dimensional model by Hungr

(1995) and the three-dimensional model developed by Chen & Lee (1998), which have been calibrated against field measurements, should be used. A frictional rheological model (Table 6) can be used for both open hillside failures and channelised debris flows. The apparent angle of friction can be determined by means of high-speed ring shear as suggested by Sassa (1988) or can be taken as the travel angle of landslide debris observed in failures of similar scale and mechanism. It is suggested that the apparent angle of friction can be taken as 25° and 20° for open hillside failures with debris volumes below and equal to or above 400 m³ respectively. For channelised debris flows, the friction model with an apparent angle of friction of 20° or the Voellmy model with an apparent angle of friction of 11° and a turbulence coefficient of 500 m/s² can be used.

If a two-dimensional continuum model, such as DAN, is used, the debris width profile along the debris trail is required as input. This should be compiled with due reference to that observed in past landslides at the site and the local topographical conditions.

6.2.2 Empirical Approach

The maximum debris velocity and maximum debris thickness on the slope can be determined based on the estimated debris volume as shown in Figure 21. The values of debris velocity and debris thickness given in Figure 21 apply to both open hillside failures and channelised debris flows. The assessment of debris runout can be carried out using the leading-edge model (Table 7). The apparent angle of friction is suggested to be taken as 25° and 20° for open hillside failures with volumes less than and equal to or exceeding 400 m³ respectively. For channelised debris flows, a friction model with an apparent angle of friction of 20° is suggested. For barriers with a sloping back, the debris runup can be estimated using the leading edge model given in Table 8.

It is prudent to temper the debris mobility data derived from these approaches with information from other sources, such as velocity estimated from super-elevation data, as far as possible.

6.3 Debris Impact

The landslide debris impact pressure can be estimated from the following equation:

$$p = 3\rho_d v_d^2 \sin \beta \dots\dots\dots (8)$$

where p = average impact pressure
 ρ_d = density of debris
 v_d = velocity of debris at impact
 β = angle between the impact face of barrier and the debris motion direction

The average impact pressure can be assumed to be uniform over the depth of the debris.

6.4 Boulder Impact

The impact loading due to boulders in the landslide debris can be estimated using the formulation which accounts for the flexural stiffness of the barrier or it can be taken as one-tenth of that predicted by the Hertz equation (Table 13). The boulder can be assumed to travel at the same velocity as the debris mass. The size of the boulder that could be entrained depends on the size of boulder in the area as well as the thickness of the debris mass.

6.5 Stability Check and Structural Design

Barriers, like retaining walls, can fail by sliding, overturning, or as a result of bearing capacity failure. Structural failures of the barrier are also possible. The stability of the barrier against different modes of failure should be checked in accordance with Geoguide 1 (GEO, 1993). Due to their transient nature, the partial load factor for the debris and boulder impact loads may be taken as unity. The structural design of the barrier should be carried out in accordance with the requirements of the relevant structural code and standards.

As the debris may occur in pulses, the stability of the barrier should also be checked for various scenarios, including:

- (a) first frontal impact by debris,
- (b) subsequent impact with debris accumulated behind the barrier, and
- (c) static loading on the wall when the debris has come to rest after impact.

For scenarios involving a layer of debris riding on previously deposited debris, the effect of the weight of the upper debris acting as surcharge on the underlying layers need to be accounted for.

7. OTHER DESIGN CONSIDERATIONS

The retention capacity of the barrier is affected by the size of the buffer zone, the height of the barrier and the storage angle which is the angle between the upper surface of the debris piled up behind the barrier and the horizon. The location of the barrier should be chosen judiciously to allow ample space to accommodate the volume of the design debris event. It is also necessary to ensure that the barrier is high enough to account for the possibility of debris runup. PWRI (1988) recommended that the storage angle could be taken between horizontal and $1/2$ to $2/3$ of the channel bed angle. Possible bulking of the debris material should be taken into account in assessing the required retention capacity. The amount of bulking will be dependent on the original structure of the material. King (1996) reported that for Tsing Shan debris flow, the bulking factor was found to be about 8%.

There are many types of barriers, e.g. counterfort walls, gabion walls, reinforced fill

structures, and other types of gravity structures. The choice of barrier type should be made taking due cognisance of the construction and maintenance costs, land take and buildability. Whether the barrier is to be designed as a sacrificial or permanent structure should also be considered. The barrier should be well maintained, e.g. by regular removal of debris accumulated behind the barrier, to ensure there is adequate storage capacity.

For a barrier that straddles a streamcourse, special provisions such as decanting or straining structures that allow normal streamflow should be incorporated in the design. Figure 22 shows a variety of barrier design with different straining and drainage provisions.

An assessment of the likely path to be traversed by landslide debris should be made taking due consideration of, inter alia, the topography and ground surface characteristics. Avulsion may occur when a debris mass blocks its own path, e.g. a stream channel, causing it to divert. This could lead to the spreading of debris material to other areas adjacent to the original flow path. For example, mobile debris when passing through a bend may be deflected away from its original path. Davies & Hall (1992) reported an incident in New Zealand where the super-elevation effect of the debris in a bend caused it to overflow the channel banks and shot into the adjacent facilities killing four people.

In the event where the debris impact loading is considerable, a second line of defence involving some form of sacrificial elements, e.g. rows of wooden piles, rubber tires, or rubble placed behind the barrier can 'soften' the impact on the primary barrier and minimise its damage.

Due consideration should also be given to selecting an appropriate constituent material for a barrier. For example, combustible material should be avoided where the risk of hill fire is high. There has been an incident in Hong Kong in 1989 in which the geosynthetic gabion material of four gabion barrier walls was badly damaged (Au & Chan, 1991).

8. RECOMMENDED R&D STUDIES

A number of areas requiring development work have been identified. In general, there is a lack of consistent terminology used in the different case histories for describing the various landslide phenomena, such as debris flow and debris flood. Therefore, a standard set of terminology should be developed to facilitate better communication and possible extrapolation of empirical data.

The debris mobility and the interaction between debris and barrier are key considerations in the design of debris-resisting barriers. Further studies by means of literature review and laboratory and field studies should be conducted to improve the current state of knowledge on the mechanisms of natural terrain landslides and the relevant factors contributing to failure and mobility of debris, with a view to developing a practical scheme for the classification of mechanisms of debris movements, assessment of debris mobility and identification of mobile mechanisms.

Investigation into the impact loading on barriers may be further examined through laboratory simulation testing and field trials. For example, flume tests and centrifuge studies could provide valuable insights into the effects of various factors, such as shearing resistance

of debris, water content of debris, etc, on the impact load. These measurements can also provide a basis for critical examination of the various existing formulations as well as the suggested methods, for possible improvement in methodology to estimate impact load.

Some exploratory work has been carried out with the use of advanced numerical models (e.g. FLAC, LS-DYNA) to assist in gaining an insight into the impact process. Suitable formulation needs to be used to overcome the difficulty in modelling the large strain behaviour of a particulate medium associated with debris motion. Numerical models based on a particulate formulation may be worthy of trial use to assess the behaviour of debris impact on a barrier.

9. CONCLUSIONS

Barriers are, in some situations, a practical mitigation measure that can help to reduce the risks posed by natural terrain landslide hazards to vulnerable facilities. The rational design of barriers, in particular the assessment of the design landslide events and the likely impact loads, is however fraught with difficulties. Although some of the design procedures can be based on theoretically rigorous methods, the determination of many of the design parameters is not an exact science and often involves field estimates, rules of thumb and engineering judgement. An under-designed barrier can result in disastrous consequences and it can provide a false sense of security.

The reliability of the barrier design depends critically on the quality of information for assessing the locations of potential failure or debris detachment and on the likely volume, mobility, travel path and deposition of landslide debris. The importance of collecting good quality data locally such as volume, velocity (e.g. to be deduced from super-elevation data) and thickness of landslide debris cannot be over-emphasised.

Various approaches put forward for evaluating the impact loads on barriers have been reviewed and these illustrate, inter alia, the considerable scatter in the predictions as well as in some of the reported field measurements. Based on the present state of knowledge, some suggestions (summarised in Figure 21) are put forward to facilitate the assessment of debris mobility and debris impact loads in the design of landslide debris-resisting barriers. Given the developments in the subject, the suggestions are intended to be interim. They will be reviewed and updated when new data and results of further research become available.

Further research is needed to gain a better fundamental understanding of the nature and mechanisms of natural hillside failures in Hong Kong and to improve the methods for assessment of debris mobility and debris impact loads under local conditions.

Pending the results of further R&D work, it is strongly recommended that the assessment of debris impact loads on barriers should be conducted in a cautious and conservative manner, with due allowance made for the uncertainties involved.

10. REFERENCES

- Armanini, A. & Scotton, P. (1992). Experimental analysis on the dynamic impact of a debris flow on structures. Proceedings of the International Symposium INTERPRAEVENT 1992, Bern, pp 107-116.
- Au, S.W.C. & Chan, C.F. (1991). Boulder Treatment in Hong Kong. Selected Topics in Geotechnical Engineering - Lumb Volume, edited by K.S. Li, pp 39-71.
- Ayotte, D. & Hungr, O. (1998). Runout Analysis on Debris Flows and Debris Avalanches in Hong Kong. Report prepared for the Geotechnical Engineering Office, Hong Kong, 90 p.
- Chan, Y.C., Chan, C.F. & Au, S.W.C. (1986). Design of a boulder fence in Hong Kong. Proceedings of the International Conference on Rock Engineering and Excavation in an Urban Environment, Hong Kong, pp 87-96.
- Chau, K.T., Chan, L.C.P., Wu, J.J., Liu, J., Wong, R.H.C. & Lee, C.F. (1998). Experimental studies on rockfall and debris flow. Proceedings of the One Day Seminar on Planning, Design and Implementation of Debris Flow and Rockfall Hazards Mitigation Methods, Hong Kong, pp 115-128.
- Chen, C.L. (1986). Bingham plastic or Bagnold's dilatant fluid as a rheological model of debris flow? Proceedings of the Third International Symposium on River Sedimentation, Mississippi, pp 1 624-1 637.
- Chen, H. & Lee, C.F. (1998). Debris flow modelling with three-dimensional Lagrangian finite elements. Proceedings of the One Day Seminar on Planning, Design and Implementation of Debris Flow and Rockfall Hazards Mitigation Methods, Hong Kong, pp 29-45.
- Chu, T., Hill, G., McClung, D.M., Ngun, R. & Sherkat, R. (1995). Experiments on granular flows to predict avalanche runup. Canadian Geotechnical Journal, vol. 32, pp 285-295.
- Corominas, J. (1996). The angle of reach as a mobility index for small and large landslides. Canadian Geotechnical Journal, vol. 33, pp 260-271.
- Cruden, D.M. & Varnes, D.J. (1996). Landslide types and processes. Landslides: Investigation and Mitigation, edited by A.K. Turner & R.L. Schuster, Transportation Research Board Special Report 247, National Research Council, pp 36-75.
- Czerny, F. (1998). Wildbachsperren aus Beton und Stahlbeton. Medieninhaber und Herausgeber: Zement + Beton Handels- und Werbeges.m.b.H im Auftrag der österreichischen Zementindustrie, 18 p.
- Davies, T.R. (1993). Research needs for debris flow disaster prevention. Proceedings of Hydraulic Engineering'93, San Francisco, pp 1 284-1 289.

- Davies, T.R. & Hall, R.J. (1992). A realistic strategy for disaster prevention. Proceedings of the International Symposium INTERPRAEVENT 1992, Bern, pp 381-390.
- Dawson, D.F., Morgenstern, N.R. & Gu, W.H. (1992). Instability Mechanisms Initiating Flow Failures in Mountainous Mine Waste Dumps. University of Alberta, 80 p.
- DeNatale, J.S., Fiegel, G.L. & Fisher, G.D. (1996). Response of the Geobruigg Cable Net System to Debris Flow Loading. California Polytechnic State University, 90 p.
- Du, R., Kang, Z., Chen, X. & Zhu, P. (1987). A Comprehensive Investigation and Control Planning for Debris Flow in the Xiaojiang River Basin of Yunnan Province. Science Press, 287 p (in Chinese).
- Duffy, J.D. (1998). Case studies on debris and mudslide barrier systems in California. Proceedings of the One Day Seminar on Planning, Design and Implementation of Debris Flow and Rockfall Hazards Mitigation Methods, Hong Kong, pp 77-90.
- Evans, N.C., Huang, S.W. & King, J.P. (1997). The Natural Terrain Landslide Study - Phases I and II (Special Project Report, SPR 5/97). Geotechnical Engineering Office, Hong Kong, 119 p.
- Evans, N.C. & King, J. (1998). The Natural Terrain Landslide Study: Debris Avalanche Susceptibility (Technical Note TN 1/98). Geotechnical Engineering Office, Hong Kong, 96 p.
- Fang, Y.S. & Zhang, Z.Y. (1988). Kinematic mechanism of catastrophic landslides and prediction of their velocities and travelling distance. Proceedings of the Fifth International Symposium on Landslides, Toronto, vol. 1, pp 125-128.
- Franks, C.A.M. (1998). Study of Rainfall Induced Landslides on Natural Slopes in the Vicinity of Tung Chung New Town, Lantau Island (GEO Report No. 57). Geotechnical Engineering Office, Hong Kong, 102p.
- Franks, C.A.M. & Woods, N.W. (1997). Natural Terrain Landslide Study: Preliminary Review of natural Terrain Landslide Hazard Mitigation Measures (Technical Note No. 8/97). Geotechnical Engineering Office, Hong Kong, 52p.
- Frenette, R., Eyheramendy, D. & Zimmermann, T. (1997). Numerical modeling of dam-break type problems for Navier-Stokes and granular flows. Proceedings of the First International Conference on Debris-Flow Hazards Mitigation: Mechanics, Prediction and Assessment, San Francisco, pp 586-595.
- GEO (1993). Guide to Retaining Wall Design (Geoguide 1). (Second Edition). Geotechnical Engineering Office, Hong Kong, 267p.
- Haller, B. (1999). Personal Communication.

- Haller, B. & Gerber, W. (1998). Field testing and design of high energy absorption rockfall barriers. Proceedings of the One Day Seminar on Planning, Design and Implementation of Debris Flow and Rockfall Hazards Mitigation Methods, Hong Kong, pp 99-104.
- Highways Department (1993). Structures Design Manual for Highways and Railways. Hong Kong Government, 210 p.
- Ho, K.K.S. & Wong, H.N. (1999). Lessons Learnt from Landslide Investigations. Presented at the Hong Kong Institution of Engineers Geotechnical Division Technical Meeting in July 1999, Hong Kong. (Unpublished).
- Huang, Z. (1996). Engineering Techniques for Debris Flow Mitigation. China Railroad Press, 301 p (in Chinese).
- Hungr, O. (1995). A model for the runout analysis of rapid flow slides, debris flows, and avalanches. Canadian Geotechnical Journal, vol. 32, pp 610-623.
- Hungr, O. (1998). Mobility of Landslide Debris in Hong Kong: Pilot Back Analyses using a Numerical Model. Report prepared for the Geotechnical Engineering Office, Hong Kong, 50 p.
- Hungr, O., Dawson, R., Kent, A., Campbell, D. & Morgenstern, N.R. (1997). Rapid flow slides of coal mines in British Columbia, Canada. Proceedings of Reviews in Engineering Geology, Geological Society of America (in press).
- Hungr, O. & Evans, S.G. (1996). Rock avalanche runout prediction using a dynamic model. Proceedings of the Seventh International Symposium on Landslides, Trondheim, vol. 1, pp 233-238.
- Hungr, O. & McClung, D.M. (1987). An equation for calculating snow avalanche runup against barrier. Proceedings of the Davos Symposium on Avalanche Formation, Movement and Effects, pp 605-612.
- Hungr, O., Morgan, G.C. & Kellerhals, R. (1984). Quantitative analysis of debris torrent hazards for design of remedial measures. Canadian Geotechnical Journal, vol. 21, pp 663-677.
- Hungr, O., Morgan, G.C., VanDine, D.F. & Lister, D.R. (1987). Debris flow defences in British Columbia. Reviews in Engineering Geology, Volume VII, pp 201-222.
- Hungr, O., Sun, H.W. & Ho, K.K.S. (1999). Mobility of selected landslides in Hong Kong - pilot back-analysis using a numerical model. Proceedings of the Hong Kong Institution of Engineers Geotechnical Division Annual Seminar on Geotechnical Risk Management, Hong Kong, pp 167-175.
- Innes, J.L. (1983). Lichenometric dating of debris flow deposits in the Scottish Highlands. Earth Surface Processes and Landforms, vol. 8, pp 579-588.

- Itasca Consulting Group (1995). FLAC-Fast Lagrangian Analysis of Continua, Version 3.3. Volume 1: User's manual.
- Iverson, R.M. & Lehusen, R.G. (1989). Dynamic pore-pressure fluctuations in rapidly shearing granular materials. Science, vol. 246, pp 796-799.
- Japan Forest Conservation and Flood Control Association (1985). Forest Conservation in Japan. 66 p.
- Julien, P.Y. & O'Brien, J.S. (1997). On the importance of mud and debris flow rheology in structural design. Proceedings of the First International Conference on Debris-Flow Hazards Mitigation: Mechanics, Prediction and Assessment, San Francisco, pp 350-359.
- Kang, Z. (1996). Debris Flow Hazards and Their Control in China. Science Press, 118 p.
- Kang, Z. (1999). Personal Communication.
- Kang, Z., Wang S., Lee, C.F. & Law, K.T. (1999). A Study of Debris Flow Hazard Prevention. The Jockey Club Research and Information Centre for Landslip Prevention and Land Development, Hong Kong, 33 p (in Chinese).
- Kawaken (1998). Product Catalogue (in Japanese).
- King, J.P. (1996). The Tsing Shan Debris Flow (Special Project Report SPR 6/96). Geotechnical Engineering Office, Hong Kong, 3 volumes.
- Koch, T. (1998). Testing various constitutive equations for debris flow modelling. Proceedings of the HeadWater 98 Conference (IAHS Publication No. 248), Italy, pp 249-257.
- Lau, K.C. & Woods, N.W. (1997). Review of Methods for Predicting the Travel Distance of Debris from Landslides on Natural Terrain (Technical Note TN7/97). Geotechnical Engineering Office, Hong Kong, 48 p.
- Lin, P.S., Chang, W.J. & Liu, K.S. (1997). Retaining function of open-type Sabo dams. Proceedings of the First International Conference on Debris-Flow Hazards Mitigation: Mechanics, Prediction and Assessment, San Francisco, pp 636-645.
- Mak, N. & Bloomfield, D. (1986). Rock trap design for presplit rock slopes. Proceedings of the International Conference on Rock Engineering and Excavation in an Urban Environment, Hong Kong, pp 263-269.
- Matsushita, T. & Ikeya, H. (1992). Methods for the evaluation of debris flow counter measures. Proceedings of the International Symposium INTERPRAEVENT 1992, Bern, pp 337-348.
- McClung, D.M. & Schaerer, P.A. (1985). Characteristics of flowing snow and avalanche impact pressures. Annals of Glaciology, vol. 6, pp 9-14.

- Mizuyama, T., Kobashi, S. & Ou, G. (1992). Prediction of debris flow peak discharge. Proceedings of the International Symposium INTERPRAEVENT 1992, Bern, pp 99-108.
- Morgan, G.C., Rawlings, G.E. & Sobkowicz, J.C. (1992). Evaluating total risk to communities from large debris flows. Proceedings of the Symposium on Geotechnique and Natural Hazards, Vancouver, B.C. pp 225-236.
- Morgenstern, N.R. (1978). Mobile soil and rock flows. Geotechnical Engineering, vol. 9, pp 123-141.
- Okubo, S., Ikeya, H., Ishikawa, Y. & Yamada, T. (1996). Development of new methods for countermeasures against debris flows. Recent Developments on Debris Flows, Lecture Notes in Earth Science, vol. 64, pp 166-185.
- Ove Arup & Partners Hong Kong (1998). Rockfall Fence - Assessment of Impact Resistance. Report prepared for the Housing Department, Hong Kong, 59 p.
- Perla, R., Cheng, T.T. & McClung, D.M. (1980). A two-parameter model of snow-avalanche motion. Journal of Glaciology, vol. 26(94), pp 197-207.
- Pierson, T.C. & Costa, J.E. (1987). A rheological classification of subaerial sediment-water flows. Reviews in Engineering Geology, Volume VII, pp 1-12.
- Public Works Research Institute (1988). Technical Standard for the Measures Against Debris Flow (Draft) (Technical Memorandum of PWRI No. 2632). Japan, 45 p.
- Reid, M.E., Lahusen, R.G. & Iverson, I. (1997). Debris-flow initiation experiments using diverse hydrologic triggers. Proceedings of the First International Conference on Debris-Flow Hazards Mitigation: Mechanics, Prediction and Assessment, San Francisco, pp 1-11.
- Rickenmann, D. & Koch, T. (1997). Comparison of debris flow modelling approaches. Proceedings of the First International Conference on Debris-Flow Hazards Mitigation: Mechanics, Prediction and Assessment, San Francisco, pp 576-585.
- Roberds, W.J. & Ho, K.K.S. (1997). A quantitative risk assessment and risk management methodology for natural terrain in Hong Kong. Proceedings of the First International Conference on Debris-Flow Hazards Mitigation: Mechanics, Prediction and Assessment, San Francisco, pp 207-218.
- Sassa, K. (1988). Geotechnical model for the motion of landslide. Proceedings of the Fifth International Symposium on Landslides, Lausanne, vol. 1, pp 37-55.
- Sawada, T., Suwa, H. & Takahashi, T. (1999). Rainfall condition for the occurrence of debris flow in the Jiangjia Gully. China-Japan Joint Research on the Mechanism and the Countermeasures for the Viscous Debris Flow, pp 11-17.
- Scheidegger, A.E. (1975). Physical Aspects of Natural Catastrophes. Elsevier, 289 p.

- Scotton, P. & Deganutti, A.M. (1997). Phreatic line and dynamic impact in laboratory debris flow experiments. Proceedings of the First International Conference on Debris-Flow Hazards Mitigation: Mechanics, Prediction and Assessment, San Francisco, pp 777-786.
- Sun, H.W. (1998). Review of Fill Slope Failures in Hong Kong (Special Project Report SPR 4/98). Geotechnical Engineering Office, Hong Kong, 86 p.
- Takahashi, T. (1991). Debris Flow. IAHR Monograph, Balkema, 165 p.
- Takahashi, T. & Yoshida, H. (1979). Study on the Deposition of Debris Flows. Part I - Deposition due to Abrupt Change of Bed Slope. Annuals, Disaster Prevention Research Institute, Kyoto University, vol. 22, paper B-2.
- Thommen, R.A. (1998). Testing and experiences gained in the field with flexible wire rope netting barriers to retain mud and debris flow. Proceedings of the One Day Seminar on Planning, Design and Implementation of Debris Flow and Rockfall Hazards Mitigation Methods, Hong Kong, pp 67-76.
- Threadgold, L. & McNicholls, D.P. (1984). The design and construction of polymer grid boulder barriers to protect a large public housing site for the Hong Kong Housing Authority. Proceedings of the Symposium on Polymer Grid Reinforcement in Civil Engineering, London, pp 212-219.
- Thurber Consultants Ltd (1984). Debris Torrents: A Review of Mitigative Measures. Report to Ministry of Transportation & Highways, British Columbia, 32 p.
- Tse, C.M., Chu, T., Lee, K., Wu, R., Hung, O. & Li, F.H. (1999). A risk-based approach to landslide hazard mitigation measure design. Proceedings of the Hong Kong Institution of Engineers Geotechnical Division Annual Seminar on Geotechnical Risk Management, Hong Kong, pp 33-42.
- VanDine, D.F. (1985). Debris flows and debris torrents in the southern Canadian Cordillera. Canadian Geotechnical Journal, vol. 22, pp 44-68.
- VanDine, D.F. (1996). Debris Flow Control Structures for Forest Engineering. British Columbia Ministry of Forests, Working Paper 22/1996, 68 p.
- Van Gassen W. & D.M. Cruden (1989). Momentum transfer and friction in the debris of rock avalanches. Canadian Geotechnical Journal, vol. 26, pp 623-628.
- Voellmy, A. (1955). Über die Zerstörungskraft von Lawinen. Schweizerische Bauzeitung, vol. 73, pp 159-165, 212-217, 246-249, 280-285.
- Wong, H.N. & Ho, K.K.S. (1996). Travel distance of landslide debris. Proceedings of the Seventh International Symposium on Landslides, Trondheim, vol. 1, pp 417-422.

- Wong, H.N., Lam, K.C. & Ho, K.K.S. (1998). Diagnostic Report on the November 1993 Natural Terrain Landslides on Lantau Island (GEO Report No. 69). Geotechnical Engineering Office, Hong Kong, 98 p.
- Wong, H.Y. (1995). Preliminary Report on Design of Free-standing Reinforced Concrete Wall as a Barrier & Energy Absorber against Debris Flow. Architectural Services Department, Hong Kong, 26 p.
- Wu, J., Tian, L., Kang, Z., Zhang, Y. & Liu, J. (1993). Debris Flow and Its Comprehensive Control. Science Press, 332 p (in Chinese).
- Wyllie, D.C. & Norrish, N.I. (1996). Stabilization of rock slopes. Landslides: Investigation and Mitigation, edited by A.K. Turner & R.L. Schuster, Transportation Research Board Special Report 247, National Research Council, pp 474-504.
- Xanthakos, P.P. (1995). Bridge Substructure and Foundation Design. Prentice Hall PTR, 844 p.
- Zhang, S. (1993). A comprehensive approach to the observation and prevention of debris flows in China. Natural Hazards, vol. 7, pp 1-23.
- Zhang, S., Hungr, O. & Slaymaker, O. (1996). The calculation of impact force of boulders in debris flow. Debris Flow Observation and Research, edited by R. Du, Science Press, pp 67-72 (in Chinese).
- Zhou, B., Li, D., Luo, D., Lu, R. & Yang, G. (1991). Guide to Mitigation of Debris Flows. Science Press, 217 p (in Chinese).

LIST OF TABLES

Table No.		Page No.
1	Summary of Active Landslide Mitigation Measures	51
2	Types of Barrier Structures in Hong Kong	52
3	Classification of Channels in British Columbia Developed by Hungr et al (1984)	53
4	Summary of Formulations for Determination of Peak Debris Discharge	54
5	Summary of Various Flow Models for the Determination of Debris Velocity	55
6	Summary of Base Shear Resistances of Some Rheological Models	56
7	Summary of Approaches for Determination of Runout Distance	57
8	Summary of Approaches for Determination of Vertical Runup Distance	58
9	Empirical Impact Pressure Values Derived from Russian Studies on Debris Flows (Wu et al, 1993)	59
10	Measurements of Debris Impact Pressures in Japan (after Wu et al, 1993)	59
11	Measurements of Debris Impact Pressures in China (after Du et al, 1987)	60
12	Summary of Formulations for Determination of Debris Impact Load	61
13	Summary of Formulations for Determination of Boulder Impact Force	62
14	Comparison of Predicted Boulder Impact Forces Obtained Using Various Formulations	63

Table 1 - Summary of Active Landslide Mitigation Measures

Area of Application	Action	Mitigation Methods
Source Area	Inhibition of Occurrence	Scaling, splitting and removal of unstable rock Excavation of unstable material Modification of slope gradient, e.g. terracing, and construction of check dams
	Stabilisation	Reinforcement, e.g. rock bolts, chains and cables, anchored mesh nets, anchors/dowels, soil nails, and piles Buttresses Soil treatment, e.g. grouting, electro-osmosis, and thermal treatment Structural retention systems Dentition Afforestation
	Drainage and Infiltration Prevention	Surface drainage Subsurface drainage Surface protection
Hazard Trail	Flow Control	Promotion of deposition, e.g. unconfined deposition area, storage basin, debris flow breaker screens, and rock trap (ditch) Flow impediments and debris straining structures, e.g. sacrificial baffles, debris racks, steel cell dams, check dams (or cascaded dams), slit dams, and grid type Sabo dam Flow direction control, e.g. deflection walls, chutes, lateral walls (or guideways), and lined channel
	Protective Structures	Terminal walls Debris barriers Boulder fences Debris sheds and viaducts

Table 2 - Types of Barrier Structures in Hong Kong

Type of Barrier	Height (m)	Hazards	Design Event	Location
steel fence	1.5 - 3	boulders	1.3 m diameter (boulder weighing 30 kN)	Below Seymour Cliff, Midlevels
steel fence	4	boulders	1 m (diameter)	Baguio Villa
steel fence	2 - 3	boulders	1.3 m diameter (boulder weighing 30 kN)	Extension above Conduit Road
steel fence	1.5	boulders	0.3 m in size	Ngau Mei Hoi
steel fence	4	boulders	1 m ³	Fanling Area 49A
gabion	3 - 4	boulders	2 m to 4 m (diameter)	Chuk Yuen
gabion	3 - 7	boulders	3 m to 5 m (diameter)	Shaukeiwan
reinforced concrete wall	2 - 4	boulders	1 m (diameter)	Baguio Villa
gabion	3	debris	300 m ³	Tsing Yi North Coastal Road
reinforced concrete wall	3	debris	125 m ³	Fei Ngo Shan Road
reinforced concrete L-shaped wall	5	debris	66 m ³ /m	Tsing Lung Tau
reinforced concrete T-shaped wall	5	debris	11 m ³ /m	Kowloon Medical Rehabilitation Centre
reinforced concrete T-shaped wall	5	debris	15.5 m ³ /m	Hospital Authority Building
reinforced concrete wall	4	debris	70 m ³	Bowen Road
reinforced concrete L-shaped wall	7 - 9	debris/ boulders	1 475 - 2 225 m ³	Fanling Area 49A
reinforced concrete L-shaped and cantilever wall	7	debris/ boulders	600 - 700 m ³	Tsing Yan
check dam	5	debris	3 000 m ³	Tuen Mun Road
check dam	6	debris/ boulders	1 400 m ³	Sham Tseng
earthfill terminal berm	1.5	debris	1 500 m ³	Tuen Mun Area 19

Table 4 - Summary of Formulations for Determination of Peak Debris Discharge

Reference	Du et al (1987)	Zhou et al (1991)	Du et al (1987)	Zhou et al (1991)	PWRI (1988)																		
Equation	$q_d = (1 + \omega)q_w$	$q_d = (1 + \omega)Dq_w$	$q_d = (1 + \omega)q_w \omega_e$	$q_d = (1 + \omega_w)q_w$	$q_d = \frac{C_s}{C_s - C_{sm}} q_w$																		
	<p>q_d = peak discharge of debris</p> <p>q_w = peak discharge of water</p> <p>$\omega = \frac{\gamma_d - \gamma_w}{\gamma_s - \gamma_d}$</p> <p>$\gamma_d$ = unit weight of debris flow</p> <p>γ_w = unit weight of water</p> <p>γ_s = unit weight of debris solids</p>	<table><tr><td><p>D = coefficient accounting for debris damming the channel</p><p>Degree of channel damming</p></td><td><p>D</p><table><tr><td>Little or none</td><td>1-1.4</td></tr><tr><td>Moderate</td><td>1.5-1.9</td></tr><tr><td>Severe</td><td>2.0-2.5</td></tr><tr><td>Very Severe</td><td>2.6-3.0</td></tr></table></td></tr></table>	<p>D = coefficient accounting for debris damming the channel</p> <p>Degree of channel damming</p>	<p>D</p> <table><tr><td>Little or none</td><td>1-1.4</td></tr><tr><td>Moderate</td><td>1.5-1.9</td></tr><tr><td>Severe</td><td>2.0-2.5</td></tr><tr><td>Very Severe</td><td>2.6-3.0</td></tr></table>	Little or none	1-1.4	Moderate	1.5-1.9	Severe	2.0-2.5	Very Severe	2.6-3.0	<p>ω_e = coefficient accounting for erodibility of debris accumulated within the channel</p> <p>Based on field observations, Du et al (1987) suggested:</p> <p>$\omega_e = 11.7q_w^{-0.21}$ with q_w in (m³/s)</p> <p>which roughly corresponds to</p> <table><tr><td>q_w (m³/s)</td><td>ω_e</td></tr><tr><td>10-50</td><td>7-13</td></tr><tr><td>50-100</td><td>3-6</td></tr><tr><td>>100</td><td>3-5</td></tr></table>	q_w (m ³ /s)	ω_e	10-50	7-13	50-100	3-6	>100	3-5	<p>ω_w = coefficient accounting for soil solids concentration and moisture content of the debris prior to entrainment</p> <p>Zhou et al (1991) suggested:</p> <p>$\omega_w = \frac{(\gamma_d - \gamma_w)}{\gamma_s (1 + w) - \gamma_d (1 + \gamma_s w)}$</p> <p>where w = moisture content of debris before entrainment</p> <p>The higher the insitu moisture content of the debris, the more likely it will be mobilized and consequently a higher ω_w.</p>	<p>C_s = volumetric solids concentration of debris before entrainment</p> <p>C_{sm} = volumetric solids concentration of debris flow</p> <p>PWRI (1988) suggested that C_s was generally about 0.6.</p> <p>For channel bed angle, $\theta > 20^\circ$:</p> <p>$C_{sm} = 0.9C_s$</p> <p>For $\theta \leq 20^\circ$:</p> <p>$C_{sm} = \frac{\gamma_w \tan \theta}{(\gamma_s - \gamma_w)(\tan \phi - \tan \theta)}$</p> <p>$\phi$ = angle of internal friction of debris</p>
<p>D = coefficient accounting for debris damming the channel</p> <p>Degree of channel damming</p>	<p>D</p> <table><tr><td>Little or none</td><td>1-1.4</td></tr><tr><td>Moderate</td><td>1.5-1.9</td></tr><tr><td>Severe</td><td>2.0-2.5</td></tr><tr><td>Very Severe</td><td>2.6-3.0</td></tr></table>	Little or none	1-1.4	Moderate	1.5-1.9	Severe	2.0-2.5	Very Severe	2.6-3.0														
Little or none	1-1.4																						
Moderate	1.5-1.9																						
Severe	2.0-2.5																						
Very Severe	2.6-3.0																						
q_w (m ³ /s)	ω_e																						
10-50	7-13																						
50-100	3-6																						
>100	3-5																						

Table 5 - Summary of Various Flow Models for the Determination of Debris Velocity

	Flow Model														
	Newtonian Laminar Flow	Bingham Laminar Flow	Newtonian Turbulent Flow	Dilatant Flow	Empirical										
Equation	$v = \frac{\rho_d g h^2 S}{k \mu_d}$	$v = \frac{\rho_d g h^2 S}{k \mu_B} (1 - 1.5 \frac{\tau_B}{\tau_o} + 0.5 \frac{\tau_B^3}{\tau_o^3})$	$v = \frac{1}{n} h^{\frac{2}{3}} S^{\frac{1}{2}}$	$v = \xi h^{\frac{3}{2}} S^{\frac{1}{2}}$	$v = k^* h^{\frac{2}{3}} S^{\frac{1}{5}}$										
	<p>v = debris velocity h = flow depth S = gradient of channel bed ρ_d = density of debris μ_d = debris viscosity g = gravitational acceleration k = coefficient accounting for cross-sectional shape: 3 for a wide rectangular channel 5 for a trapezoidal one 8 for a semicircular one Hungr et al (1984) found that a value of $\mu_d = 3 \text{ kPa}\cdot\text{s}$ gave reasonably good agreement between computed and observed unit discharge for selected debris events in Canada and Japan.</p>	<p>μ_B = Bingham viscosity τ_o = basal shear stress τ_B = Bingham yield stress</p>	<p>n = Manning's roughness coefficient Du et al (1987) reported that the following correlation between n and h was established based on field measurements in Yunnan, China: $\frac{1}{n} = 28.5 h^{-0.34}$</p>	<p>ξ = coefficient accounting for grain properties and concentration of solids Hungr et al (1984) found that a value of $\xi = 2.17 \text{ m}^{-1/2}\text{s}^{-1}$ gave reasonably good agreement between computed and observed unit discharge for selected debris events in Canada and Japan.</p>	<p>Du et al (1987) suggested the following k^* values:</p> <table><tr><th>$h \text{ (m)}$</th><th>k^*</th></tr><tr><td>< 2.5</td><td>10</td></tr><tr><td>3</td><td>9</td></tr><tr><td>4</td><td>7</td></tr><tr><td>5</td><td>5</td></tr></table>	$h \text{ (m)}$	k^*	< 2.5	10	3	9	4	7	5	5
$h \text{ (m)}$	k^*														
< 2.5	10														
3	9														
4	7														
5	5														

Table 6 - Summary of Base Shear Resistances of Some Rheological Models

Rheological Model	Base Shear Resistance, τ		
Friction (or Apparent Friction)	$\tau = \rho_d g h \cos \theta \tan \phi_a$ or $\tau = \rho_d g h \cos \theta (1 - r_u) \tan \phi'$		
Newtonian Laminar Flow	$\tau = \frac{3 v \mu_d}{h}$		
Newtonian Turbulent Flow	$\tau = \rho_d g v^2 n^2 h^{\frac{1}{3}}$		
Dilatant Flow	$\tau = \frac{\rho_d g v^2}{\xi^2 h^2}$		
Bingham Flow	$v = \frac{\rho_d g h^2 S}{3 \mu_B} \left(1 - 1.5 \frac{\tau_B}{\tau} + 0.5 \frac{\tau_B^3}{\tau^3} \right)$		
Voellmy	$\tau = \rho_d g \left(h \cos \theta \tan \phi_a + \frac{v^2}{\zeta} \right)$		
Legend:			
θ	Slope angle	ζ	Turbulence coefficient
v	Debris velocity	h	Flow depth
S	Gradient of channel bed (= $\tan \theta$)	g	Gravitational acceleration
μ_d	Debris viscosity	ρ_d	Density of debris
ξ	Coefficient accounting for grain properties and concentration of solids	τ_B	Bingham yield stress
		μ_B	Bingham viscosity
n	Manning's roughness coefficient	ϕ'	Angle of shearing resistance of debris in terms of effective stress
r_u	Pore water pressure ratio	ϕ_a	Apparent angle of friction

Table 7 - Summary of Approaches for Determination of Runout Distance

Model	Lumped-mass Model	Leading-edge Model (Hungr et al, 1984; Hungr & McClung, 1987)	Constant Rate of Deposition (Van Gassen & Cruden, 1989)
Equations	$x_L = \frac{v_o^2}{2g \cos \theta (\tan \phi_a - \tan \theta)}$ $v_x = \sqrt{2g \cos \theta (\tan \phi_a - \tan \theta)(x_L - x)}$ $v_x = v_o \sqrt{1 - \frac{x}{x_L}}$	$x_L = \frac{v_o^2 \cos^2(\theta_o - \theta) \left[1 + \frac{gh_o \cos \theta_o}{2v_o^2} \right]^2}{G}$ $G = g(S_f \cos \theta - \sin \theta)$ $v_x = \sqrt{G(x_L - x)}$	$x_L = \frac{3}{2} \frac{v_o^2}{2g \cos \theta (\tan \phi_a - \tan \theta)}$ $v_x = v_o \sqrt{1 - \frac{x}{2x_L}}$
	x_L = runout distance ϕ_a = apparent angle of friction of debris θ = runout slope angle v_o = entry velocity v_x = debris velocity at a distance x from entry point (point of initial deposition) g = gravitational acceleration	θ_o = entry channel slope angle S_f = friction slope (see Hungr et al, 1984) It can be shown that: $S_f = (1 - \frac{\rho_w}{\rho_d}) \tan \phi_d'$ Hungr & McClung (1987) suggested that: $S_f = \tan \phi_a$ h_o = debris thickness at entry point ρ_w = density of water ρ_d = density of debris ϕ_d' = effective dynamic friction angle	

Table 8 - Summary of Approaches for Determination of Vertical Runup Distance

Model	Lumped-mass Model	Lumped-mass Model Corrected for Momentum Change (Perla et al, 1980)	Leading-edge Model (Hung & McClung, 1987; Takahashi & Yoshida, 1979)
Equation	$\Delta h = \frac{v_o^2 \tan \theta}{2g(\tan \phi_a + \tan \theta)}$	$\Delta h = \frac{v_o^2 \cos^2(\theta_o + \theta) \tan \theta}{2g(\tan \phi_a + \tan \theta)}$	$\Delta h = \frac{v_o^2 \cos^2(\theta_o + \theta) \tan \theta}{g(\tan \phi_a + \tan \theta)} \left(1 + \frac{gh_o \cos \theta_o}{2v_o^2} \right)^2$
	Δh = runup distance ϕ_a = apparent angle of friction of debris θ = runup slope angle v_o = entry velocity	θ_o = entry channel slope angle	h_o = approach debris thickness

Table 9 - Empirical Impact Pressure Values Derived from Russian Studies on Debris Flows
(Wu et al, 1993)

Scale of Debris Flow	Maximum Flow Depth (m)	Diameter of the Largest Entrained Boulder (m)	Impact Pressure (kPa)
Small	< 2	< 0.5	50 - 60
Medium	2 - 3	< 0.7	70 - 80
Medium-large	3 - 5	< 1.5	90 - 100
Large	5 - 10	2.5 - 3	110 - 150
Very Large	> 10	< 3	150 - 300

Table 10 - Measurements of Debris Impact Pressures in Japan (after Wu et al, 1993)

Measurement Number	Measured Debris Impact Pressure, p_m (kPa)	Measured Debris Velocity (m/s)	Density of Debris* (kg/m ³)	Computed Debris Impact Pressure, p_c (kPa)	p_m / p_c
1	80	6.0	2 100	76	1.1
2	31	6.0	2 100	76	0.4
3	36	6.0	2 100	76	0.5
4	2151	6.0	2 100	76	28.5
5	818	3.3	2 100	23	35.8
6	342	3.3	2 100	23	15.0
7	293	3.3	2 100	23	12.8
8	391	3.7	2 100	29	13.6
9	382	3.3	2 100	23	16.7
Note: * denotes value assumed in the computation of debris impact pressure					

Table 11 - Measurements of Debris Impact Pressures in China (after Du et al, 1987)

Measurement Number	Measured Debris Impact Pressure, p_m (kPa)	Measured Debris Velocity (m/s)	Density of Debris (kg/m^3)	Computed Debris Impact Pressure, p_c (kPa)	p_m / p_c
1	383	7.2	2 200	114	3.4
2	314	7.2	2 200	114	2.8
3	255	6.4	2 200	90	2.8
4	230	6.9	2 100	100	2.3
5	242	6.9	2 100	100	2.4
6	281	6.9	2 100	100	2.8
7	230	6.6	2 100	91	2.5
8	204	6.2	2 100	81	2.5
9	191	7.7	2 100	125	1.5
10	192	8.1	2 100	138	1.4
11	600	8.1	2 100	138	4.4
12	217	7.7	2 100	125	1.7
13	293	7.3	2 100	112	2.6
14	587	5.9	2 100	73	8.0
15	281	7.4	2 100	115	2.4
16	255	7.4	2 100	115	2.2
17	485	7.4	2 100	115	4.2
18	383	7.0	2 100	103	3.7
19	383	7.0	2 100	103	3.7
20	230	6.0	2 100	76	3.0
21	217	6.0	2 100	76	2.9
22	255	7.1	2 100	106	2.4
23	255	5.9	2 100	73	3.5
24	268	7.8	2 100	128	2.1
25	903	For measurements numbered 25 to 35, boulders of 1 m to 2 m in diameter were observed to be entrained in debris			
26	903				
27	903				
28	1 785				
29	1 275				
30	1 138				
31	824				
32	1 275				
33	1 020				
34	903				
35	903				

Table 12 - Summary of Formulations for Determination of Debris Impact Load

	Debris Flows					Snow Avalanches	
Reference	Hungr et al (1984)	Du et al (1987)	Thurber Consultants Ltd (1984)	Scotton & Deganutti (1997)	Lin et al (1997)	McClung & Schaerer (1985)	Scheidegger (1975)
Equations	$p = \rho_d v_d^2 \sin \beta$ $F = \rho_d A v_d^2 \sin \beta$	$p = 3\rho_d v_d^2 \sin \beta$	$F = \frac{\alpha \rho_w g d^2}{2}$	$p = \alpha g \rho_d h$	$p = 2b_r h \rho_d \Delta v_d^2$	$p = \rho v_s^2$	$p = \rho g \left(h + \frac{v_s^2}{2g} \right)$
	<p>p = impact pressure</p> <p>F = impact force</p> <p>ρ_d = density of debris</p> <p>v_d = velocity of debris</p> <p>A = cross-sectional area of debris mass</p> <p>β = angle between velocity vector and surface of obstruction</p>		<p>ρ_w = density of water</p> <p>d = debris height against barrier</p> <p>α = impact load factor</p> <p>g = gravitational acceleration</p> <p>Austria:</p> <p>$\alpha = 3$ to 5</p> <p>Switzerland:</p> <p>$\alpha = 3$</p>	<p>h = flow depth</p> <p>$\alpha = 5.3$ for more viscous fluid to 3.5 for less viscous fluid</p>	<p>b_r = ratio of width of debris flow to width of barrier</p> <p>Δv_d = change of debris velocity</p>	<p>ρ = density of snow</p> <p>v_s = velocity of snow avalanche</p>	

Table 13 - Summary of Formulations for Determination of Boulder Impact Force

	Boulder Impact						Vehicles
Reference	Hertz Equation (PWRI, 1988)	Flexural Stiffness Method (Hung et al, 1984; Zhang et al, 1996)	Compressible Barrier Method (Huang, 1996)	Allowance for Sliding of Barrier (Threadgold & McNicholls, 1984)	Wave Theory (Zhang et al, 1996)	Momentum Equation (Wu et al, 1993)	Highways Department, Hong Kong Government (1993)
Equations	$F = \lambda \left(\frac{5m_b v_b^2}{4\lambda} \right)^{\frac{3}{5}}$ $\lambda = \frac{4r_b^{\frac{1}{2}}}{3 \left(\frac{1 - \mu_b^2}{E_b} + \frac{1 - \mu_B^2}{E_B} \right)}$ <p>The above can be rewritten as:</p> $F = 1.14 v_b^{1.2} \lambda^{0.4} m_b^{0.6}$	$F = v_b \sin \beta \sqrt{m_b K_B}$	$F = \eta v_b \sin \beta \sqrt{\frac{m_b}{c_b + c_B}}$	$F = \frac{(m_b v_b)^2}{m_b + m_B} \times \frac{1}{2s}$ $s = \left(\frac{m_b v_b}{m_b + m_B} \right)^2 \times \frac{1}{2g \tan \phi}$ <p>The above can be rewritten as:</p> $F = (m_b + m_B) 2g \tan \phi$	$F = \rho_b C_b v_b A_c$ $C_b = \sqrt{\frac{E_b}{\rho_b}}$	$F = \frac{m_b v_b}{\Delta t}$	$F = \frac{m(v \sin \beta)^2}{2(c^* \sin \beta + b^* (\cos \beta - 1) + z^*)}$
	m_b = mass of boulder v_b = velocity of boulder r_b = radius of boulder μ_B = Poisson's ratio of barrier E_B = elastic modulus of barrier μ_b = Poisson's ratio of boulder E_b = elastic modulus of boulder	K_B = stiffness factor $= \frac{3EI}{L_B^3 (1 - \psi)^2 \psi^2}$ for a simply-supported beam $= \frac{3EI}{(\psi L_B)^3}$ for a cantilever beam or wall EI = bending stiffness of barrier L_B = length or height of barrier ψ = ratio of distance between impact location and barrier support to length of barrier	η = reduction factor, assumed to be 0.3 c_b = coefficient of elastic deformation of boulder c_B = coefficient of elastic deformation of barrier β = angle between the face of barrier and the debris motion direction	m_B = mass of barrier s = displacement of barrier ϕ = angle of friction between base of barrier and foundation g = gravitational acceleration	A_c = contact area C_b = velocity of compression wave through boulder ρ_b = density of boulder	Δt = duration of impact	m = vehicle mass v = vehicle velocity β = vehicle impact angle (measured between velocity vector of vehicle and wall face) b^* = lateral position of vehicle centre of gravity c^* = longitudinal position of vehicle centre of gravity z^* = sum of vehicle crumpling and parapet deflection

Table 14 - Comparison of Predicted Boulder Impact Forces Obtained Using Various Formulations

Case Histories	Estimated Failure Capacity +	Estimated Impact Force				
		Hertz Equation $F = 1.14v_b^{1.2}\lambda^{0.4}m_b^{0.6}$	Flexural Stiffness Method $F = v_b \sin \beta \sqrt{m_b K_B}$	Compressible Barrier Method $F = \eta v_b \sin \beta \sqrt{\frac{m_b}{c_b + c_B}}$	Wave Theory $F = \rho_b C_b v_b A_c$	Momentum $F = \frac{m_b v_b}{\Delta t}$
<p>On 7 September 1981, a 6 m diameter boulder entrained in a debris flow severed the centre pier of a bridge on the Chengdu-Kuming Railroad into three fragments (Zhang et al, 1996).</p> <p>$E_b = 49 \text{ GPa}$ $E_B = 26 \text{ GPa}$ $\mu_b = 0.2$ $\mu_b = 0.18$ $v_b = 8.9 \text{ m/s}$ $I_B = 12.56 \text{ m}^4$ $\rho_b = 2700 \text{ kg/m}^3$ $\psi = 0.6$ $m_b = 414 \text{ Mg}$ $L_B = 22 \text{ m}$ $r_b = 3.32 \text{ m}$ $A_c = 0.5 \text{ m}^2$</p>	12 000 kN	2 623 000 kN (218.6)	121 000 kN (10.1)	770 kN (0.06)	51 200 kN (4.3)	3 700 kN (0.3)
<p>In June 1983, a 5.5 m boulder entrained in a debris flow buckled two 1 m diameter steel pipes in Dongchuan, Yunnan. These pipes were welded together side by side with a wall thickness of 1 cm (Zhang et al, 1996).</p> <p>$E_b = 42 \text{ GPa}$ $E_B = 210 \text{ GPa}$ $\mu_b = 0.2$ $\mu_B = 0.3$ $v_b = 12 \text{ m/s}$ $A_c = 0.2 \text{ m}^2$ $m_b = 230.6 \text{ Mg}$ $\rho_b = 2700 \text{ kg/m}^3$</p>	28 600 kN	3 413 000 kN (119.3)	-	770 kN (0.03)	25 600 kN (0.9)	2 800 kN (0.1)
<p>On 30 June 1981, a debris flow severed a concrete bridge pier in Dongchuan, Yunnan. The cross-sectional area of the bridge pier normal to the debris flow direction is 21 m^2. A 3 m diameter boulder was later found nearby the bridge pier and it was believed that this boulder probably contributed to the failure of the pier (Wu et al, 1993).</p> <p>$E_b = 42 \text{ GPa}^*$ $E_B = 26 \text{ GPa}^*$ $\mu_b = 0.2^*$ $\mu_B = 0.18^*$ $v_b = 12.5 \text{ m/s}$ $A_c = 0.25 \text{ m}^2$ $\rho_b = 2700 \text{ kg/m}^3$ $\rho_d = 2190 \text{ kg/m}^3$ $m_b = 38.2 \text{ Mg}$</p>	28 770 kN	787 000 kN (27.4)	-	330 kN (0.01)	33 300 kN (1.2)	480 kN (0.02)
<p>On 10 August 1968, a boulder estimated to be 2 m x 3 m x 4 m in size destroyed a reinforced concrete structure in a debris flow event in Dongchuan, Yunnan (Wu et al, 1993).</p> <p>$E_b = 42 \text{ GPa}^*$ $E_B = 26 \text{ GPa}^*$ $\mu_b = 0.2^*$ $\mu_B = 0.18^*$ $v_b = 10.5 \text{ m/s}$ $I_B = 0.16 \text{ m}^4$ $\rho_b = 2700 \text{ kg/m}^3$ $L_B = 16 \text{ m}$ $m_b = 64.8 \text{ Mg}$ $A_c = 0.2 \text{ m}^2^*$</p>	1 290 kN	123 000 kN (95.3)	4 440 kN (3.4)	340 kN (0.26)	21 300 kN (16.5)	648 kN (0.5)
+ provided by original authors * assumed values adopted in this study () denotes ratio of the estimated impact force to the failure capacity of the structure						

LIST OF FIGURES

Figure No.		Page No.
1	Possible Hazardous Scenarios Posed by Natural Hillside	66
2	Landslide Zones and Mechanisms of a Debris Flow (Franks & Woods, 1997)	67
3	Methods of Landslide Mitigation	68
4	Schematic Diagram Showing Some Active Mitigation Measures for Debris Flows	69
5	Construction of Site-specific Landsliding Frequency versus Source Volume Relationship (based on Tse et al, 1999)	70
6	Plot of Debris Volume versus Catchment Area	71
7	Peak Debris Flow Discharge versus Scale of Debris Flow (after Hungr et al, 1984; PWRI, 1988; Mizuyama et al, 1992)	72
8	Debris Volume in Debris Flow Events in Val Varuna, Switzerland, 1772-1987 (after Davies, 1993)	73
9	Principles of the Sled Model	74
10	Flow Depth-Unit Discharge Relationships Predicted by Various Formulations	75
11	Classification of Debris Flow Events (after Kang et al, 1999)	76
12	Simulated and Observed Velocities for a Debris Flow Event in Kamikamihori Valley (Rickenmann & Koch, 1997)	77
13	Source Volume versus Apparent Angle of Friction Correlation for Open Hillside Failures (Ayotte & Hungr, 1998)	78
14	Schematic of Runup Process Assumed by Different Models	79
15	Comparison of Computed and Measured Debris Impact Pressures	80

Figure No.		Page No.
16	Comparison of Apparent Angle of Friction Used in DAN Analysis with Observed Travel Angle of Debris	81
17	Data on Debris Mobility for Different Mechanisms and Scales of Natural Terrain Landslides in Hong Kong	82
18	Comparison of Data Extracted from DAN Analysis with Those Predicted by Flow Models	83
19	Maximum Debris Frontal Velocity and Debris Thickness Corresponding to the Four Debris Volume Ranges	84
20	Comparison of Measured and Computed Vertical Runup Distances Using Various Models	85
21	Suggestions for Assessment of Debris Mobility and Debris Impact Loading	86
22	Some Typical Decanting or Straining Structures (Czerny, 1998)	87

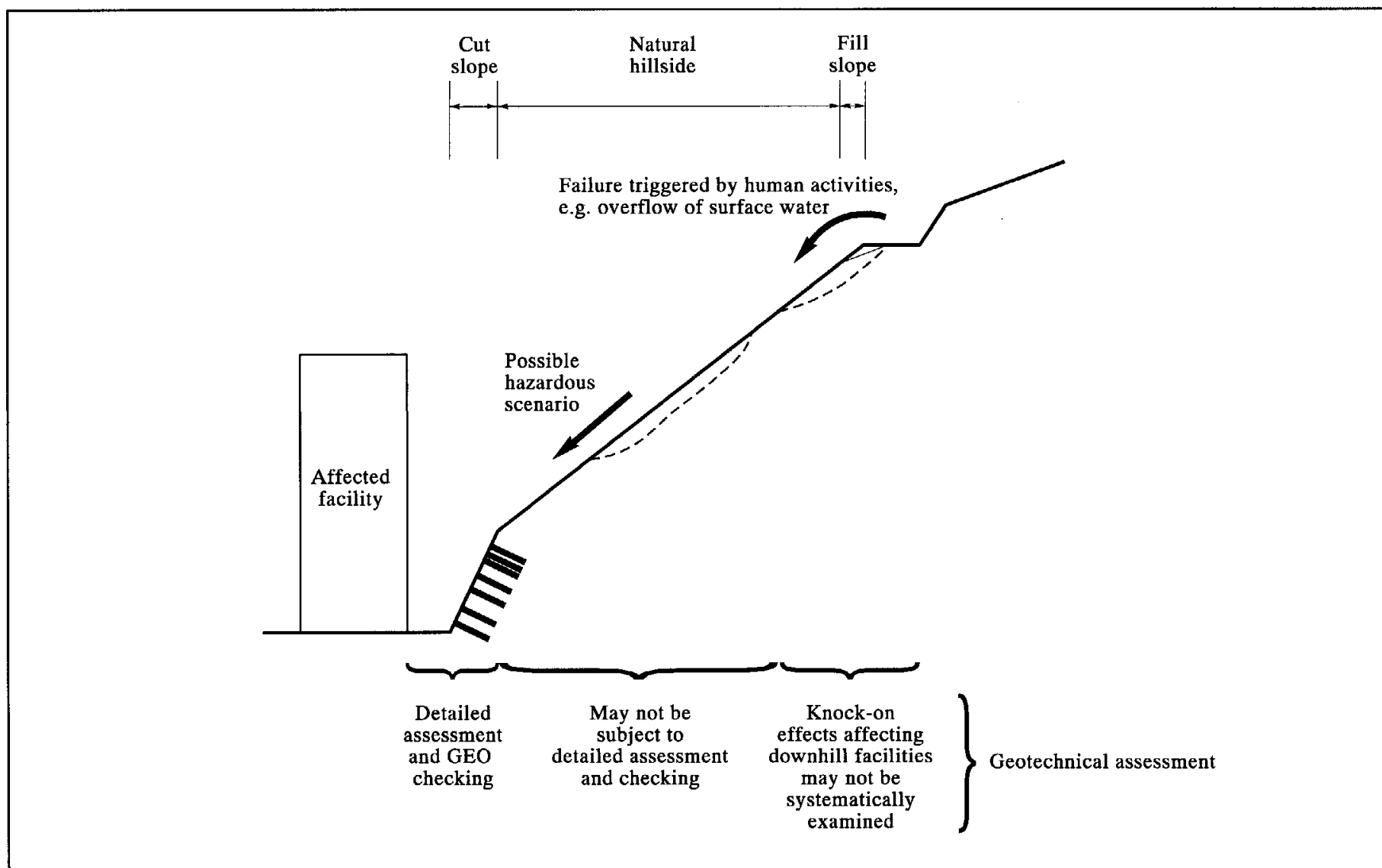


Figure 1 - Possible Hazardous Scenarios Posed by Natural Hillside

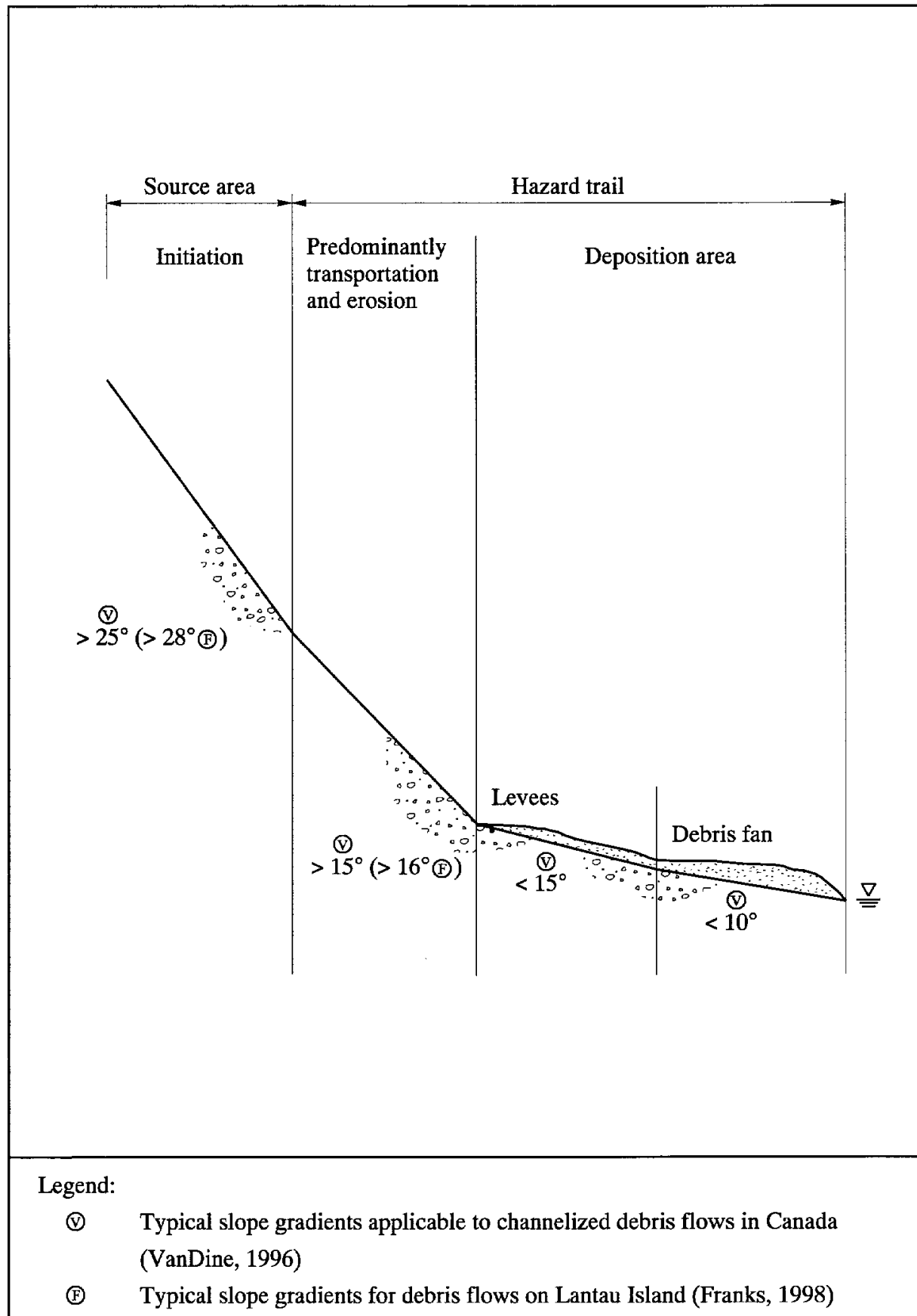


Figure 2 - Landslide Zones and Mechanisms of a Debris Flow (Franks & Woods, 1997)

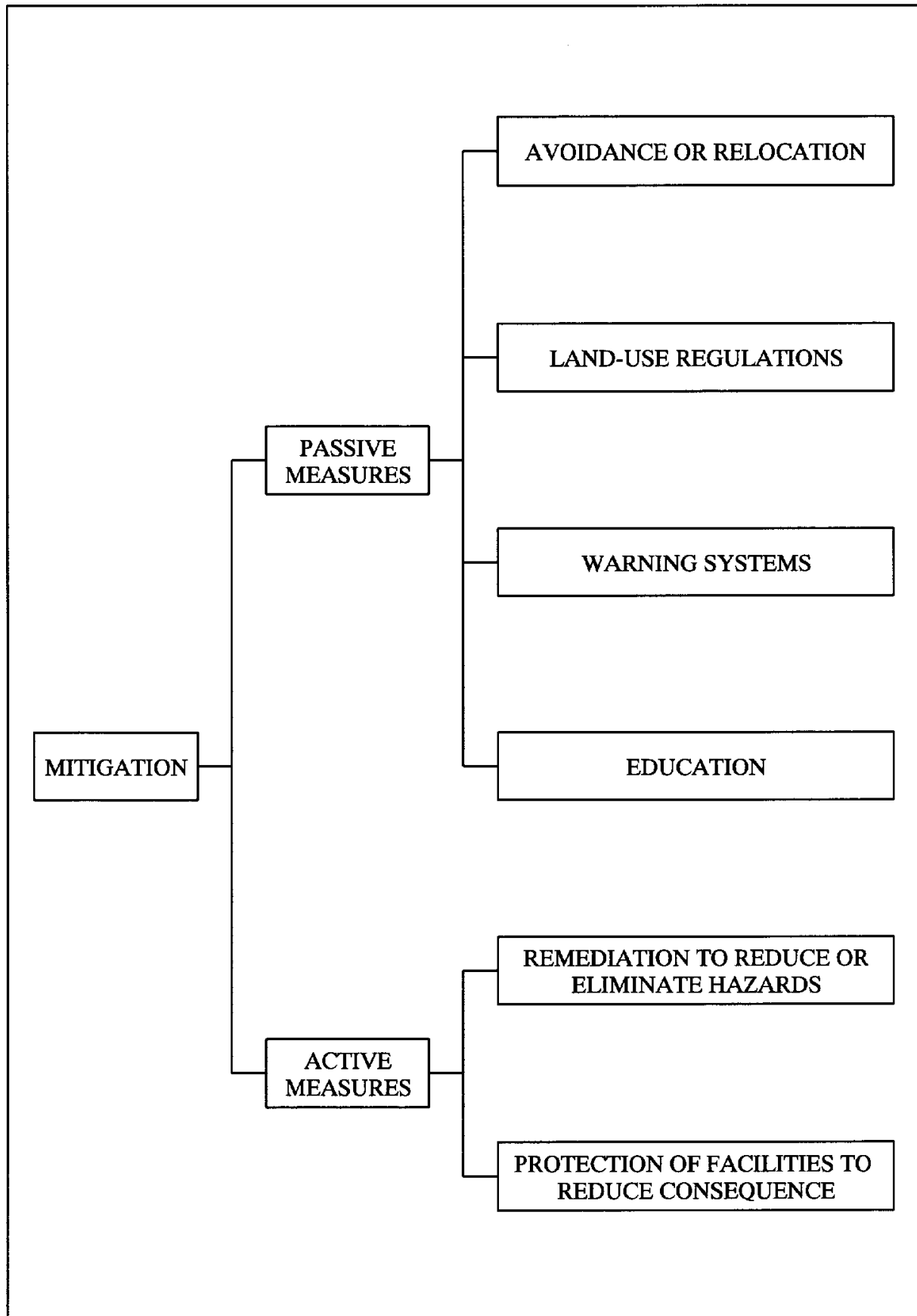


Figure 3 - Methods of Landslide Mitigation

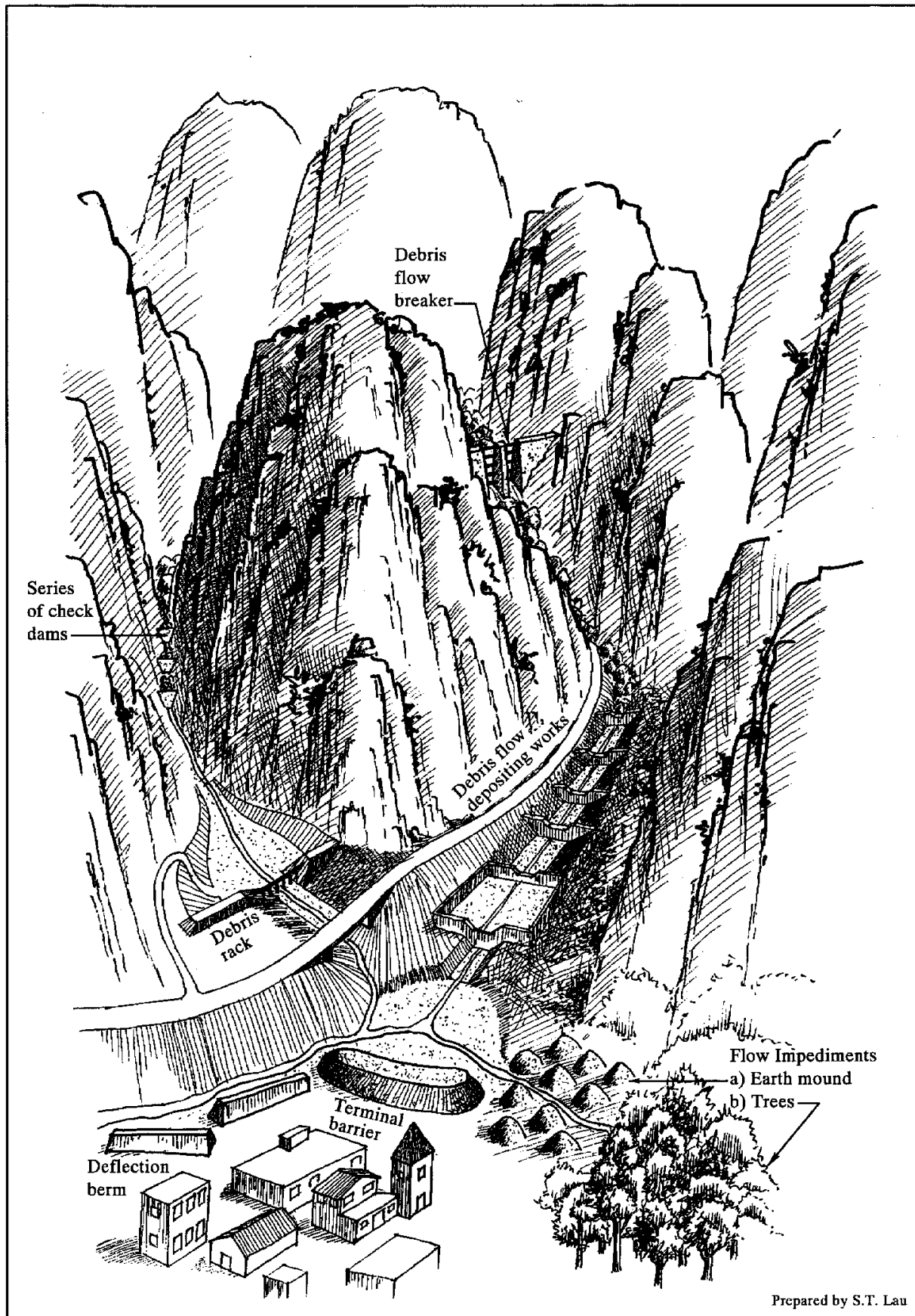
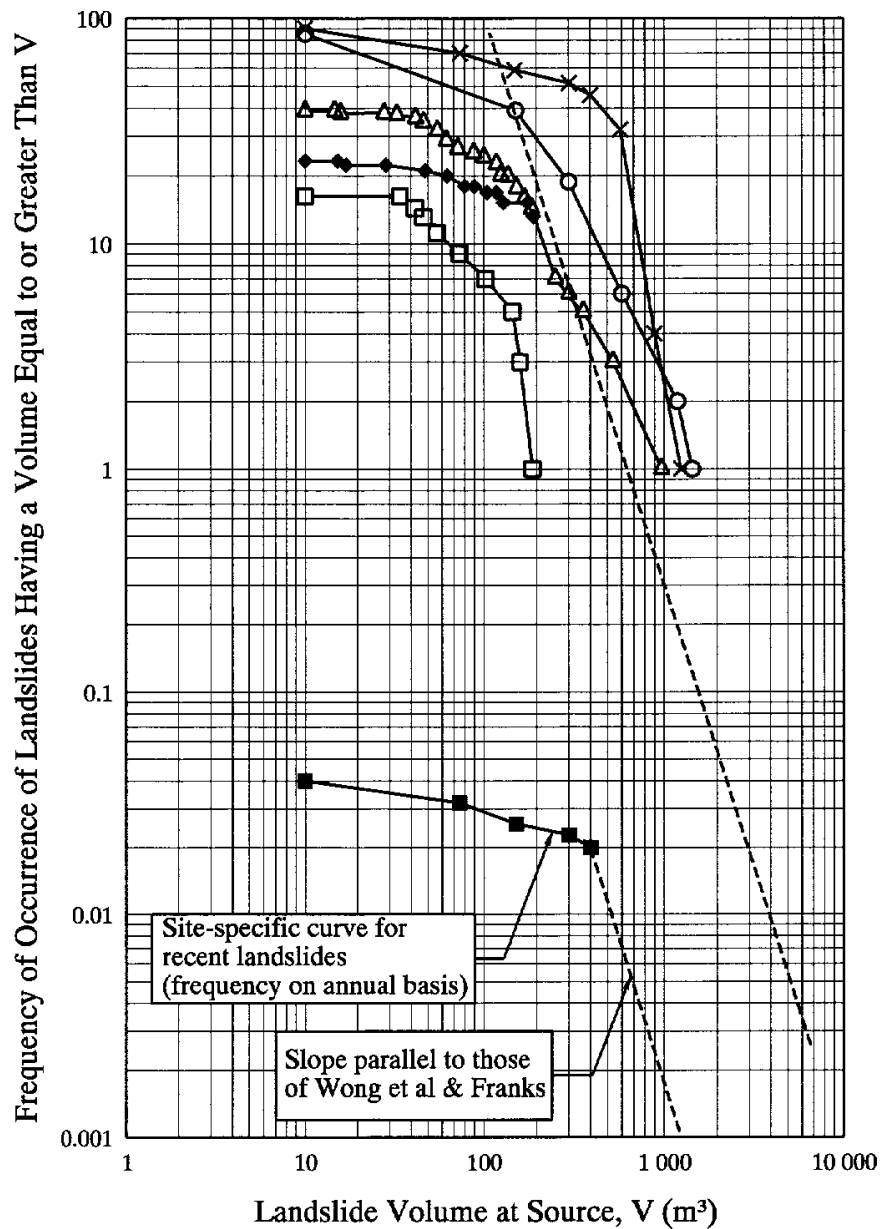


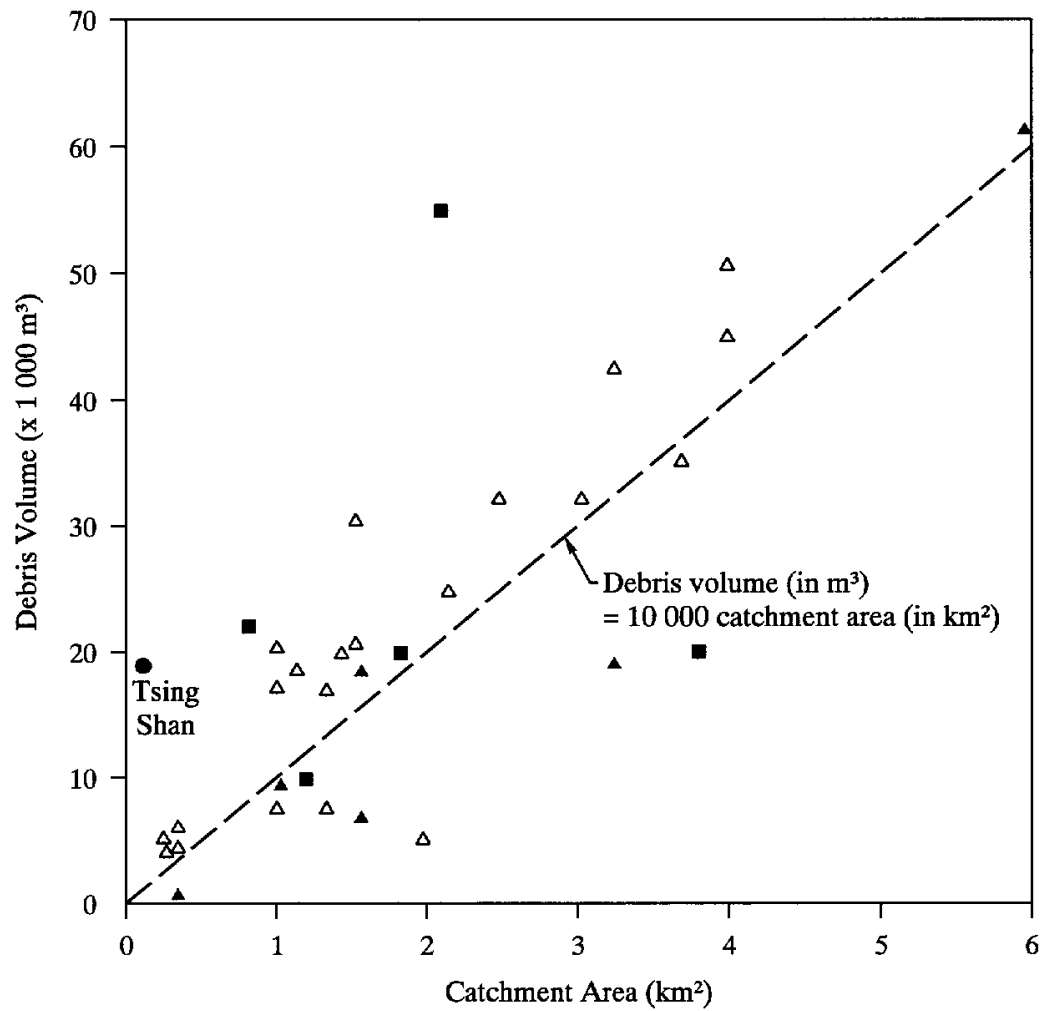
Figure 4 - Schematic Diagram Showing Some Active Mitigation Measures for Debris Flows



Legend:

- ◆— Failures on open hillsides (based on Wong et al, 1998)
- Failures adjacent to streamcourses (based on Wong et al, 1998)
- △— Failures on open hillsides and adjacent to streamcourses (based on Wong et al, 1998)
- Failures documented in a landslide study on Lantau (based on Franks, 1998)
- ×— Site-specific curve from API (based on recent and relict landslides)
- Site-specific curve from API (based on recent landslides)

Figure 5 - Construction of Site-specific Landsliding Frequency versus Source Volume Relationship (based on Tse et al, 1999)



Legend:

Data points from past channelised debris flows

● King (1996)

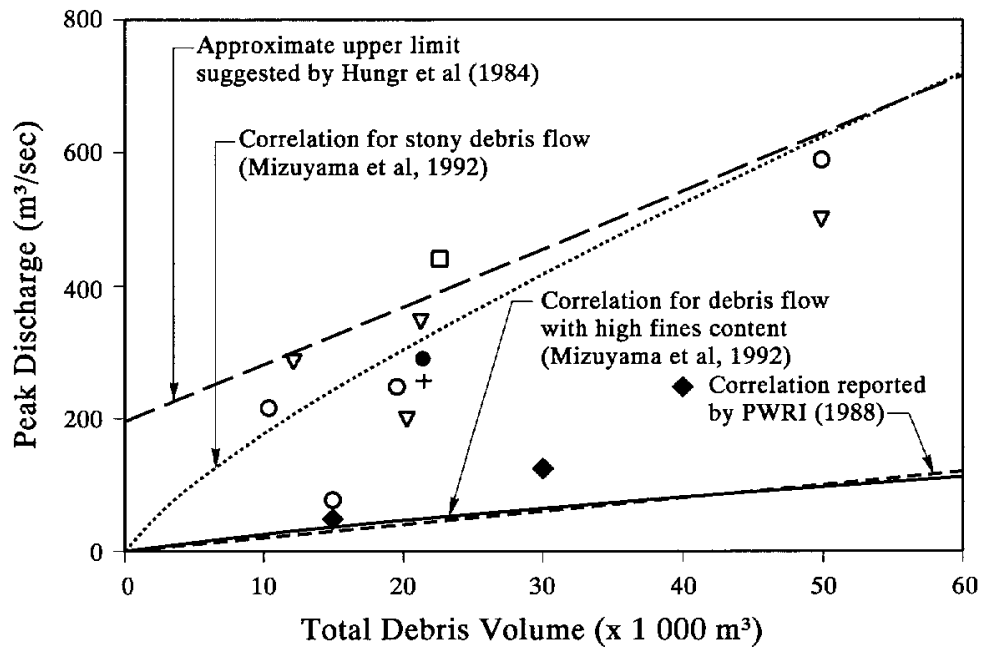
■ Hungr et al (1984)

▲ VanDine (1996)

△

Estimated design volumes
reported by VanDine (1996)

Figure 6 - Plot of Debris Volume versus Catchment Area



Legend:

Methods of estimating peak discharge for debris flow events in British Columbia:

- Eyewitness records
- ◆ Flood discharge
- ▽ Super-elevation data
- + Weir formula
- Model tests
- Velocity equation

Figure 7 - Peak Debris Flow Discharge versus Scale of Debris Flow
(after Hungr et al, 1984; PWRI, 1988; Mizuyama et al, 1992)

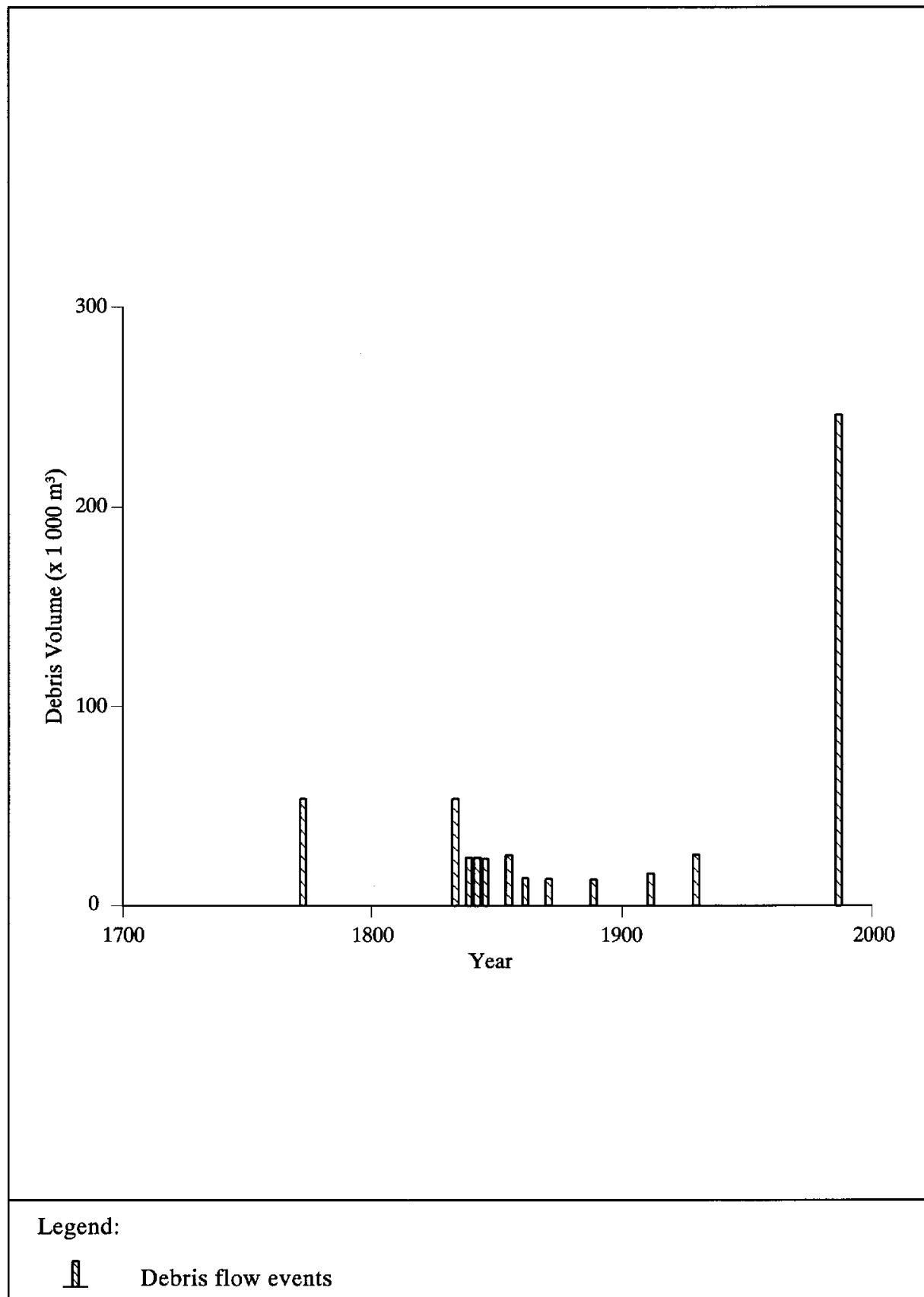


Figure 8 - Debris Volume in Debris Flow Events in Val Varuna, Switzerland, 1772-1987 (after Davies, 1993)

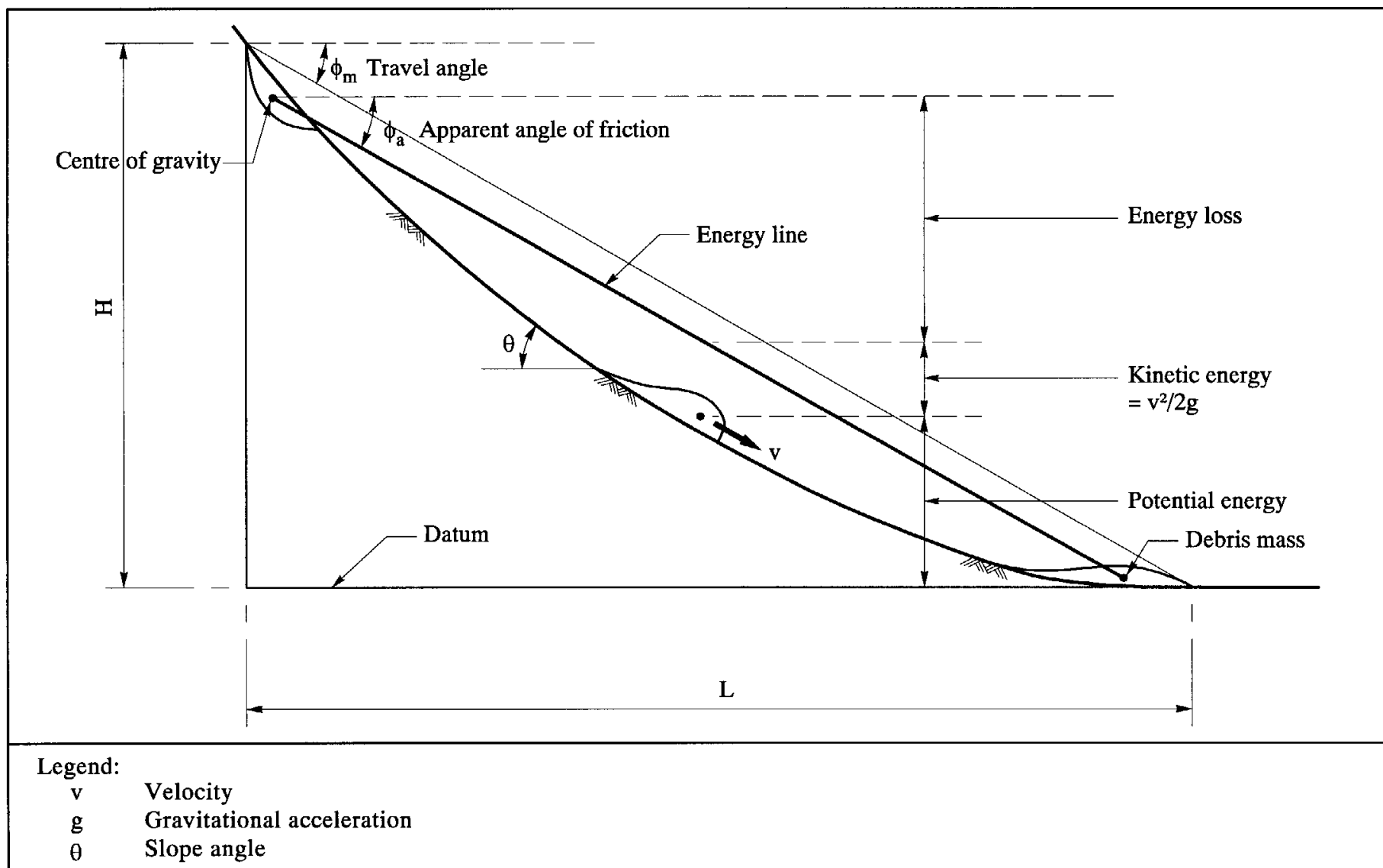


Figure 9 - Principles of the Sled Model

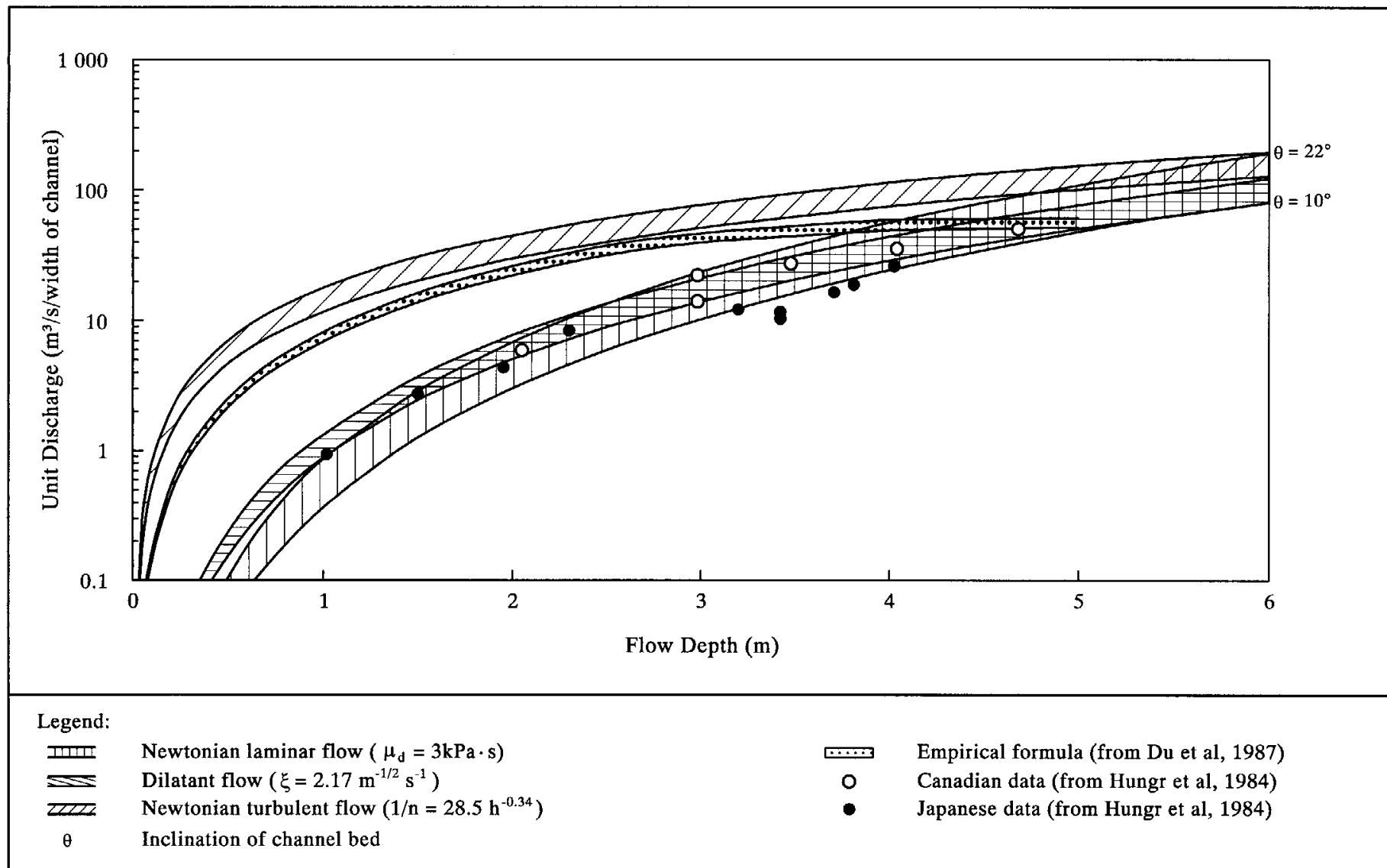


Figure 10 - Flow Depth-Unit Discharge Relationships Predicted by Various Formulations

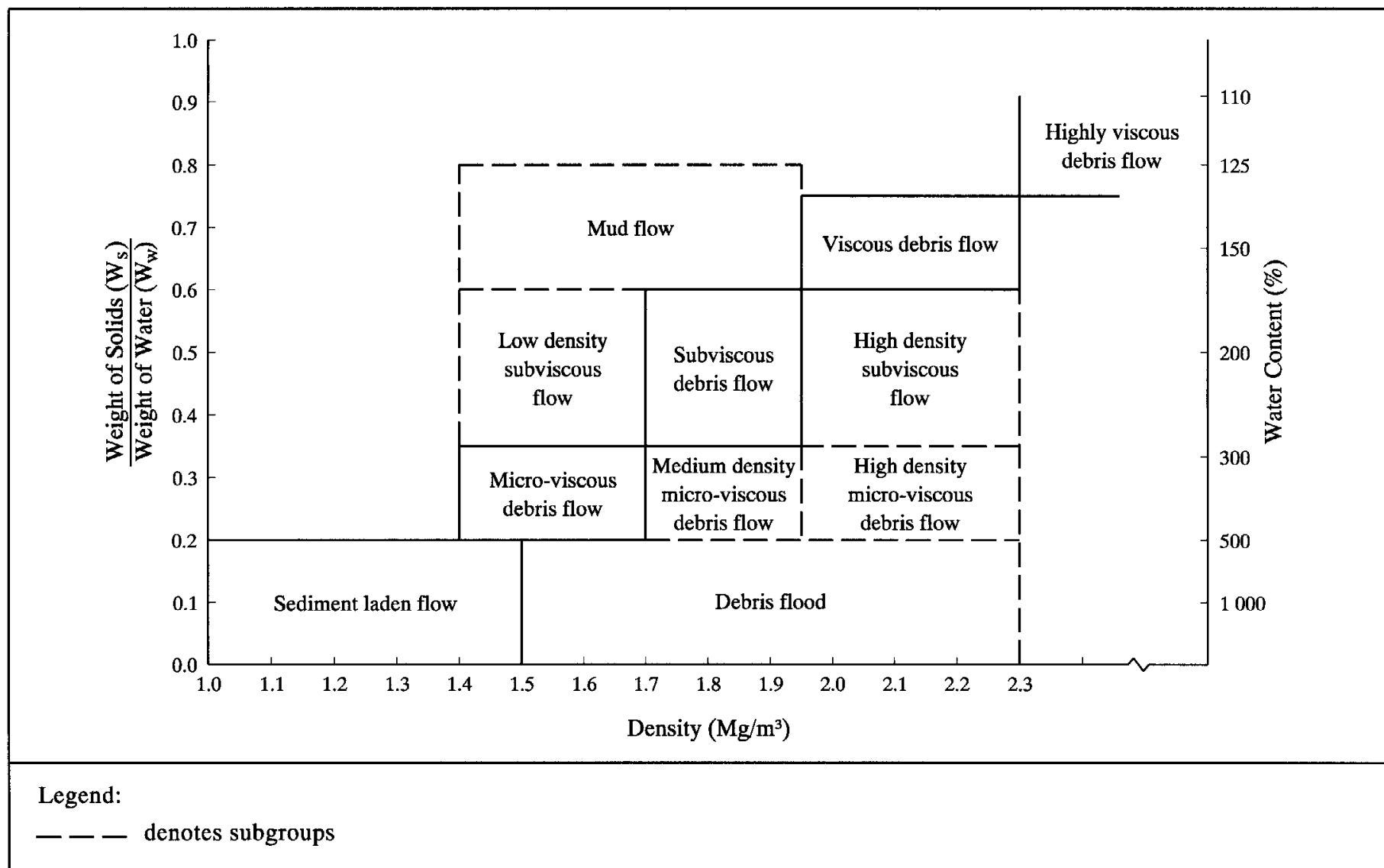
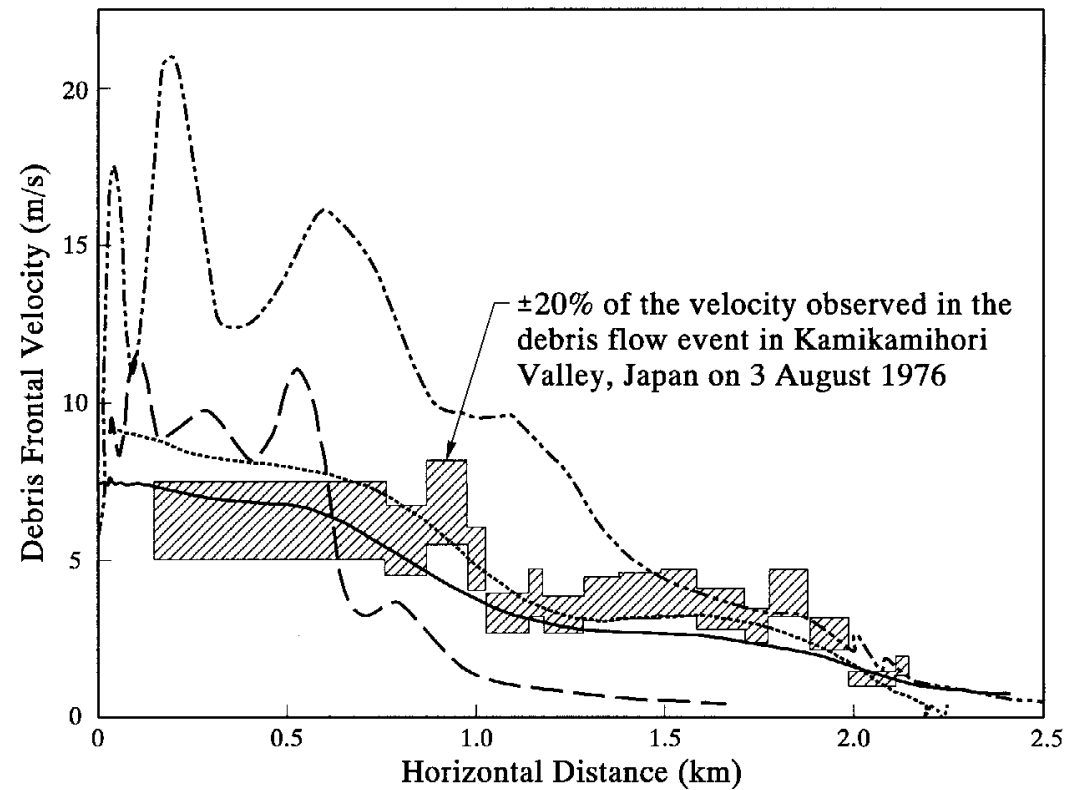


Figure 11 - Classification of Debris Flow Events (after Kang et al, 1999)



Legend:

———— Turbulent: $n = 0.15$

..... Voellmy: $\phi_a = 3.5^\circ$, $\zeta = 120 \text{ m/s}^2$

— — — Bingham: $\tau_B = 100 \text{ Pa}$, $\mu_B = 0.8 \text{ kPa}\cdot\text{s}$

- - - - Dilatant: $\xi = 31 \text{ m}^{-1/2} \text{ s}^{-1}$

Note: Horizontal distance is measured from a location at the elevation of about 1 940 m above sea level with a maximum flow depth of 2.5 m and a mean flow velocity of 6.5 m/s.

Figure 12 - Simulated and Observed Velocities for a Debris Flow Event in Kamikamihori Valley (Rickenmann & Koch, 1997)

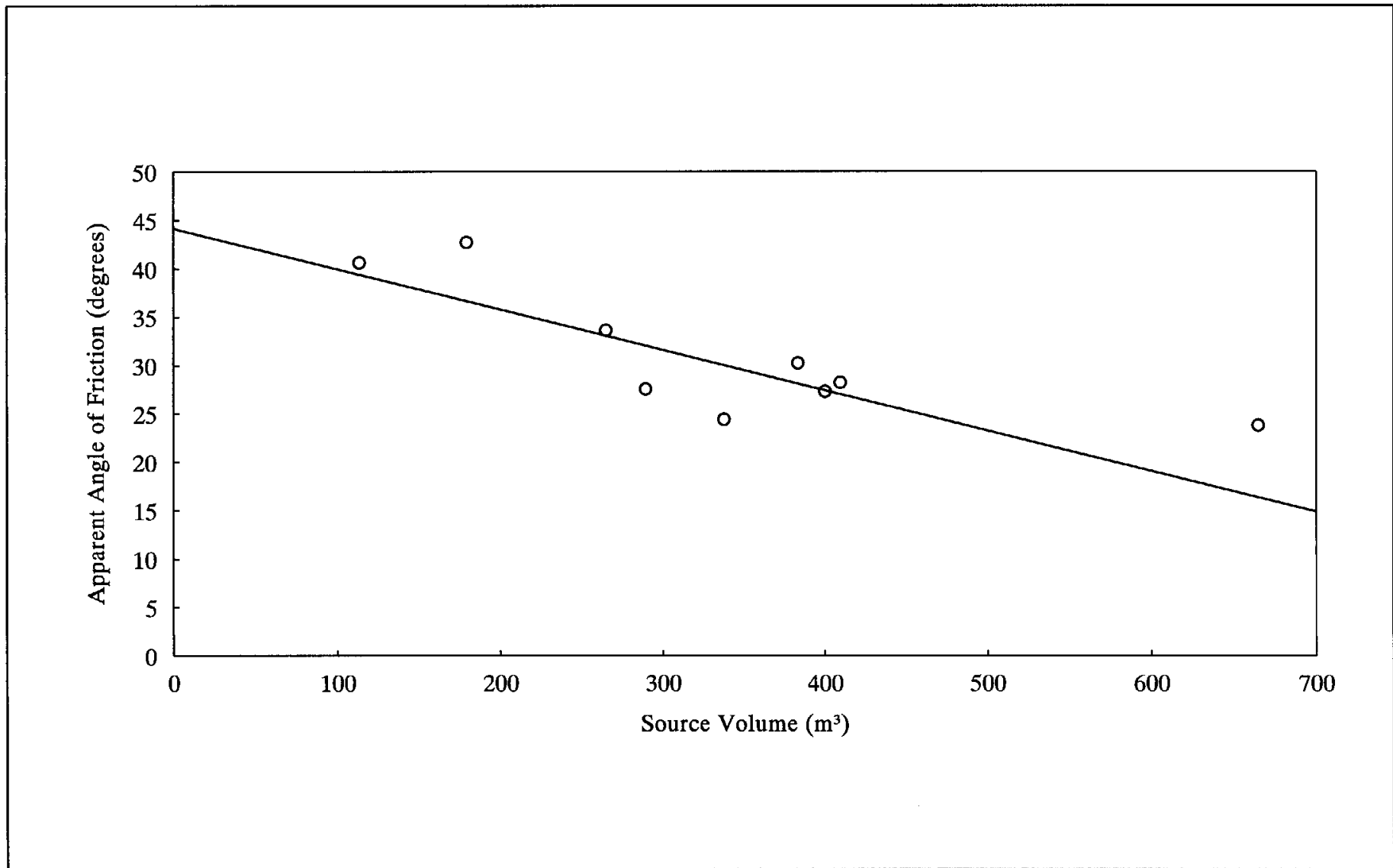
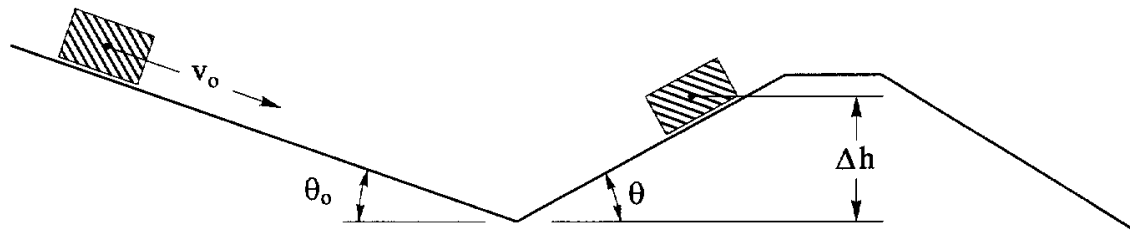
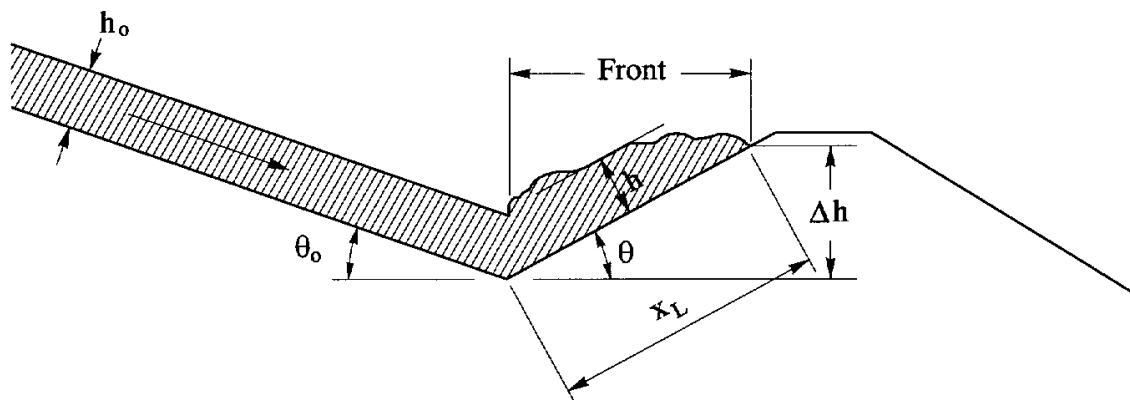


Figure 13 - Source Volume versus Apparent Angle of Friction Correlation for Open Hillside Failures (Ayotte & Hungr, 1998)



(a) Lumped-mass formulation



(b) Leading-edge model

Figure 14 - Schematic of Runup Process Assumed by Different Models

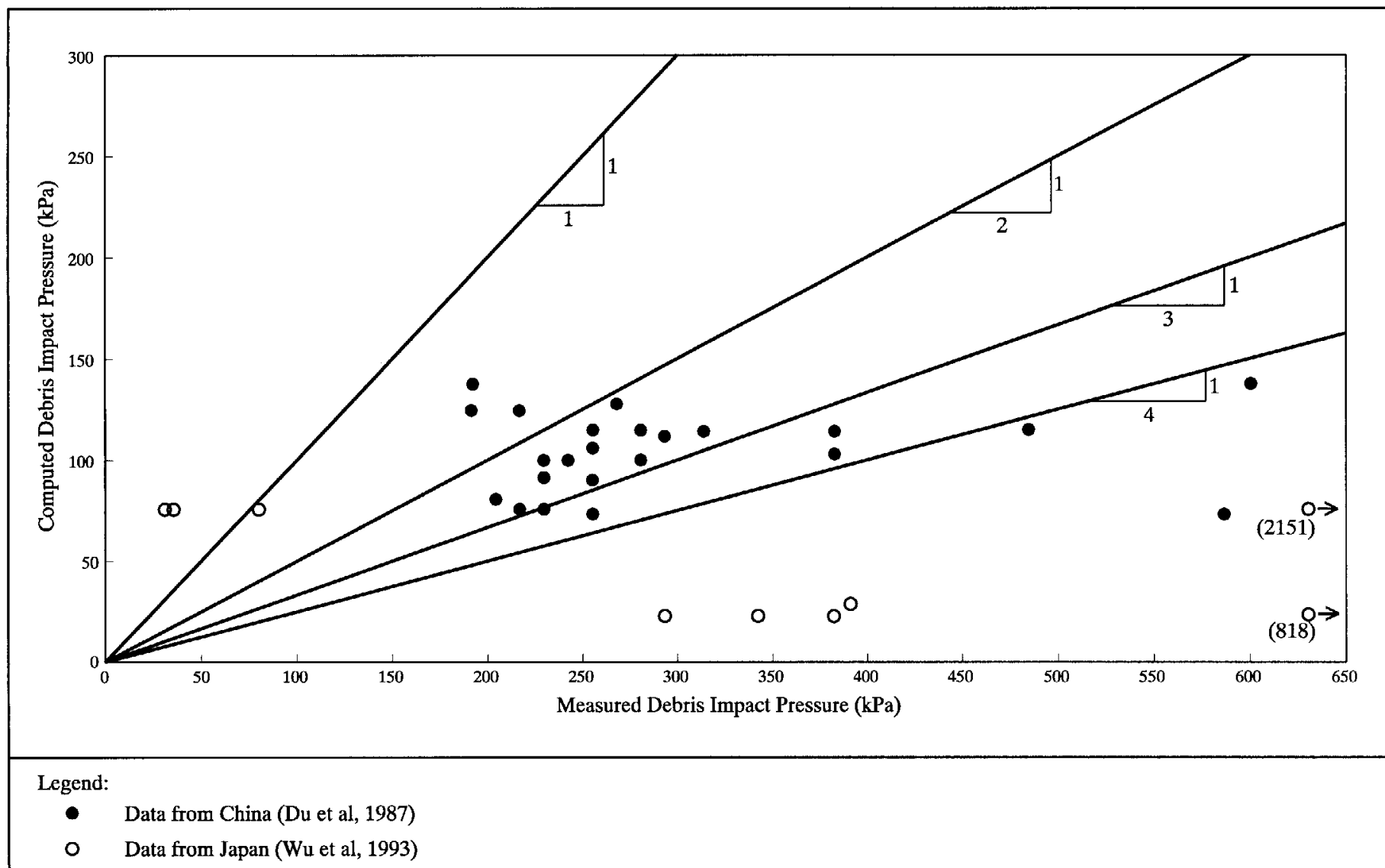


Figure 15 - Comparison of Computed and Measured Debris Impact Pressures

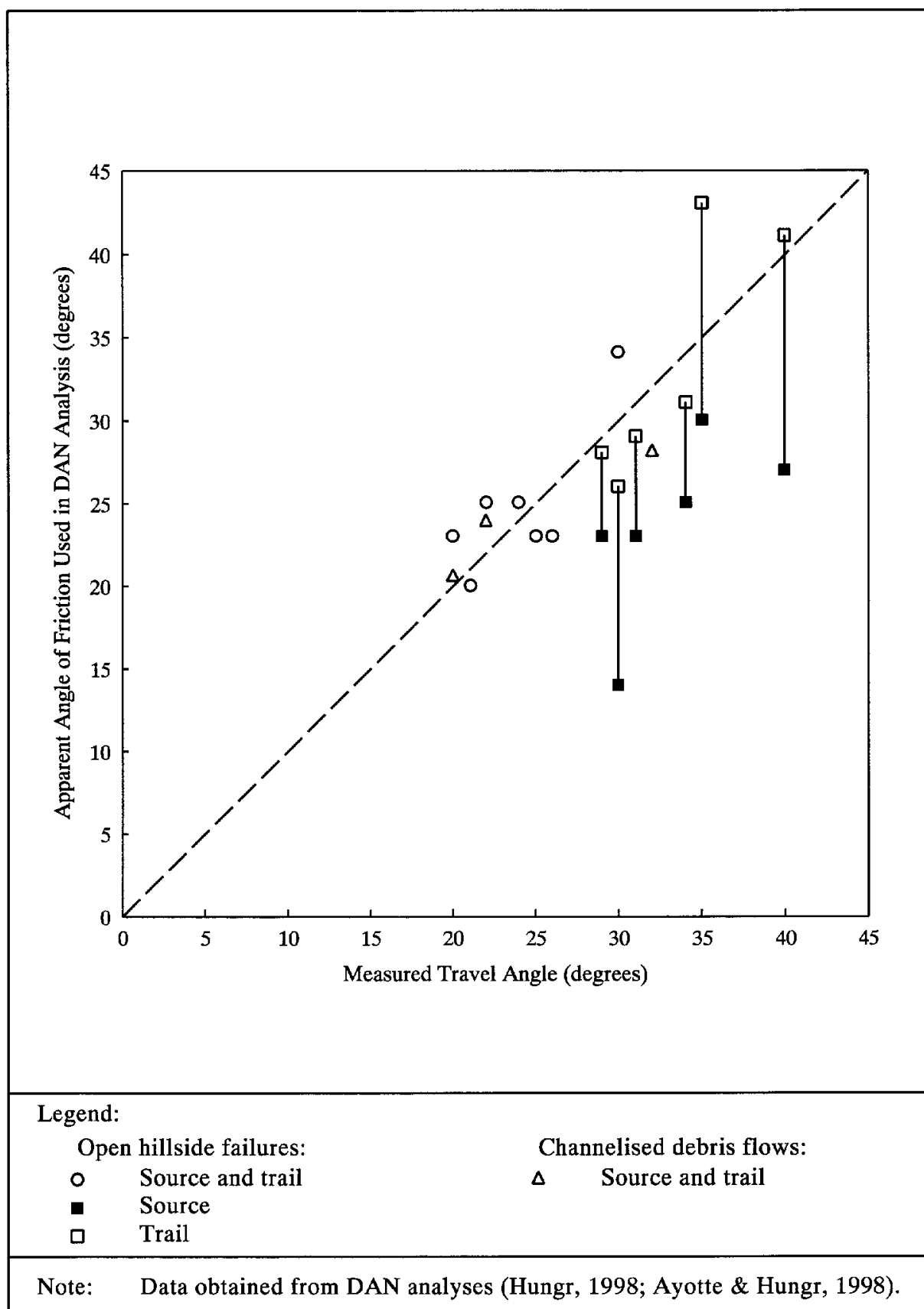
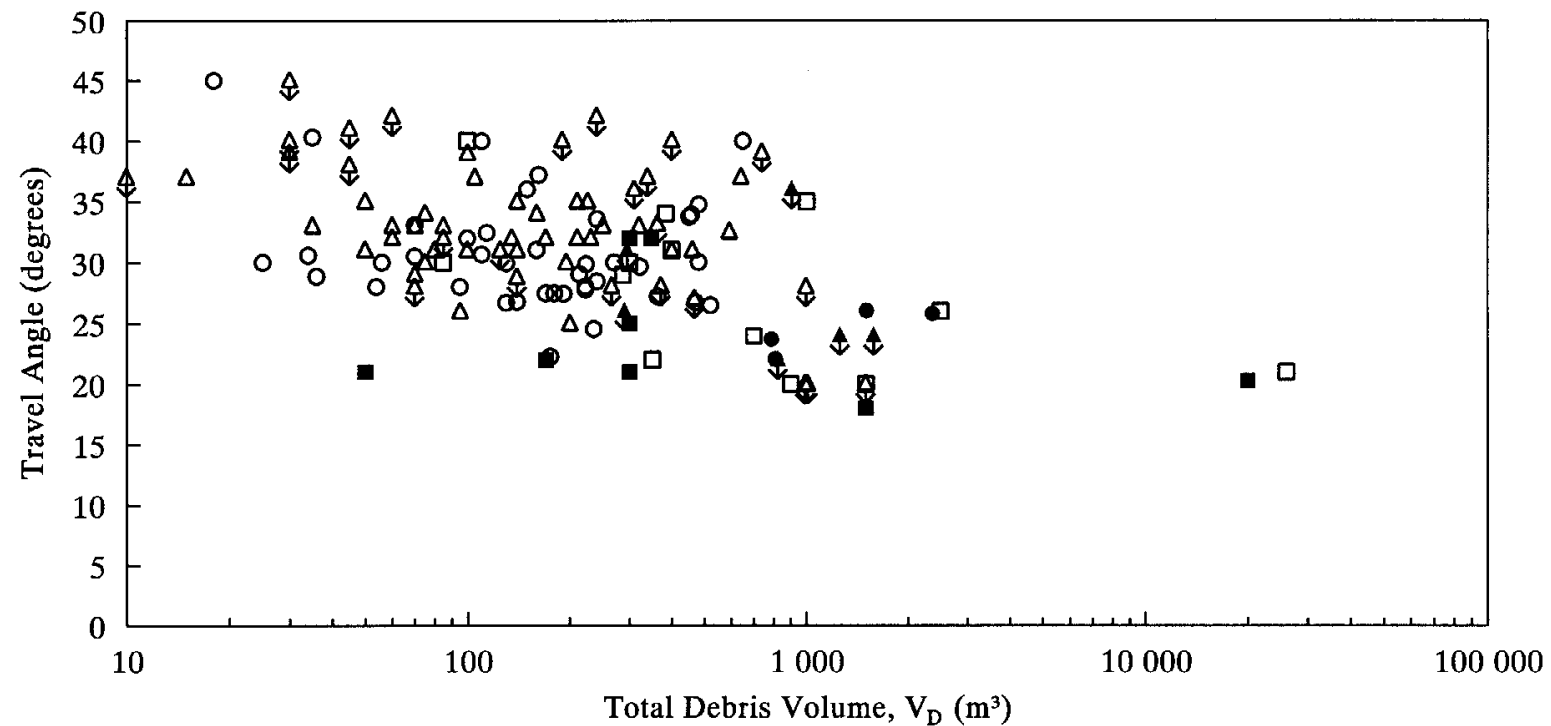


Figure 16 - Comparison of Apparent Angle of Friction Used in DAN Analysis with Observed Travel Angle of Debris



Legend:

Open hillside failures:

- △ Wong et al (1998)
- ◈ Wong et al (1998) (upper bound)
- Franks (1998)
- Data extracted from landslide study reports and values reported in Hungr (1998) and Ayotte & Hungr (1998)

Channelised debris flows:

- ◈ Wong et al (1998) (upper bound)
- Franks (1998)
- Data extracted from landslide study reports and values reported in Hungr (1998) and Ayotte & Hungr (1998)

Figure 17 - Data on Debris Mobility for Different Mechanisms and Scales of Natural Terrain Landslides in Hong Kong

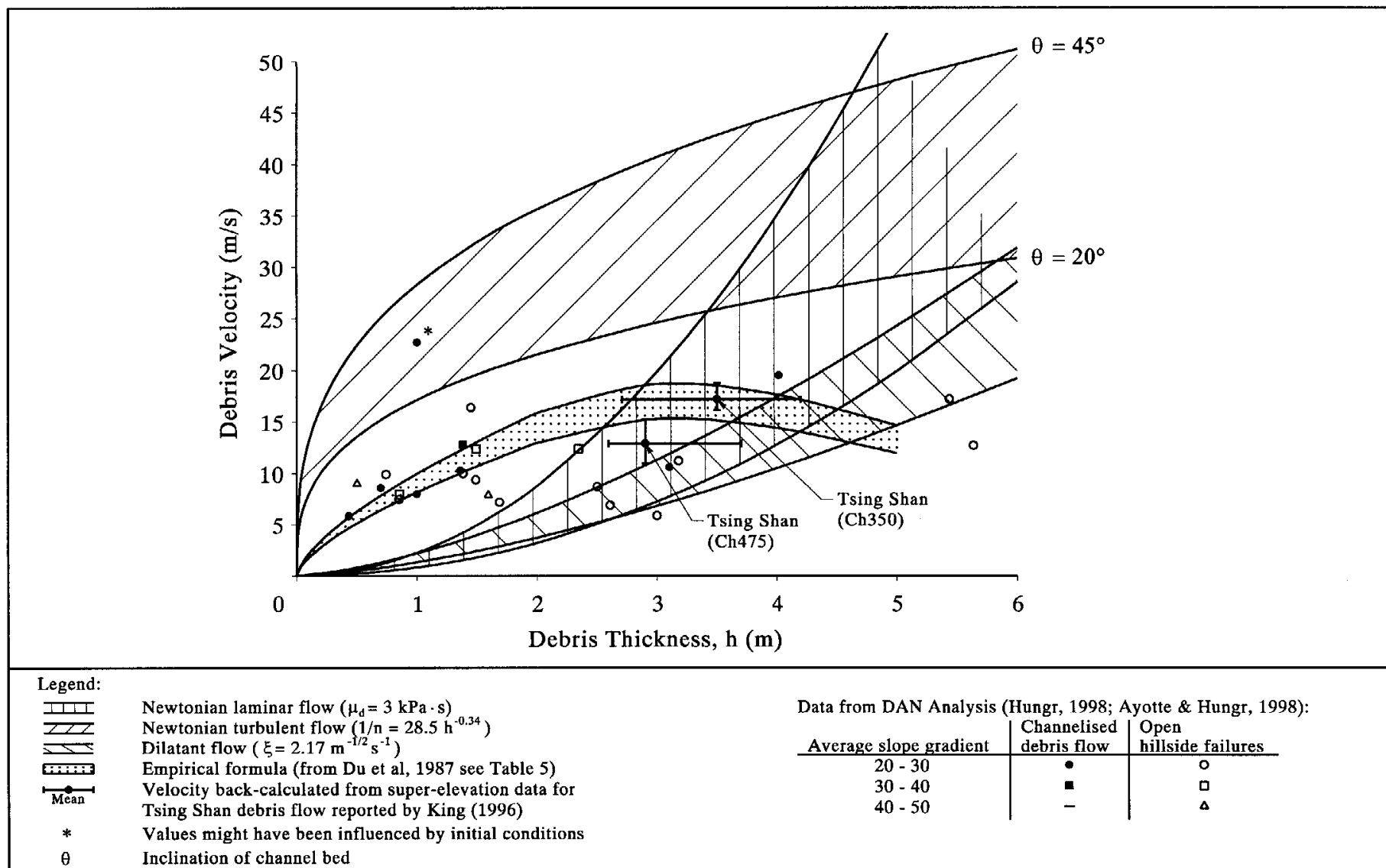


Figure 18 - Comparison of Data Extracted from DAN Analysis with Those Predicted by Flow Models

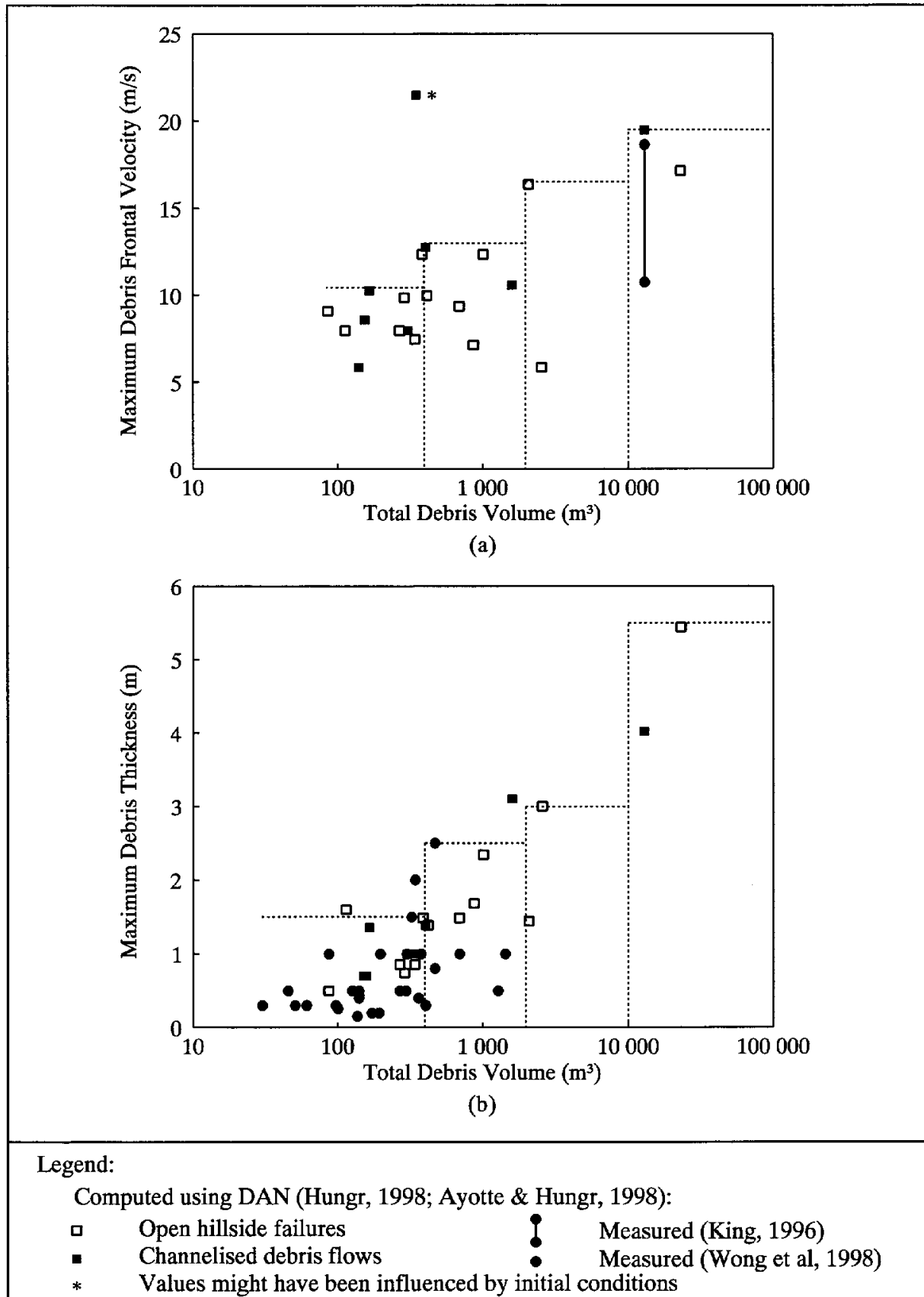
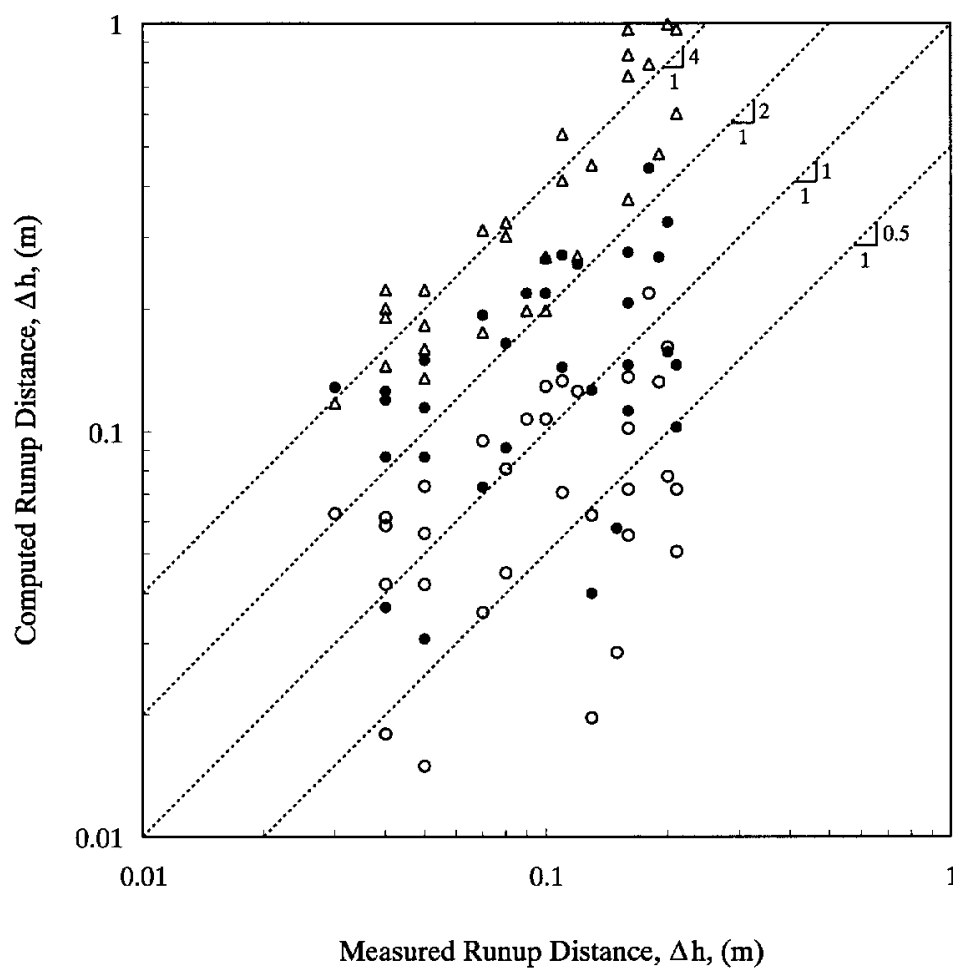


Figure 19 - Maximum Debris Frontal Velocity and Debris Thickness Corresponding to the Four Debris Volume Ranges



Legend:

- △ Sled Model
- Sled Model Corrected for Changes in Slope Gradient (Perla et al, 1980)
- Leading-edge Model (Hung & McClung, 1987; Takahashi & Yoshida, 1979)

Note: Measured data obtained from Chu et al (1995).

Figure 20 - Comparison of Measured and Computed Vertical Runup Distances Using Various Models

Suggestions for Assessment of Debris Mobility					
Analytical Approach			Empirical Approach		
Determine debris mobility using continuum models which have been calibrated against field observations			Determine maximum debris velocity and maximum debris thickness from estimated debris volume		
Rheological Model	Model Parameters		Debris Volume, V_D (m ³)	Maximum Debris Velocity on Slope, v_o (m/s)	Maximum Debris Thickness (m)
	Open Hillside Failures	Channelised Debris Flows			
	Friction	$V_D < 400 \text{ m}^3$ $\phi_a=25^\circ$ $V_D \geq 400 \text{ m}^3$ $\phi_a=20^\circ$			
Voellmy	-	$\phi_a=11^\circ$ $\zeta=500 \text{ m/s}^2$	$V_D < 400$	10.5	1.5
Refer to Table 6 for description of rheological models.			$400 \leq V_D < 2000$	13.0	2.5
			$2000 \leq V_D < 10000$	16.5	3.0
			$V_D \geq 10000$	19.5	5.5
			Runout		
			$v_x = \sqrt{G(x_L - x)}$ $x_L = \frac{v_o^2 \cos^2(\theta_o - \theta)(1 + \frac{gh_o \cos \theta_o}{2v_o^2})^2}{G}, \text{ where}$ $G = g(\tan \phi_a \cos \theta - \sin \theta)$		
			Runup		
			$\Delta h = \frac{v_o^2 \cos^2(\theta_o + \theta) \tan \theta}{g(\tan \phi_a + \tan \theta)} (1 + \frac{gh_o \cos \theta_o}{2v_o^2})^2$		
			Refer to Tables 7 & 8 for legend.		
Rheological Model	Model Parameters		Debris Volume, V_D (m ³)	Maximum Debris Velocity on Slope, v_o (m/s)	Maximum Debris Thickness (m)
	Open Hillside Failures	Channelised Debris Flows			
	Friction	$V_D < 400 \text{ m}^3$ $\phi_a=25^\circ$ $V_D \geq 400 \text{ m}^3$ $\phi_a=20^\circ$			
Suggestions for Assessment of Debris Impact Loading					
Debris Impact Pressure $p=3\rho_d v_d^2 \sin \beta$					
Boulder Impact					
One-tenth of the value estimated using Hertz equation: $F = 1.14 v_b^{1.2} \lambda^{0.4} m_b^{0.6}$					
Flexural stiffness method: $F = v_b \sin \beta \sqrt{m_b K_B}$					
Refer to Table 13 for legend.					

Figure 21 - Suggestions for Assessment of Debris Mobility and Debris Impact Loading

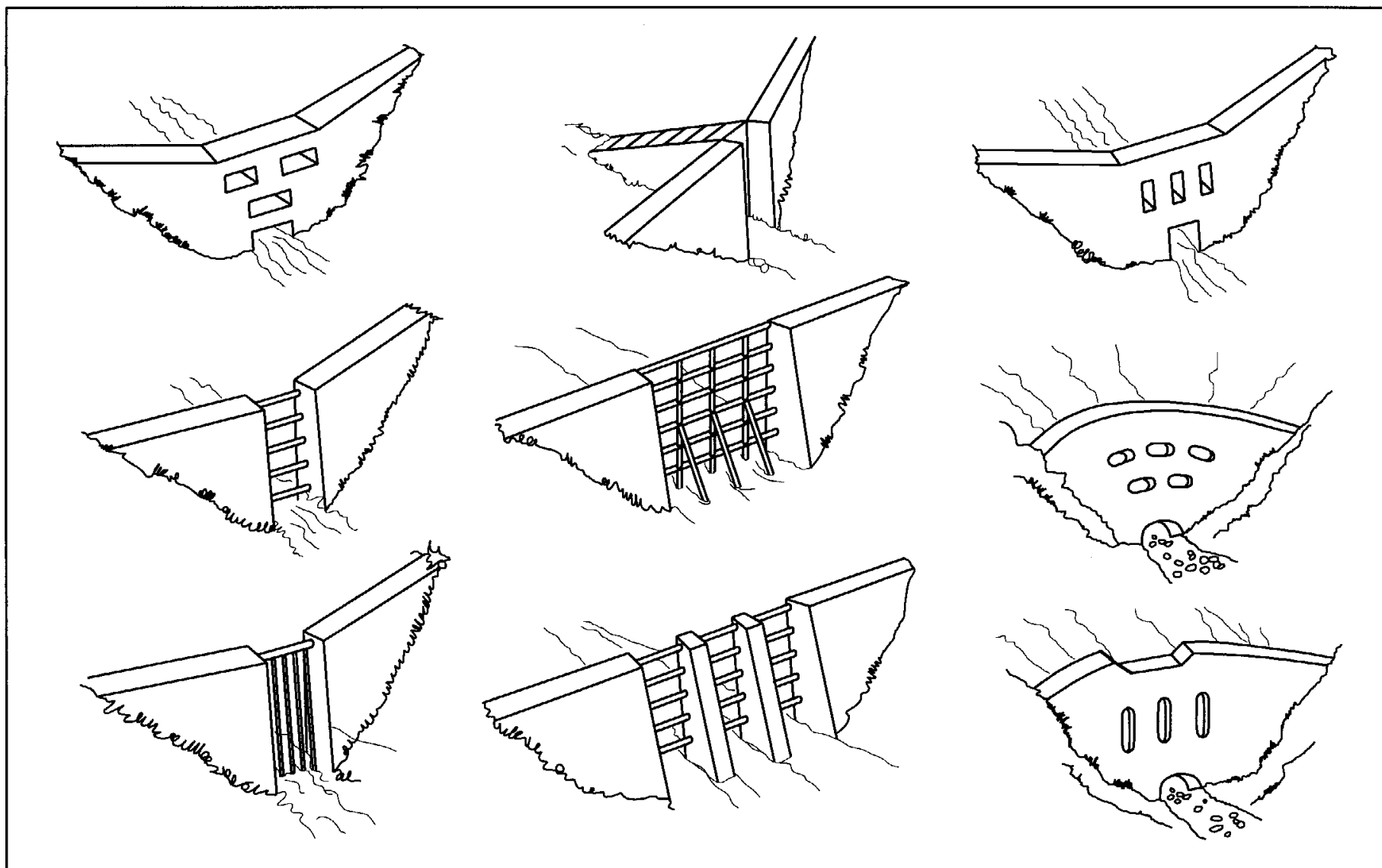


Figure 22 - Some Typical Decanting or Straining Structures (Czerny, 1998)

LIST OF PLATES

Plate No.		Page No.
1	Series of Check Dams in Nagano Prefecture, Japan (Japan Forest Conservation and Flood Control Association, 1985)	89
2	Grid-type Steel Sabo Structure on Komu River in Japan (Kawaken, 1998)	89
3	5-m High Slit Dam in Japan (Kawaken, 1998)	89
4	Gabion-type Check Dam in Japan (Kawaken, 1998)	89
5	Reinforced Concrete Barrier with Counterforts (Czerny, 1998)	89
6	Steel Cell Dams on Yotagiri River in Japan (Okubo et al, 1996)	90
7	Steel Boulder Fence below Seymour Cliff, Midlevels	90
8	Steel Boulder Fence in Fanling Area 49A	90
9	Gabion-type Boulder Barrier Constructed at Yiu Hing Estate, Shaukeiwan	90
10	Reinforced Concrete Boulder Barrier at Baguio Villa	90
11	Reinforced Concrete Landslide Debris/Boulder Barrier in Fanling Area 49A	90
12	5-m High Reinforced Concrete Barrier at Kowloon Medical Rehabilitation Centre	91
13	Debris Containment Berm in Tuen Mun Area 19	91
14	6-m High Check Dam under Construction in Sham Tsang	91
15	Use of Rubber Tires to Soften Impact on Barrier (Kawaken, 1998)	91



Plate 1 - Series of Check Dams in Nagano Prefecture, Japan (Japan Forest Conservation and Flood Control Association, 1985)



Plate 2 - Grid-type Steel Sabo Structure on Komu River in Japan (Kawaken, 1998)



Plate 3 - 5-m High Slit Dam in Japan (Kawaken, 1998)



Plate 4 - Gabion-type Check Dam in Japan (Kawaken, 1998)



Plate 5 - Reinforced Concrete Barrier with Counterforts (Czerny, 1998)

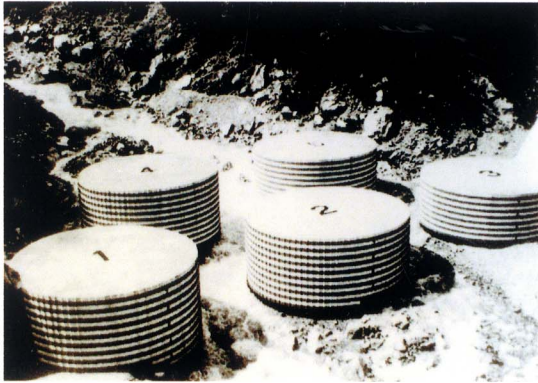


Plate 6 - Steel Cell Dams on Yotagiri River in Japan (Okubo et al, 1996)



Plate 7 - Steel Boulder Fence below Seymour Cliff, Midlevels



Plate 8 - Steel Boulder Fence in Fanling Area 49A



Plate 9 - Gabion-type Boulder Barrier Constructed at Yiu Hing Estate, Shaukeiwan



Plate 10 - Reinforced Concrete Boulder Barrier at Baguio Villa



Plate 11 - Reinforced Concrete Landslide Debris/Boulder Barrier in Fanling Area 49A



Plate 12 - 5-m High Reinforced Concrete Barrier at Kowloon Medical Rehabilitation Centre



Plate 13 - Debris Containment Berm in Tuen Mun Area 19

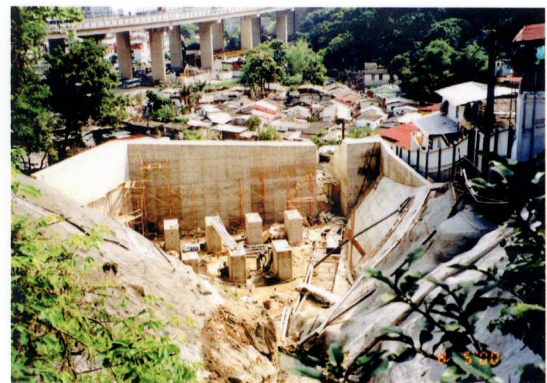


Plate 14 - 6-m High Check Dam under Construction in Sham Tseng

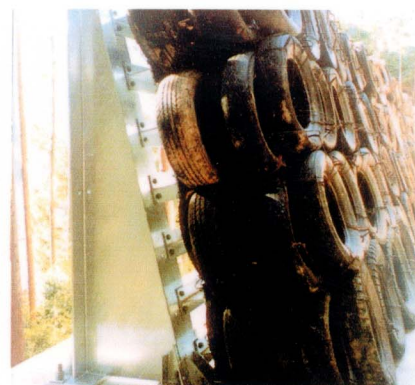


Plate 15 - Use of Rubber Tires to Soften Impact on Barrier (Kawaken, 1998)